Smart Polymers as Flocculants for Oil Sands Tailings Treatment

by

Atreya Krishna Nittala

A thesis submitted in partial fulfillment of the requirements for the degree of

Master of Science

In

CHEMICAL ENGINEERING

Department of Chemical and Materials Engineering
University of Alberta

ABSTRACT

The by-product slurry resulting from the bitumen extraction process from oil sands sources, known as tailings, holds substantial amount of water along with clays and fugitive bitumen. Current polymer-based dewatering technologies are centred on acrylamide-based polymers such as polyacrylamide (PAM). The main motivation to develop smart polymers is to replace PAM with more efficient polymer flocculants. This research deals with the synthesis and testing of polymers that are sensitive to pH. Solution pH levels can be tuned by introducing carbon dioxide (CO_2) in the medium, which is advantageous since CO_2 can be easily removed from the system by depressurization. In this work, homopolymers of dimethyl amino ethyl methacrylate (DMAEMA) and N-isopropyl acrylamide (NIPAM) and their copolymers having different molecular weight averages were synthesized using free radical addition polymerization. Their performance as flocculants and dewatering agents for mature fine tailings (MFT) was systematically evaluated using different metrics: initial settling rate (ISR), capillary suction time (CST), and turbidity of the supernatant, in the presence and absence of CO_2. The best conditions from these studies were adapted to study the performance of blends made out of these polymers. The polymer blends proved to be more effective as flocculants than the individual polymers.

ACKNOWLEDGEMENTS

I would like to sincerely thank my thesis advisor Dr. João B. P. Soares of the Department of Chemical and Materials Engineering at the University of Alberta for his unconditional support and guidance. Prof. Soares has always been helpful in giving valuable input upon encountering any hiccups in my research and steered me in the right direction at the time of need which helped a new grad student like me, to work effectively without any pressure. Prof. Soares and his wife Maria always made everyone in the group feel at home, giving us second family in Edmonton, for which I am deeply indebted to.

Special thank you to Dr. João B. P. Soares, Dr. Qi Liu, Dr. Hyun-Joong Chung and Dr. Natalia Semagina for being part of my defense committee members for the Master of Science program.

I would like to acknowledge deeply Marco Antonio da Silva, Postdoctoral fellow at the University of Alberta, and Ni Yang, Research Technologist at Oil Sands and Coal Interfacial Engineering Facility for their patience and expertise in helping me out for polymer characterization and flocculation studies respectively.

I would also like to thank my course instructors and research group members, particularly Vahid Vahijinehad, Sarang Gumfekar, Dr. Linda Botha, Daniel Alberto Moran Nava and Dr. Diógenes Vedoy, for providing me with different insights into understanding the subject.

My heartfelt gratitude to my friends Dr. Naresh Miriyala, Rohan Gaikwad, Khushaal Popli, Pankaj Kumar Sahu, Nitya Arunachalam Iyer, Risha Dutt and Kasturi Nagesh Pai for their unconditional support in making this journey a fun ride. I am very grateful to my brother Pavan Pramod Sripada for making the transition into life in Canada as smooth as possible, during my early days in Edmonton.

I also acknowledge the efforts of Lily Laser, Mia Law, Kevin Heidebrecht and the staff of the Chemical and Materials Engineering in providing me with support whenever required.

Finally, I would like to express my profound gratitude to my parents, family and friends for providing me with continuous encouragement and moral support throughout this adventure. This feat would not have been possible without them. The past two years have been a great experience and will be etched in my memories as one of the fondest moments of my life.

Atreya Nittala

NOMENCLATURE

CHWE	Clarke hot water extraction
CST	Capillary suction time
C-UCST	Coloumb interaction upper critical solution temperature
CT	Consolidated tailings
DMAEMA	*N, N*-dimethyl aminoethyl methacrylate
HB-UCST	Hydrogen bonding upper critical solution temperature
ISR	Initial settling rate
LCST	Lower-critical solution temperature
MFT	Mature fine tailings
NIPAM	*N*-isopropyl acrylamide
PAA	Poly(acrylic acid)
PAM	Polyacrylamide
PMMA	Poly(methyl methacrylate)
PT	Paste technology
RAFT	Reversible addition-fragmentation chain transfer
SAGD	Steam assisted gravity drainage
SRF	Specific resistance to filtration
TEMED	*N,N,N',N'*-tetramethyl ethylene diamine
UCST	Upper-critical solution temperature

The following convention was adopted to identify the several polymer types made and tested in this investigation:

1. The first letter *p* identifies a polymer flocculant

2. When the first letter *p* is followed only by an *N* or *D*, it indicates a homopolymer of NIPAM (pN) or DMAEMA (pD), respectively.
3. Copolymers are labelled pN2D1, pN1D1 and pN1D2, where the number following the letter denotes the mass ratio of monomers used during polymer synthesis. For example, pN2D1 indicates that the ratio NIPAM:DMAEMA was 2:1 during polymer synthesis.
4. Finally, the number that follows the dash at the end of the polymer label is the weight average molecular weight (M_w) of the polymer in million Daltons. For instance, pN-2 is a homopolymer of NIPAM with weight average molecular weight of 2 million Daltons.

TABLE OF CONTENTS

LIST OF FIGURES

LIST OF TABLES

1. INTRODUCTION

Alberta has the world's third largest oil reserve after Venezuela and Saudi Arabia. The continuous exploration of such large reserves, however, has generated a large amount of waste in the form of tailings (a mixture of sand, clays, unrecovered residual bitumen, and water) that accumulate in ponds occupying vast areas of land. About 170 square kilometers of land was occupied by tailing ponds in 2015, and this number keeps growing (Saidi-Mehrabad et al., 2013).

Recently, the Alberta Energy Regulator (formerly Energy Resources Conservation Board, ERCB), reported an estimated 26.4 billion cubic meters of bitumen could be mined from these reserves. The two primary methods employed for the extraction of bitumen from oil sands in Alberta are *in situ* and *surface mining*. These methods will be discussed in the sections below.

1.1 *In Situ* or SAGD Extraction

Steam assisted gravity drainage (SAGD) is an in situ method, among others such as Toe to Heal Air Injection (THAI), Vapor Extraction (VAPEX), and Cyclic Steam Stimulation (Liang et al., 2016). They are practiced when the thickness of the overburden (soil coverage) is greater than 75 meters, in which case surface mining techniques become impractical and uneconomical. *In situ* practices are popular in Peace River, Cold Lake, and some areas around the Athabasca River regions, constituting about 80% of the total oil sands reserves in Canada (Alberta Energy Regulator, 2015).

SAGD requires the construction of two parallel wells enclosing the oil sands ore (Shen, 2013). Steam is injected into the first well, increasing the temperature and reducing the viscosity of bitumen. This allows the bitumen to flow downwards, due to gravity, into the second well. The light bitumen collected in this well is transported to the surface via pumps. A schematic of the *in situ* method is shown in Figure 1.1.

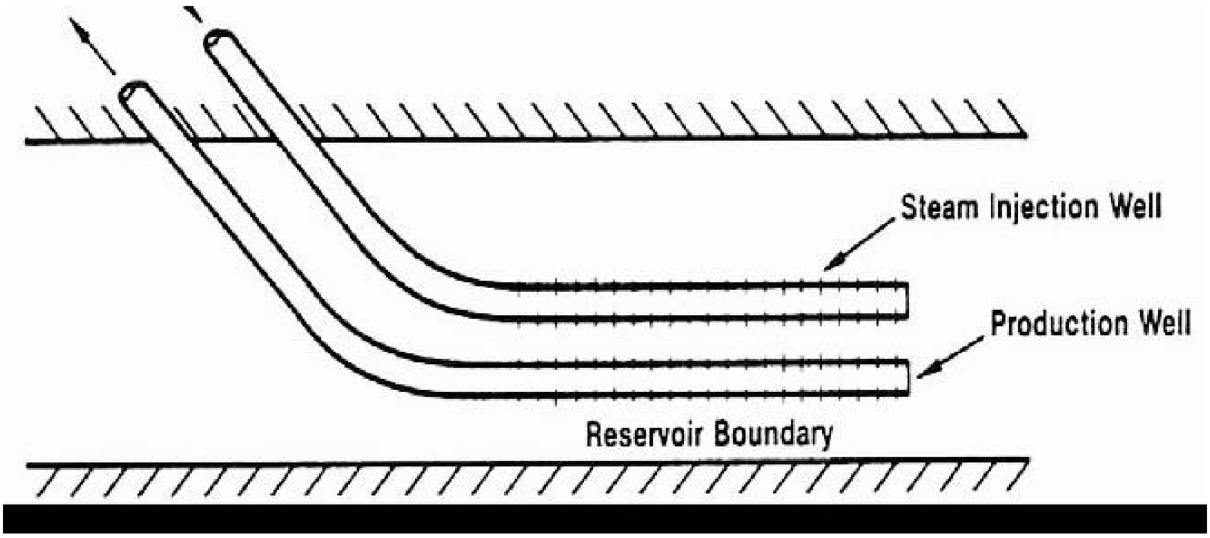

Figure 1.1. Schematic of a SAGD operation (reproduced from Speight, 2009).

The SAGD process is attractive because it does not generate oil sands tailings. Although SAGD has high energy requirements, it is environmentally friendlier than the traditional surface mining technique.

1.2 Surface Mining

Surface mining, or open pit mining, is practiced in areas where the oil sands deposits are not very far from the surface. The thickness of the overburden should be less than 75 meters for this method to be practiced economically. Only about 20% of Alberta's oil reserves are explored using surface mining operations (Alberta Energy Regulator, 2009), including areas north of Fort McMurray along the Athabasca river valley**.** This extraction method is also called the Clark Hot Water Extraction (CHWE) process. The basics of the CHWE process are outlined below.

The muskeg (vegetation) and the overburden are removed using shovels and other mechanical equipment. Next, the oil sands are mixed with hot water (80 ^{o}C – 85 ^{o}C) and chemical additives (NaOH), and then crushed. The crushed ore is hydrotransported in long pipelines to the bitumen recovery unit. Due to the added chemicals and the mechanical shear experienced during this transport, the bitumen trapped in the ore is liberated. The bitumen, due to its hydrophobic nature, attaches itself to the air bubbles present in the mixture. The slurry is diluted with water and discharged into huge settling vessels at the bitumen extraction unit. The aerated bitumen froth rises to the top of the vessel, while the heavy ore particles settle at the bottom due to gravity. The bitumen froth from the settling tanks and floatation cells is deaerated and transferred to the bitumen froth treatment unit to remove the water and solids present, achieving a final purity of 96% to 98% (Masliyah et al., 2011).

The tailings resulting from the surface mining operation are transported to large tailing ponds where the heavier particles settle down due to gravity. This is shown in Figure 1.2.

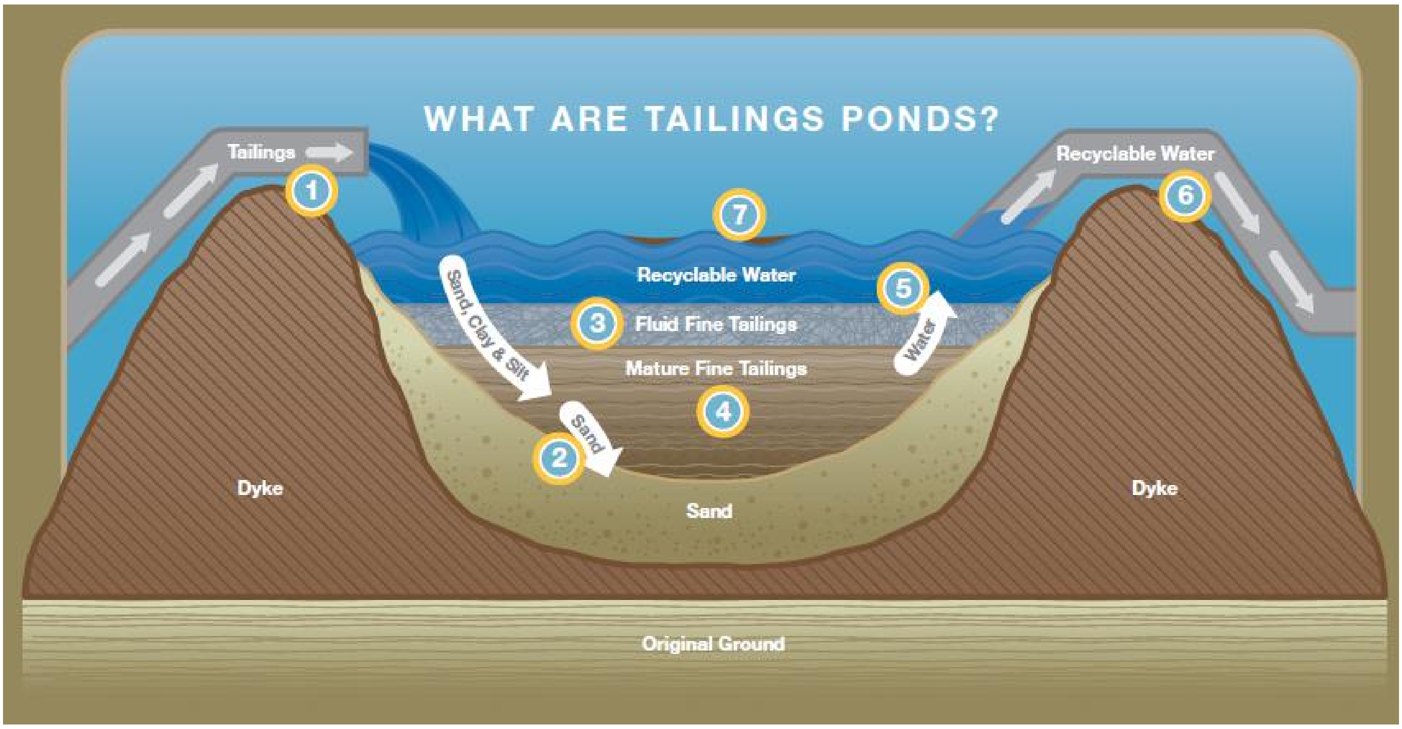

Figure 1.2. Cross sectional view of a typical tailings pond (extracted from Alberta Energy Regulator, 2009).

However, the clays and silt form a stable colloidal suspension layer above the layer of the deposited coarse sand fraction, which takes a longer period of time to separate from the aqueous phase. The bottom fraction of this layer, having a higher fraction of fines (particles with diameters below 44 µm), is known as mature fine tailings (MFT), and the upper fraction, having a higher percentage of ultrafines (particle size less than 2 µm) is known as fluid fine tailings or FFT.

The typical composition of this MFT layer is shown in Table 1.1.

Table 1.1. Typical composition of MFT.

COMPONENT	PERCENTAGE (%)
Bitumen	5
Water	35
Solids	60

1.3 Challenges in Tailings Treatment

The challenges faced by the oil sands industry is tailings storage, land reclamation and water recovery. Large areas of open land are being used as tailing ponds for the purpose of dewatering tailings by gravity, posing an environmental hazard that affects flora and fauna (Timoney et al., 2009). Water management is another issue, as the water recycled from tailings treatment units comes with a certain ion concentration. Recycled water from the tailings ponds should satisfy requirements with respect that include, but not limited to, hardness, pK_a and turbidity. Calcium ion concentration in the recycled water should be in the range of 17-25 mg/L (Allen, 2008), as a high ion concentration in the recycled stream can lead to effects such as low bitumen recovery and corrosion damage to pumps and pipelines.

One volumetric unit of bitumen requires up to 10 volumetric units of water (Flint, 2005), which implies that any contribution that helps reduce water usage can have a significant economic and environmental impact. About 65% of the water used in the extraction of bitumen is recycled, but the remaining 35%, which corresponds to three volumetric units for every unit of bitumen produced, remains trapped in tailing ponds (BGC Engineering Inc., 2010). This water must be separated from the tailings to increase the percentage of recycled water, as well as to minimize the space being used for storage.

In order to minimize environmental damage, the Alberta Energy Regulator (AER) has passed legislations to reclaim lands used as tailing ponds. The aim is, firstly, to increase the quantity of recycled water from tailing ponds, thereby reducing the demand of fresh water from natural resources and, secondly, to strengthen the particle deposits at the bottom of these ponds by removing the water present so as to obtain “dry” lands for reclamation.

Being cognizant of this issue, we will discuss how we can contribute to the goal of tailing ponds reclamation using established treatment practices. This work deals with the use of these practices for polymers that are sensitive to pH changes.

The adopted strategy consisted in making three types of flocculants: 1) homopolymers of *N,N*-dimethyl aminoethyl methacrylate (DMAEMA), 2) homopolymers of N-isopropyl acrylamide (NIPAM), and 3) copolymers of DMAEMA and NIPAM. The polymer synthesis conditions were adjusted to make polymers with varying molecular weight and compositions. Homopolymers of DMAEMA are sensitive to both temperature and pH, whereas homopolymers made with NIPAM are only sensitive to temperature. In this study, homopolymers of NIPAM and DMAEMA and their copolymers are synthesized. Including both the monomers in the polymer chain imparts the polymers with both, temperature and pH sensitive properties, however, only the pH sensitivity of the polymers was investigated. The performances of these polymers by themselves and as blends are investigated in this study.

2. LITERATURE REVIEW

A recent article stated that the composition of the MFTs has a significant influence on its flocculation characteristics (Botha et al., 2015). A typical composition of clays present in MFT is shown in Figure 2.1.

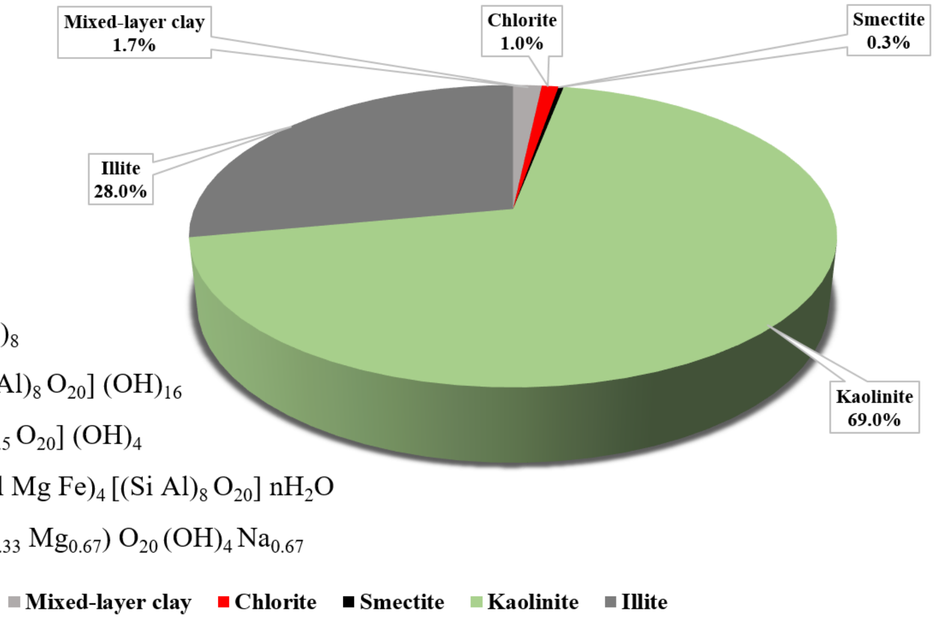

Kaolinite: $Al_4 [Si_4O_{10}] (OH)_8$

Chlorite: $(Mg\ Al\ Fe)_{12}[(Si\ Al)_8\ O_{20}]\ (OH)_{16}$

Illite: $K_{1\text{-}1.5}\ Al_4\ [Si_{7\text{-}6.5}\ Al_{1\text{-}1.5}\ O_{20}]\ (OH)_4$

Smectite: $(0.5\ Ca\ Na)_{0.7}\ (Al\ Mg\ Fe)_4\ [(Si\ Al)_8\ O_{20}]\ nH_2O$

Montmorillonite: $(Si_8)\ (Al_{3.33}\ Mg_{0.67})\ O_{20}\ (OH)_4\ Na_{0.67}$

Figure 2.1. Typical composition of clays in MFT (adapted from Masliyah et al., 2011).

Mature fine tailings are stable colloidal suspensions of solids in water, where water accounts for approximately 65% of the total mass. The solids are mostly comprised of different clay types; in Athabascan oil sands, kaolinite is the most common clay type. Other clays include illite, smectite and montmorillonite. These clays have varying structures, as shown in Figure 2.2.

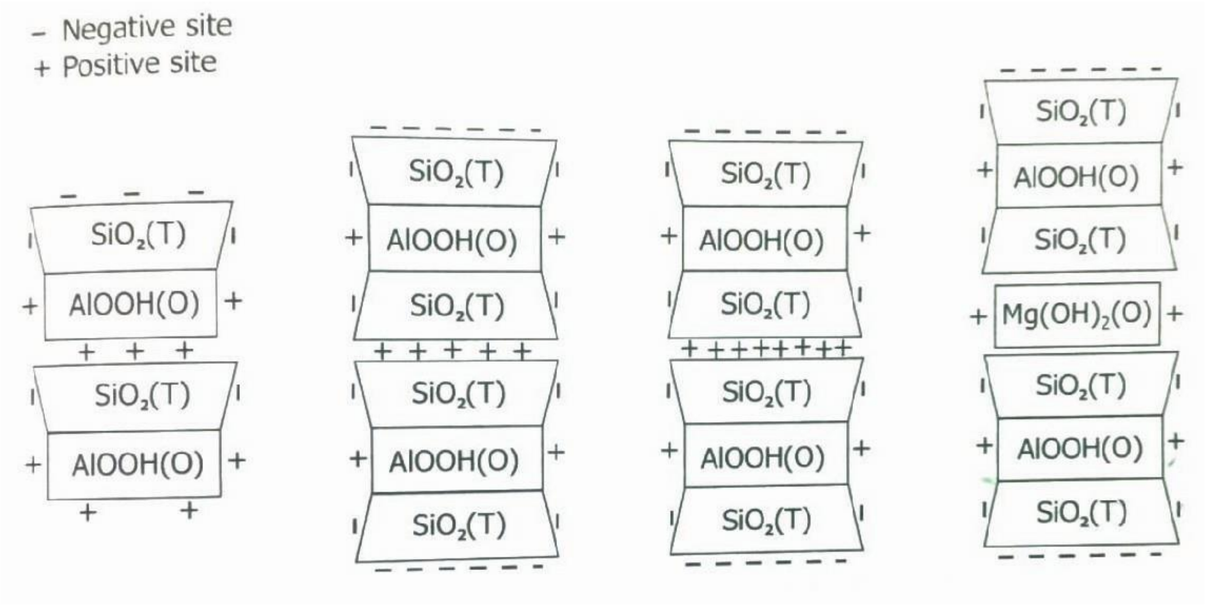

Figure 2.2. Schematics of kaolinite, illite, montmorillonite, and chlorite (reproduced from Masliyah et al., 2011).

Kaolinite clays make up the majority of clays in MFT. Since kaolinite is the most common clay type in MFTs, let us discuss it in some detail. Kaolinite is a two layered clay with alternating tetrahedron and octahedron sheets (Konan et al., 2007), as shown in Figure 2.3.

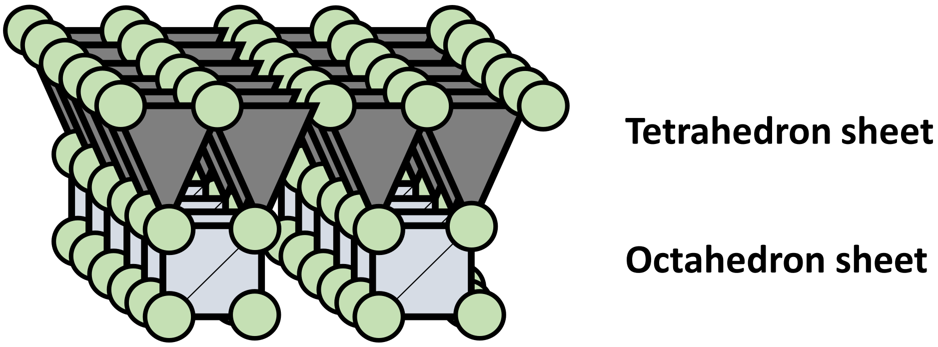

Figure 2.3. Tetrahedron and octahedron structures of kaolinite clays (adapted from Masliyah et al., 2011).

The tetrahedron sheet consists of a covalently bonded silicon and oxygen layer, whereas the octahedron sheet consists of a covalently bonded aluminum (or magnesium) and oxygen layer (Masliyah et al., 2011). Kaolinite has a recurring structure of a silicon atom bonded with oxygen atoms. The tetrahedron and the octahedron layers are bonded by hydrogen bonds between the oxygen of the tetrahedron and the hydroxyl of the octahedron. These clays do not swell in water (Chalaturnyk et al., 2002), and therefore do not increase substantially the viscosity of the slurry.

Oil sands tailings contain small concentrations of ionic species such as magnesium (Mg^{2+}), aluminum (Al^{3+}), silicon (Si^{4+}), sodium (Na^+), potassium (K^+) and iron (Fe^{2+}) that are present in both clays and water. An interesting phenomenon occurs where the lower valence ions in the clays tend to substitute the higher valence ions, with negligible impact on the clay structure. As the lower valence ions take the place of higher valence ions, the valence of the ions at the site is not "satisfied", leading to a charge imbalance. This phenomenon is called isomorphic substitution. As a consequence of isomorphic substitution, kaolinite clays have a characteristic negative charge. However, the entire system is charge balanced as the metal ions present in the system neutralize this charge.

Other clays, such as illite or smectite, have a three-layer structure as opposed to the two-layer structure of kaolinite. The tetrahedron layer undergoes easier isomorphic substitution than the octahedron layer. As a result, these clays undergo isomorphic substitution to a greater extent, as their structure comprises of two tetrahedron layers surrounding each octahedron layer, thus having a greater negative charge. Among these clays, illite clays are known to be non-swelling clays whereas montmorillonite (smectite) clays are swelling clays, in spite of them having the same structure (Figure 2.2). This is due to presence of compensating ions, like Na^+ and K^+ among others, resting in between the different blocks, which weakens the intermolecular forces between the clays. This allows for easier ion exchange between the blocks. This effect is not observed in illite clays where the compensating rest in the octahedral layer which forms strong bonds between the building blocks. Illite clays exhibit significant isomorphic substitution only through the tetrahedral layers, whereas smectite clays show ion exchange through both the tetrahedral and octahedral layers (Masliyah, J. H et al., 2011).

As the majority of the clays present in oil sands tailings are negatively charged kaolinite clays, they repel each other forming a stable suspension. In order to settle these particles, these repulsive forces have to be compensated for. This is achieved by adding chemical agents that either neutralizes surface charges or adsorbs onto the particle surfaces. The result of either of these actions leads to the formation of aggregates. These processes are called coagulation and flocculation respectively. Coagulation involves charge neutralization of the suspended particles through the addition of coagulant aids. The main purpose of the coagulant aid is to destabilize the system. Flocculation, on the other hand, is a process that involves bridging or enmeshment of the suspended particles (Dentel, 1991). Particle aggregation is achieved using coagulating agents like gypsum via ion neutralization, and by flocculating agents via polymer bridging mechanisms. The polymer molecules get adsorbed on the particle surface thereby forming a physical link between the particles. These particles then come closer to each other through surface forces (i.e. they adsorb on to each other).

The force driving the polymer chains to adsorb onto clay surfaces are the electrostatic force of attraction between the negatively charged clays and the positively charged polymeric chains. The polymer chains get adsorbed on more than one particle which leads to the formation of flocs that settle down due to gravity. This is represented as a schematic in Figure 2.4.

Figure 2.4. Polymer adsorption on a particle and a representation of a single floc.

One of the main performance requirements of polymer flocculants is the settling rate of the flocs they produce. The general trend for the change in the initial settling rate (ISR) of the mudline with polymer dosage (Vedoy et al., 2015) is shown in Figure 2.5. The ISR increases until it reaches a peak value, known as the optimum dosage, after which it drops and plateaus.

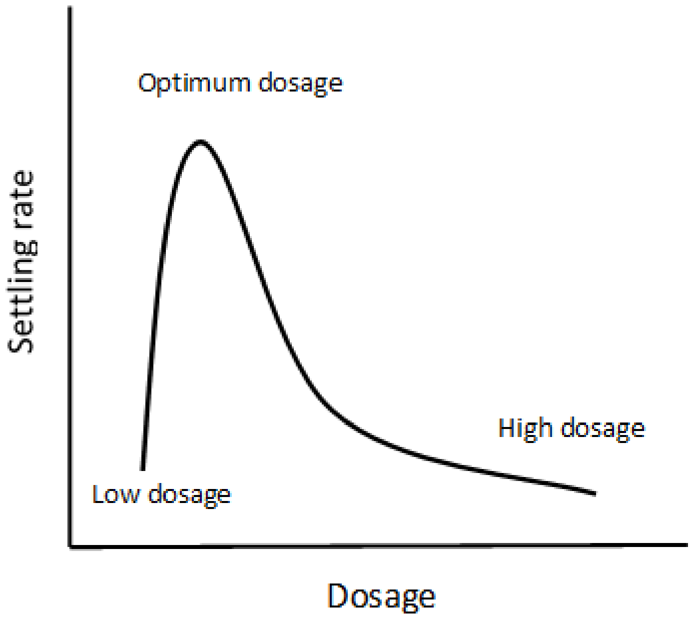

Figure 2.5. General trends in initial settling rate (ISR) with polymer dosage.

The optimum dosage of the flocculant is the dosage at which the flocculant covers less than the entire surface area of the solids being flocculated, as sections of the particle surface have to be left exposed so to allow for the bridging mechanism to occur during particle collisions (Sworska, Laskowski, & Cymerman, 2000). It has been observed that if more than half the particle surface is covered by the polymer, further adsorption of the polymer gets difficult (Bolt, 2007). This might have an adverse effect on the settling rate. The curve drops and levels out due to the particle surface being surrounded by excess polymer which causes repulsions among the flocs, thus stabilizing the system (Li et al., 2005; Long et al., 2006). With these concepts in mind, let us discuss some common techniques that have been employed in managing tailing ponds.

2.1 Tailings Management Technology

One of the popular methods of tailings management is the Consolidated Tailings (CT) process, practiced by Suncor and Syncrude (MacKinnon et al., 2001). This process involves mixing MFTs with coarse sand from raw tailings and a coagulant aid, such as gypsum or calcium sulphate. The CT process creates a highly permeable mixture, and the coarse sand added to the mixture, aids in dewatering, by acting as a physical load on the deposited solids. The water obtained from the CT process can be re-used or recycled in many ways. The typical course taken by the recycle water is represented in Figure 2.6.

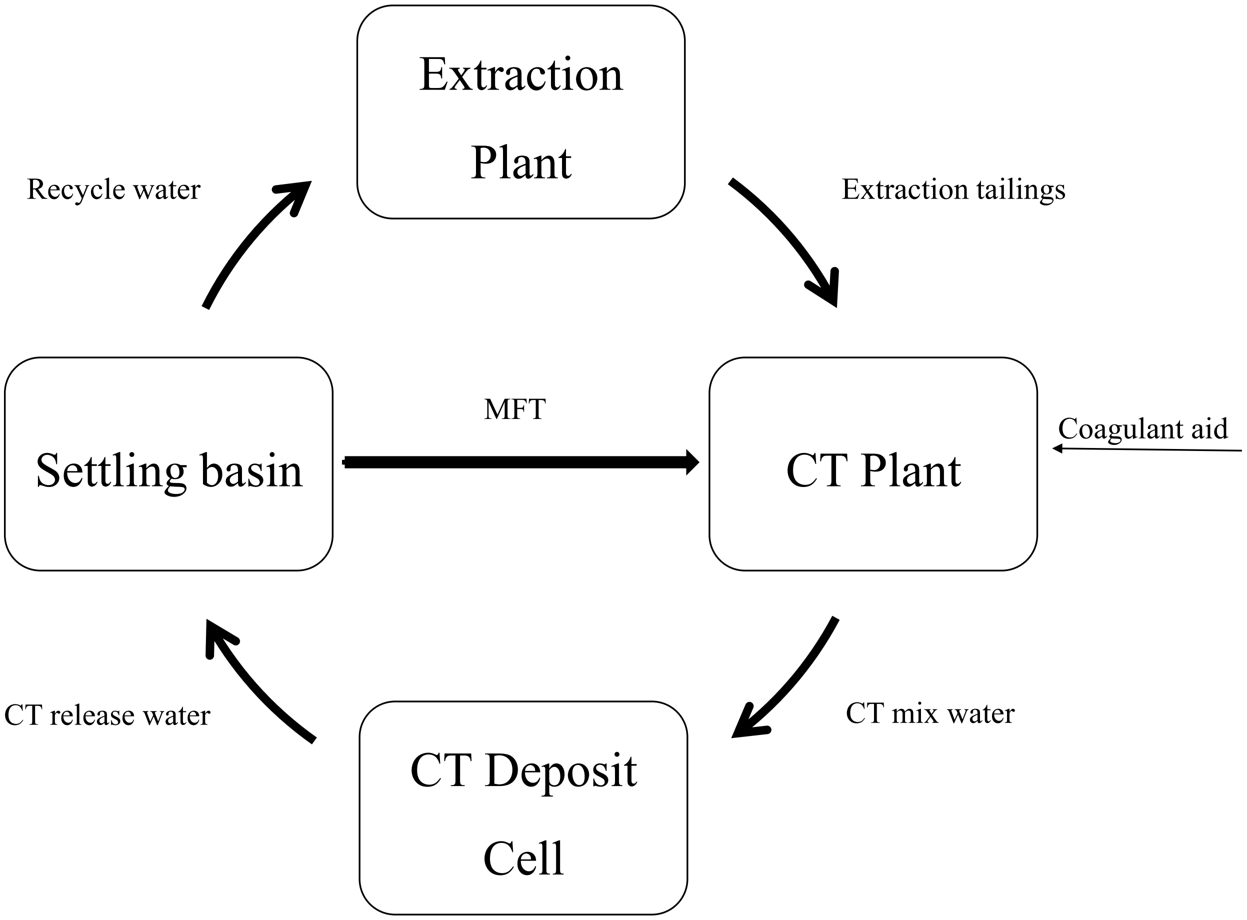

Figure 2.6. Path of water after bitumen extraction (adapted from MacKinnon et al., 2001).

Most of the recovered water is used in tailings management or for upstream processes like bitumen extraction. In the majority of the cases, the recycled water contains calcium ions which creates problems during the extraction process because they interfere with bitumen liberation, thereby lowering the total oil recovery (Fong et al., 2004; Kasongo et al., 2000). In addition, the sulphate ions left behind in the sediment bed can release a potentially harmful gas, hydrogen sulphide (H_2S), upon anaerobic reduction.

Means to avoid the high calcium ion concentrations are being studied. Apex Engineering Inc. (AEI) studied the effect of calcium hydroxide along with a thickener for tailings management (Chalaturnyk et al., 2002). The tailings, upon mixing with calcium hydroxide, were treated with carbon dioxide which converts the calcium hydroxide into insoluble calcium carbonate, which precipitates from the water solution. This reduces the concentration of calcium in the recovered water.

2.2 Paste Technology

An alternative to the CT process is Paste Technology (PT). This method uses polymeric flocculants, reducing complications caused by metal ions such as Ca^{2+} that are introduced in the CT process. This enables the recycling of the recovered water for upstream applications with reduced water treatment. Although PT requires higher operational and initial costs, some polymer flocculants can dewater tailings more efficiently than inorganic coagulants (Vedoy et al., 2015) (Zhu et al., 2011). Water soluble polymeric flocculants are effective as their degree of hydrophilicity permits them to have an extended conformation (C. Wang et al., 2014), allowing them to adsorb onto the clay surfaces, bringing the solid particles together.

2.2.1 PAM-based flocculants

Polyacrylamide (PAM) is the most commonly used polymeric flocculant for oil sands tailings treatment. PAM gained popularity because its molecular weight and charge density can be modified to suit specific process requirements. Acrylamide (AM) can be polymerized to make PAM, an inexpensive neutral polymer, or it can be copolymerized with other co-monomers to produce anionic or cationic PAM.

The structures of neutral, anionic, and cationic PAM are compared in Figure 2.7 (Vedoy et al., 2015). PAM may be synthesized with molecular weights up to 20 million Daltons. Polymers with high molecular weights are considered to be efficient in flocculating oil sands tailings via the bridging mechanism. However, these high molecular weight PAM flocculants cannot capture some of the fines that remain in the supernatant water, and they tend to retain significant amounts of water in the sediment bed. In spite of this fact, PAM-based flocculants have widespread uses in water treatment, mining industries and paper making (Vedoy et al., 2015).

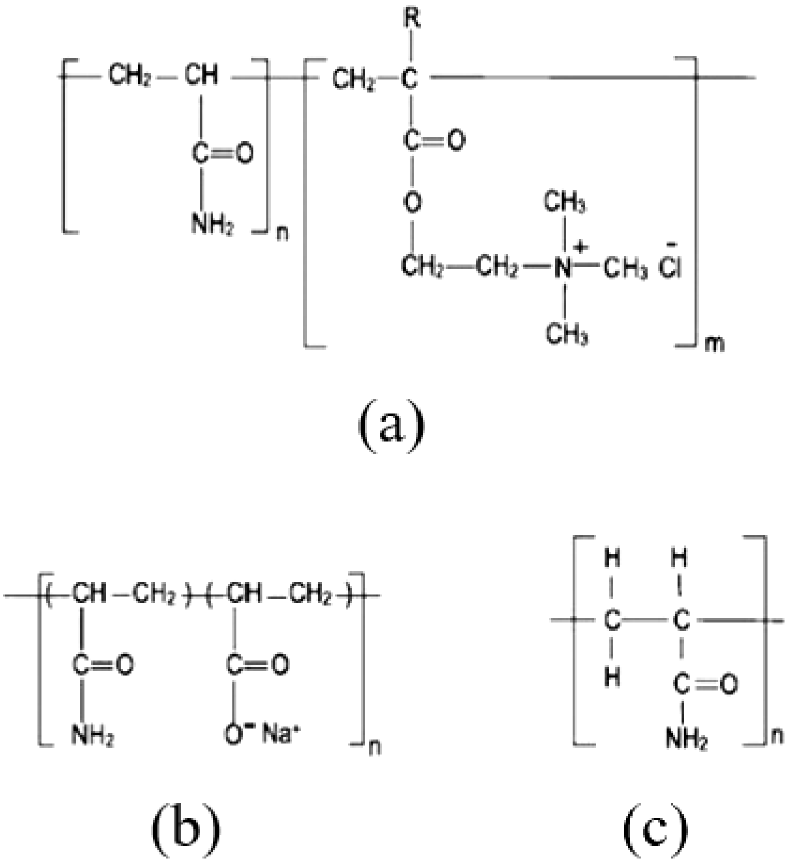

Figure 2.7. PAM molecular structures: a) cationic PAM, b) anionic PAM, c) neutral PAM (adapted from Vedoy et al., 2015).

Charged polymers take a more extended configuration than their neutral counterparts due to the repulsion caused by the charged groups in their backbones (Henderson et al., 1987). This, in principle, conveys an advantage to these polymers, since they “reach out” to more clay particles through the bridging flocculation mechanism. It has been shown that anionic PAM of medium charge density of around 25% is a good flocculant for oil sands tailings (Sworska et al., 2000). The authors tested anionic PAM flocculants under different pH values and concluded that their flocculation performance, to be specific, supernatant turbidity got better with the introduction of divalent cations like Ca^{2+} and Mg^{2+}. The expected behavior of ionic polymers interacting with clays is illustrated in Figure 2.8.

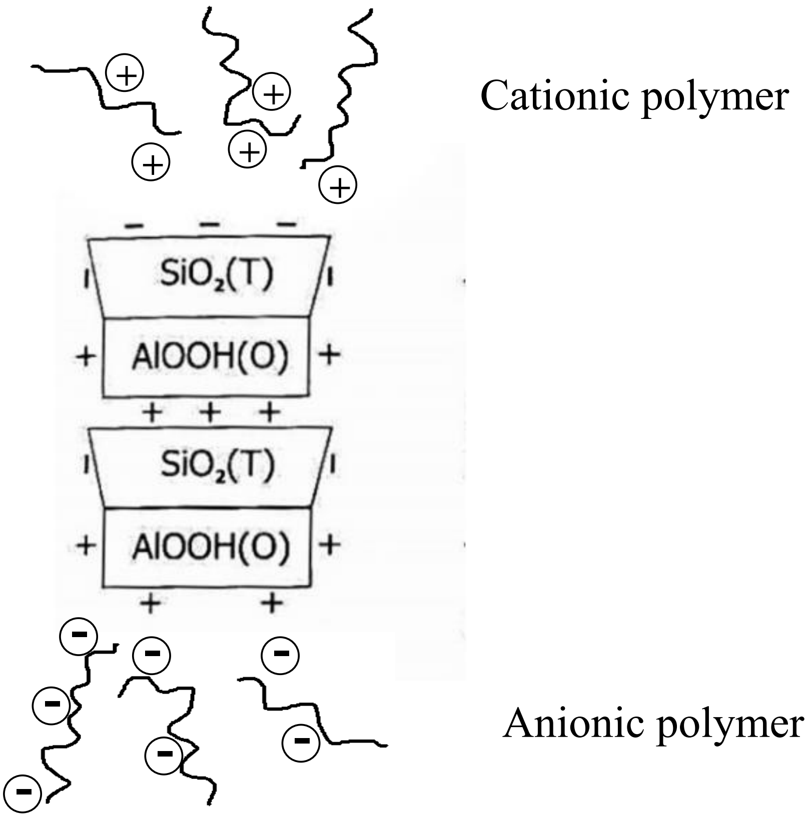

Figure 2.8. Interaction of ionic polymers with kaolinite.

Mpofu et al. (2004) compared anionic PAM with non-ionic poly(ethylene oxide) (PEO) to flocculate smectite clays, and reported that the structure and functionality of the polymers affected the dewatering characteristics of the smectite suspension. PEO produced higher settling rates of greater than 10 m/h at low dosages of 500 ppm compared to PAM, which produced settling rates in the range of 1 m/h to 10 m/h at dosages from 200-1000 ppm. This was due to the negative charges of anionic PAM that mitigates the adsorption on the negative clay surfaces, which form majority of the clay surfaces.

Wang et al. (2010) made cationic Al-PAM flocculants, and showed that these polymers could settle oil sands tailings effectively. They produced a clear supernatant and a filter cake that was strong and supportive enough to be used as reclaimed land. The Al-PAM polymers were also tested as effective filtration aids for tailings flocculation (Alamgir et al., 2012). The mature fine tailings were diluted to 10% solids (by weight), and the filtration studies that were performed showed an increase in dewatering as compared to the undiluted samples. This was due to compensation of the repulsive forces through dilution.

Paste Technology produced good results, such as when high molecular weight anionic PAM is used as flocculant, with some polymers like PEO producing even better results (Mpofu et al., 2004), which stimulated the development of better polymer flocculants, such as smart polymers that respond to a change in stimuli, like temperature and pH, causing them to experience changes in their physical properties. They are labelled as *smart* polymers as they can revert back to their original state on the removal of the stimulus (Ward et al., 2011).

2.2.2 Temperature-sensitive polymers

Temperature-sensitive polymers are those that undergo a transition in their physical properties with a change in temperature. These polymers are capable of switching between hydrophobic and hydrophilic states when temperature is changed. They can be divided into two main categories: upper critical solution temperature (UCST) polymers, and lower critical solution temperature (LCST) polymers. The LCST and UCST phase diagrams are shown in Figure 2.9.

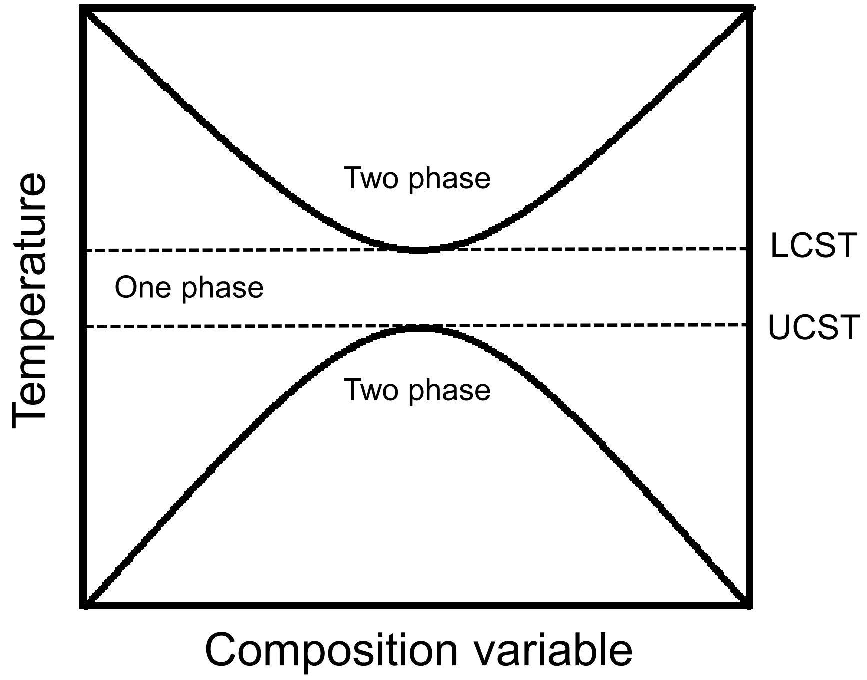

Figure 2.9. Phase diagram depicting LCST and UCST transition.

The phase diagram illustrates the hydrophobic-to-hydrophilic transition, or vice versa, of polymer solutions. The region labelled as “two phase” depicts the region in which the polymer is insoluble in water (hydrophobic), whereas the “one phase” region depicts the region in which the polymer is soluble in water (hydrophilic). With an increase in temperature, a hydrophobic-to-hydrophilic transition takes place at UCST, and with a decrease in temperature, a hydrophobic to hydrophilic transition takes place at LCST (Clark et al., 2012).

The upper critical solution temperature is the temperature above which the polymer transitions from a hydrophobic to a hydrophilic state. On cooling below the UCST, a phase transition takes place during which the entropy of the system reduces as the polymer becomes hydrophobic. Therefore, the driving force for UCST phenomenon is the change in enthalpy. Enthalpy changes are achieved through hydrogen bonding or coulomb interactions, based on which, UCST polymers can be classified in two types: 1) hydrogen bonding upper critical solution temperature (HB-UCST) polymers, and 2) coulomb upper critical solution temperature (C-UCST) polymers.

C-UCST polymers include some zwitterionic polymers and polymeric ionic liquids (Yoshimitsu., 2012). Polymers with tetraflouro borate (BF^{4-}) counter-ions were synthesized using living cationic polymerization. These polymers were found to exhibit UCST behavior. Ionic liquids have interesting interactions with ions that are reflected in their phase transition behaviors.

Among the UCST polymers, the HB-UCST polymers have been studied a little more than C-UCST polymers. Some commercially available HB-UCST polymers are polyethylene oxide (PEO) (Seuring et al., 2012) and poly(vinylmethylether) (Van Durme et al., 2007). Poly(vinylmethylehter) has a sub-zero UCST that may come in handy if freeze-thaw is being employed to dewater tailings. Freeze-thaw technique is a process in which the sample is frozen to convert any of its liquid component to solid, followed by sample trimming and thawing. MFT samples were densified using this technique at Suncor (Proskin et al., 2010) from 35% solids to nearly 50% solids by weight.

Another HB-UCST polymer is poly(acrylic acid). This polymer (and its copolymers) exhibits a change in their UCST behavior with changes in the surrounding ionic concentrations (Buscall et al., 1982). These polymers were studied in the presence of different salts, like sodium chloride, sodium nitrate, and sodium iodide. The shape of the UCST phase diagram changed with salt type and concentrations up to 6 mol/dm^3. The phase separation temperature was found to increase with increase in salt concentration. This plays an important role if used in tailings flocculation, as the ion concentration may never always be constant in the tailings stream from the extraction unit.

Poly(N-acryloylglycinamide) is a UCST polymer which has low transition temperatures in ionic form. The cloud point (transition temperature) upon cooling is around 13 °C, and its cloud point on heating is about 22 °C for a 1% (weight) solution of the polymer in water (Seuring et al., 2012).

Poly(methyl methacrylate) (PMMA) copolymers have been synthesized to tune the UCST behavior in aqueous ethanol solutions (Zhang et al., 2015). These polymers showed a decreased UCST with dilution of the ethanol-water system they were dissolved in.

The UCST behavior of polymer is highly sensitive to environmental factors (Seuring et al., 2012) such as dilution, ion concentration, and polymer-solvent interactions. Seuring et al. have explained this phenomenon based on thermodynamic parameters like interaction parameter which depends on polymer chain connectivity and its concentration. The equation below shows the change in Gibbs free energy for mixing (Kammer et al., 1989),

$$\frac{\Delta \mathrm{G}^{M}}{\mathrm{RT}} = \phi_A \phi_B \mathrm{X} + \left(\frac{\phi_A}{\mathrm{r}_A}\right) \mathrm{In}\ \phi_A + \left(\frac{\phi_B}{\mathrm{r}_B}\right) \mathrm{In}\ \phi_B$$

where ϕ_A and ϕ_B are the volume fractions of individual components, X is the interaction parameter and r_A and r_B are the number of segments in a chain molecule, R is the universal gas constant and T is the absolute temperature.

The interaction parameter X is highly dependent on the size effect that results from difference in sizes of segments. The sizes of segments contribute to a significant change of the Gibbs energy. Keeping this concept in mind, when the concentration of ions change in a polymer solution, the sizes of the segments change. For example, a greater number of like charged ions, causes the polymer coils to become smaller thus reducing the size of segments, resulting in a change of Gibbs free energy, thus causing a shift in the transition temperature. This is probably the reason for the sensitivity of UCST and LCST towards environmental factors

Most of the UCST polymers do not have their transition temperatures in practically relevant conditions (Seuring et al., 2012b). This is probably why LCST polymers have found more applications than UCST polymers. The most commonly used LCST temperature-sensitive polymeric flocculant is poly(N-isopropyl acrylamide), or pNIPAM, which has the structure shown in Figure 2.10.

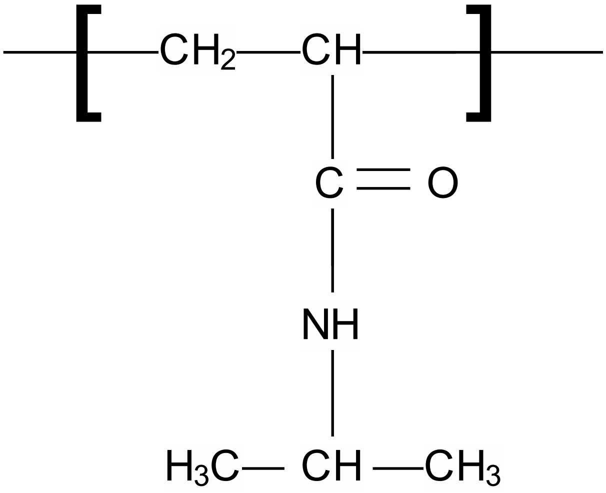

Figure 2.10. Structure of pNIPAM.

Poly(N-isopropyl acrylamide) undergoes a phase transition from hydrophilic to hydrophobic behavior (Meewes et al., 1991; Schild, 1992) at 32 °C. Studies show that using pNIPAM at temperatures above its LCST resulted in good flocculation performances (Long et al., 2011).

Adsorption studies of pNIPAM were performed on alumina and silica surfaces (O'Shea et al., 2010). It was observed that polymer deposition on the particles increased by a considerable margin above its phase transition temperature, indicating that the polymer had higher affinity towards the alumina/silica particles.

In a typical flocculation experiment, pNIPAM is added to the suspension that needs to be flocculated at a temperature below its LCST. This allows for the polymer to dissolve in water and adsorb onto the surfaces of the suspended particles to flocculate them. When the temperature is raised above the LCST, the polymer become hydrophobic, thus separating itself from the aqueous phase, expelling any entrapped water.

The homopolymer pNIPAM is neutral, but anionic or cationic charges may be introduced by copolymerizing it with suitable monomers to alter the flocculating performance of the homopolymer. Copolymers of NIPAM with acrylic acid, N,N-dimethylaminopropyl acrylamide, and N-*tert*-butylacrylamide were used as flocculants for koalinte suspensions to study the advantages of their LCST transition (Sakohara et al., 2013). In addition, their transition temperatures were studied with changes in pH. Cationic and anionic polymers showed opposite trends with pH changes. The copolymers that were tested had their LCST in the range 30 ºC to 45 ºC. However, the LCST of ionic pNIPAM copolymers is higher (20 ºC higher for cationic copolymers) than their nonionic counterparts.

Flocculation studies of oil sands tailings using pNIPAM were found to increase the settling rate by 12 times the initial value on increasing polymer dosages in the range 0 to 400 ppm, with all the tests being performed at a 40 ºC (Long et al., 2011). Under the influence of temperature, it was observed that the dosage had a prominent effect on the settling rate. Another study showed that the settling rates of kaolinite suspensions with pNIPAM were higher at 40 ºC than at room temperature (Li et al., 2007). In addition to better settling rates, an increase in temperature also resulted in better solid compaction and reduced sediment volumes. Comprehensive studies were performed to increase settling rates and reduce sediment volumes by modifying the flocculation procedure. Flocculation of alumina and silica suspensions were performed using pNIPAM at temperatures below and above the LCST (O'Shea et al., 2010). Higher settling rates and reduced solids content in the supernatant were observed when pNIPAM was used at 50 ºC than at room temperature. The solids volume fraction in the sediment bed decreased when the polymer was introduced to the alumina and silica suspensions at room temperature followed by elevating the suspension temperature to 50 ºC. A more compact sediment bed was achieved using the above flocculation template.

For oil sand tailings treatment, the main disadvantage of LCST temperature-sensitive polymers is the need to raise the temperature of the solution above the transition temperature which may incur high costs as large volumes of sludge in tailing ponds are to be heated. One of the alternatives to temperature-sensitive polymers is pH-sensitive polymers. These polymers also undergo a hydrophilic-hydrophobic transition, but the stimulus now is a change in solution pH. These polymer flocculants are described in the next section.

2.2.3 pH-Sensitive polymers

One of the commonly used pH-sensitive polymers is poly(acrylic acid) (PAA) (Dai et al., 2008). The structure of this polymer is shown in Figure 2.11.

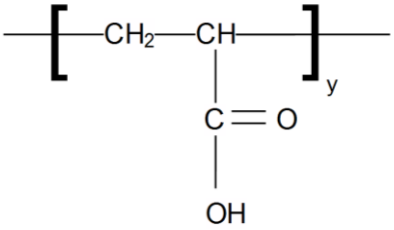

Figure 2.11. Repeating units for poly(acrylic acid).

Copolymerizing PMMA with PAA imparts PMMA with pH sensitive properties (Dai et al., 2008). Dai et al. synthesized copolymers of PMMA and PAA with ethylene oxide, NIPAM and styrene were synthesized using atom transfer radical polymerization (ATRP). Early controlled polymerization techniques include group transfer polymerizations (GTP) that involve stringent reaction conditions limiting their use to some monomers only. With the use of ATRP, the conditions necessary for polymerizations have become milder and less stringent. ATRP aids in the synthesis of polymers of a particular molecular weight. The authors studied the micelle formation of the synthesized polymers with monomer composition and concentration of salt (sodium chloride), acid or base in the environment. These polymers responded to the change in solution pH by changing their morphologies. The lower pH environment favored the formation of sphere formation of the polymer. As the pH was increased, an environment favorable to the formation of rods and vesicles were created.

Poly(acrylic acid) is hydrophobic in acidic pH. As the pH increases, PAA is ionized, turns into a polyelectrolyte, and assumes a completely extended conformation at a pH of 7 (Zhang et al., 1995).

Poly(diethyl aminoethyl methacrylate) (pDEAEMA) is another pH sensitive polymer with a high degree of hydrophobicity. This polymer was synthesized and tested for its pH sensitivity (Han et al., 2012; Hinrichs et al., 1999). The pH sensitivity was confirmed with a reversible volume transition and the reassembly and dissociation of the micelles formed on changing the pH. Due to its high hydrophobic nature, this polymer does not possess temperature dependent phase transition properties. Copolymers of pDEAEMA were studied by (Dai et al., 2008) and exhibited high solubility at low pH due to protonation of the amine groups. However, increasing the pH led to the formation of micelles followed by precipitation at a pH of 7.5.

Similar to pDEAEMA is poly(dimethyl aminoethyl methacrylate), or pDMAEMA, which has the structure shown in Figure 2.12.

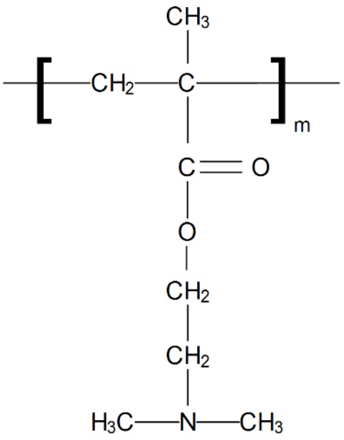

Figure 2.12. Chemical structure of DMAEMA.

The monomer DMAEMA is soluble in water with a pK_a of 8.4, whereas the pK_a of the polymer ranges from 7.4 to 7.8 depending on its molecular weight (Sevimli et al., 2012). At a pH lower than its pK_a, the amine group gets protonated whereas at high pH, above the pK_a of the polymer, the amine group loses its protonation, which is the polymer's response to pH change. Since pDMAEMA is not as hydrophobic as pDEAEMA, it also exhibits temperature sensitive properties.

Poly(dimethyl aminoethyl methacrylate) may be synthesized by free radical polymerization (Bogoeva-Gaceva et al., 1993) or controlled free radical polymerization (Creutz et al., 1997; Oh et al., 1994; Liu et al., 2004). Copolymers of DMAEMA and 2-hydroxyethyl methacrylate (HEMA) were studied for their swelling characteristics, elasticity, temperature and pH sensitive properties (Zırıh et al., 2016). These polymers tend to swell in acidic solutions, and shrink in alkaline solutions. A small decrease in pH from 8 to 7.7 resulted in a drastic increase in swelling volume of the polymer, thereby confirming the pH sensitivity of the polymer. The elastic modulus of the polymer increased slightly with increase in pH in the range of 2 to 7.7, and presented a sharp rise from pH of 7.7 to 8.

Chen et al., (2013) made block copolymers of NIPAM and other monomers, one of which being DMAEMA, via a controlled free radical polymerization techniques, namely reversible addition-fragmentation chain transfer (RAFT) polymerization. Copolymers of NIPAM and DMAEMA were synthesized so as to obtain dual stimulus responsive polymers. It was established earlier that NIPAM is a temperature sensitive polymer. In order to make the polymer responsive to another stimulus, pH, DMAEMA was used as a co-monomer. These block copolymers had narrow molecular weight distributions, defined molecular structures and compositions. The pH sensitivity and self-assembly properties of the synthesized block copolymers were investigated by studying the change in the hydrodynamic radius of the polymer chains. The hydrodynamic radius decreased when the solution pH increased, because increasing pH reduces the protonation of the amine groups in the DMAEMA blocks, thereby lowering the electrostatic repulsion among the polymer chains. Due to the protonation of the amine groups in the DMAEMA blocks at low pH, the LCST of the polymer increased from 33 ºC at pH = 9 to 38.9 ºC at pH = 4. The decrease in LCST is due to deprotonation of the amine group making the polymer less hydrophilic, due to which the transition from a hydrophilic to a hydrophobic state occurs earlier. This depicts the dependency of polymer LCST on the solution pH.

Another study showed similar results, where di-block copolymers of DMAEMA and methyl methacrylate (MMA) having different molecular weights were synthesized using group transfer polymerization (Baines et al., 1996). The effect of polymer composition was tested on solubility and micellization properties of these polymers under different pH conditions. The polymers were found to be soluble at low pH due to the amine group protonation. In addition, the hydrodynamic radius increased with salt addition from 10 nm to 24 nm indicating the sensitivity of these polymers towards the environment.

Oxyanion-initiated polymerization techniques were employed in synthesizing pDMAEMA (Liu et al., 2004). These polymers were studied to understand the effect of molecular weight on aqueous properties and micellization behavior. Critical micelle concentration (CMC) is that concentration of the surfactant (in this case polymer) at which aggregates begin to form. The CMC decreased with an increase in polymer molecular weight. This trend shows that high molecular weight polymers tend to form micelles more easily at alkaline pH (pH was set at 9 for this experiment) conditions. This study also showed the variation of the phase transition temperature (LCST) of the polymer with molecular weight. The LCST of the polymer increased from 14 ºC to 39 ºC when the molecular weight was increased from 1950 to 7660.

Due to their easy synthesis and pH sensitivity, DMAEMA polymers have found a place in many applications. DMAEMA undergoes free radical polymerization at room temperature with low polymerization times. Expensive equipment and reagents are not required for their synthesis, as will be seen in the following chapter. Free radical polymerization has the advantage of synthesizing polymers of high molecular weights at a rapid reaction rate (emulsion polymerization) (Smith et al., 1948).

Polymers of DMAEMA are popularly used in the biomedical field as fluid filled sacs or vesicles (Yan et al., 2011; Liu et al., 2003; Shen et al., 1999). Water soluble polymers or polypeptides are being studied for their pH sensitivity (Checot et al., 2002). Drug delivery, tissue engineering, and gene transport were made easier using copolymers of DMAEMA. The cationic and water soluble nature of pDMAEMA allows for it to be used as carrier systems for DNA delivery (Hinrichs et al., 1999; Cherng et al., 1996; Van De Wetering et al., 1998). The polymer attaches itself to the DNA molecule through electrostatic interactions at low pH. DMAEMA has been studied for its biocompatibility (Chen et al., 1989; Yang et al., 1997). These studies show that DMAEMA is suitable for biomaterial testing in terms of biocompatibility. Tissue engineering saw the rise in use of synthetic polymers due to their ability to not react with enzymes and being tailor made to suit chemical and mechanical requirements (Ward et al., 2011). DMAEMA when copolymerized, with NIPAM for example, possess good mechanical properties (Orakdogen, 2011). These gels were tested for their compressive strength to show that no crack formation was observed till 80% strain. Without diving too deep into the biomedical aspect, it can be understood that the cationic nature of the amine group at low pH is the key to its pH sensitivity.

In addition to the above mentioned applications, pDMAEMA is also used as a flocculant. These polymers aggregate solids in a suspension generally through coagulation and flocculation mechanisms. Parameters like settling rate, turbidity, capillary suction time and resistance to filtration are used to evaluate the performance of the flocculant, which are described in the following chapter. The performance of the flocculant may be dependent on many parameters like temperature, pH of the solution, molecular weight of the polymer among many others.

Changes in pH can be brought about by the introduction of acids like HCl or H_2SO_4. An alternative to this technique is to use CO_2 as the agent to achieve the pH change. Carbon dioxide is an inexpensive side product that may be obtained from the hydrogen generating unit during the reforming of natural gas or methane (Froment, 1989),

$$CH_4 + 2H_2O \leftrightarrow CO_2 + 4H_2$$

When CO_2 dissolves in water it forms a weak acid, as shown below,

$$CO_{2_{gas}} \leftrightarrow CO_{2_{aq}}$$

$$CO_{2_{aq}} + H_2O \xleftrightarrow{room\ temperature} H_2CO_3$$

The acid dissociates in the following two-step process,

$$H_2CO_3 \xleftrightarrow{room\ temperature} HCO_3^- + H^+$$

$$HCO_3^- \xleftrightarrow{room\ temperature} CO_3^{2-} + H^+$$

Lowering the pH of the solution by bubbling CO_2 results in the protonation of the polymer, thus increasing its ionic nature, resulting in an enhanced rate of adsorption of polymers onto the clay surfaces.

The presence of CO_2 has a positive effect on the MFT too. Particle destabilization is required to achieve a good flocculation response from the aid being used (Adin et al., 1998). Destabilization is caused either by using a strongly ionic polymer or by using CO_2. Carbon dioxide by itself can be used to obtain unsegregated tailings (Zhu et al., 2011). Canadian Natural Resources (CNRL) uses this technique by injecting CO_2 into the pipelines that are used to transport tailings (Zhu et al., 2011). This causes the CO_2 to mix with tailings which helps in their treatment. However, a high dosage of CO_2 in the system does not improve the settling rate of the sediments. The presence of a large number of CO_2 bubbles in the system hinders the settling of the flocs (Scardina et al., 1999). One must, therefore, operate in the range of CO_2 levels such that it does not appear in excess.

Guo used DMAEMA-based copolymers as flocculants (Guo, 2015) for model tailings (kaolinite suspensions) to determine how changes in pH affected solids content and mechanical properties (such as yield stress) of the sediments. It was determined that increase in polymer dosage improved the settling rate of model tailings. The optimum polymer dosage among the various dosages used for the best turbidity measurements was found to be 2 kg/ton of the polymer solution. The copolymers generated more compact sediments at pH = 6.8 than at pH = 8.2. It was thus concluded that the pH sensitive polymers produced more compact beds at lower pH.

Dimethyl aminoethyl methacrylate also found applications in the pulp and paper industry when copolymerized with biodegradable polymers like cellulose (Parviainen et al., 2014). Copolymers of DMAEMA and cellulose were synthesized for this purpose and were tested with kaolin and kaolin-pulp suspensions. Cationicity was achieved by quartenizing the amine group using iodomethane and sodium chloride. The performance of these polymers was compared to commercial cationic PAM. The cationic grafted copolymers had similar flocculation performance as compared to the commercial PAM flocculants in terms of supernatant turbidity.

The recycled water obtained from the oil sands tailings using pH sensitive flocculants may have an adverse effect on the bitumen liberation if the pH change is brought about using diluted mineral acids that introduces ions (like Cl^-, SO_4^{2-}) into the system. The ions introduced by bubbling the solution with CO_2 are in equilibrium and their concentration can be easily controlled. If needed, the CO_2 dissolved in the system can be removed by simply bubbling the solution with an inert gas.

The selection of the monomer DMAEMA was done keeping in mind the conditions under which the polymer undergoes a change in pH. MFT has a pH range from 8.3 to 9. The monomer DMAEMA is soluble in water at low pH of around 5 and becomes insoluble at higher pH (beyond its pK_a value) as mentioned earlier in this chapter. Carbon dioxide, which is used to lower the solution pH, will slowly escape from solution into the atmosphere. Therefore, as time passes, the concentration CO_2 dissolved in the system would decrease, thereby increasing the solution pH. In this case, it is advantageous to use a pH-sensitive polymer that is insoluble in water at high pH, since the water molecules trapped within the flocs will be expelled as the polymer separates from the aqueous solution due to hydrophobicity.

The usage of inorganic ions such as Ca^{2+} (Consolidated Tailings process) to generate a good flocculation performance has been heavily relied upon. This study encourages achieving good flocculation parameters, without the use of inorganic ions, by exploiting the pH sensitivity of DMAEMA in the field of oil sands tailings. Further, this study throws light on the performance of homopolymers, copolymers and polymer blends to produce the best flocculation of MFT amongst each other.

3. MATERIALS AND METHODOLOGY

3.1 Materials

All chemical compounds used to synthesize the polymer flocculants were purchased from Sigma Aldrich: N,N-dimethylaminoethyl methacrylate (DMAEMA) (98%), N-isopropyl acrylamide (NIPAM) (97%), N,N,N',N'-tetramethyl ethylene diamine (TMEDA) (99%), ammonium persulphate (APS) (>98%), isopropyl alcohol, and hexane (mixture of isomers). Mature fine tailings (MFT) were obtained from Coanda Research and Development Corporation. Nitrogen and CO_2 were procured from Praxair, Inc.

3.2 Methodology

3.2.1 Polymer synthesis

Polymers were made by free radical polymerization under different conditions to obtain distinct weight average molecular weights (M_w) and chemical compositions. Based on the monomer used, the polymers are classified into three families: NIPAM homopolymers, DMAEMA homopolymers and NIPAM-DMAEMA copolymers. The polymer molecular weights were controlled by varying the concentration of initiator (APS), and the copolymer compositions by changing the mass ratio of the two comonomers in the feed. As the polymer synthesis was performed using trial and error methods in order to achieve the desired molecular weight, the TEMED and APS molar ratio was altered accordingly, and hence these quantities do not have a set trend with polymer molecular weight (M_w).

Synthesis of pDMAEMA homopolymers

The reactor used for polymer synthesis is shown in Figure 3.1. It consists of a round bottom 250 mL glass flask with three necks. The middle neck was used to inject reagents into the reactor, whereas the outer necks were used as N_2 inlet and outlet. The reactor was washed and rinsed with distilled water and dried overnight prior to being used for polymer synthesis.

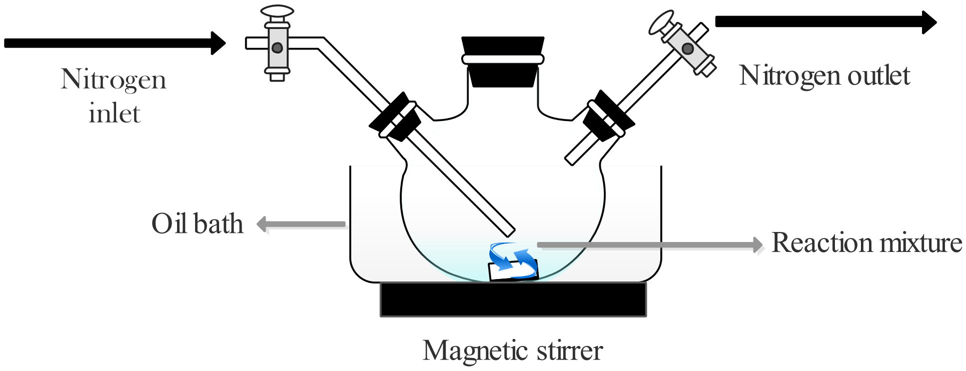

Figure 3.1. Glass reactor used for polymer synthesis.

Appropriate proportions of DMAEMA, deionized water, and TEMED, as depicted in Table 3.1, were added to the glass reactor setup shown in Figure 3.1, to obtain homopolymers of different molecular weight.

Table 3.1. Feed composition for pDMAEMA synthesis.

	pD-0.37	**pD-0.43**	**pD-0.64**	**pD-0.95**
DMAEMA (moles)	0.254	0.254	0.254	0.254
Water (moles)	2.22	2.22	2.22	2.22
TEMED (moles)	6.7×10^{-6}	3.2×10^{-6}	2.5×10^{-6}	1.6×10^{-6}
APS (moles)	440×10^{-6}	165×10^{-6}	220×10^{-6}	110×10^{-6}

Once the reagents were transferred into the reactor, the flask was sealed using rubber stoppers and placed in an oil bath at room temperature (23 ºC). The mixing speed was kept at 350 rpm and the solution was bubbled with nitrogen for 40 minutes to make the system inert. The appropriate quantity of APS initiator was injected to the reaction mixture after 40 minutes of N_2 purge through the rubber cork in the middle neck, and N_2 continued to be bubbled for 5 more minutes before its supply was stopped. The polymerization was then allowed to proceed for 24 hours, after which the polymerization was stopped by placing the reactor in an ice bath and simultaneously bubbling the reaction mixture with air to oxidize any remaining free radicals. The setup was then left aside for half an hour, after which the polymer precipitation procedures were initiated.

Synthesis of pNIPAM homopolymers

The same procedure described above was repeated to make pNIPAM homopolymers, replacing DMAEMA with NIPAM. The proportions of the reagents used are displayed in Table 3.2.

Table 3.2. Feed composition for pNIPAM synthesis.

	pN-1.27	**pN-1.85**	**pN-1.90**	**pN-2.07**	**pN-2.16**	**pN-2.57**
NIPAM (moles)	0.0221	0.0221	0.0442	0.0221	0.0221	0.0442
Water (moles)	1.11	1.11	1.11	1.11	1.11	1.11
TEMED (moles)	1.64×10^{-6}	0.85×10^{-6}	1.64×10^{-6}	0.85×10^{-6}	0.85×10^{-6}	1.64×10^{-6}
APS (moles)	110×10^{-6}	55×10^{-6}	110×10^{-6}	82.7×10^{-6}	27.5×10^{-6}	49.6×10^{-6}

Synthesis of p(NIPAM-co-DMAEMA) copolymers

The procedure employed for DMAEMA homopolymers was followed to make NIPAM/DMAEMA copolymers, with minor altercations. The net mass of monomers was kept constant and equal to 10 g, with the relative proportion of comonomers varying to achieve a mass ratios of 1:2, 1:1, and 2:1. The quantities of the reagents for each trial are shown in Table 3.3.

Table 3.3. Reagent quantities for p(NIPAM- *co*-DMAEMA) synthesis.

	pN1D2-0.97	**pN1D2-0.28**	**pN1D2-0.67**	**pN1D2-0.69**	**pN1D2-1.38**	**pN1D1-1.02**	**pN2D1-0.583**
NIPAM (moles)	0.0294	0.0294	0.0294	0.0294	0.0294	0.0442	0.0589
DMAEMA (moles)	0.0424	0.0424	0.0424	0.0424	0.0424	0.0318	0.0211
Water (moles)	2.22	2.22	2.22	2.22	2.22	2.22	2.22
TEMED (moles)	1.64×10^{-6}	6.68×10^{-6}	1.64×10^{-6}	3.34×10^{-6}	1.64×10^{-6}	3.2×10^{-6}	3.2×10^{-6}
APS (moles)	82.7×10^{-6}	330.8×10^{-6}	82.7×10^{-6}	220×10^{-6}	110×10^{-6}	31.8×10^{-6}	31.8×10^{-6}

3.2.2 Polymer purification

All homo- and copolymer solutions of DMAEMA made in the reactor were first dissolved in isopropyl alcohol, and then precipitated in excess n-hexane (1:10 volumetric ratio). The organic solvent was decanted. The obtained polymer was filtered through Whatman grade 1 filter paper, and dried in vacuum of 30 mm Hg at 40 °C for 24 hours. The dried polymers were once again washed in n-hexane to remove traces of impurities, and vacuum dried once again.

Homopolymers of NIPAM were directly precipitated in isopropyl alcohol, filtered using Whatman grade 1 filter paper, and dried in a vacuum of 30 mm Hg at 40 ºC for 24 hours.

3.2.3 Polymer characterization

Gel permeation chromatography (GPC)

The polymer molecular weight distributions were measured using a GPC unit (Agilent Technologies 1260 Infinity series) using triple detection by viscosity, refractive index, and light scattering. Two Tosoh columns (TKS gel G6000PW XL-CP 8.8 mm ID x 30 cm, 13 μm) were used, together with a guard column (Tosoh PW XL_CP 5 mm ID x 4 cm). Universal calibration method was used to calibrate the system. The polymer sample was dissolved in the solvent same as mobile phase (0.2 M sodium nitrate aqueous solution with pH of 4). Mobile phase of low pH was chosen as the polymer was more soluble at this condition. Sample polymer solutions of 4 mg/mL were stirred for at least 24 hours to ensure proper dissolution, and a volume of 100 μL was injected in the GPC columns with a flow rate of 1 ml/min at an analysis temperature of 30 ºC.

Fourier-transform infrared spectroscopy (FTIR)

Fourier-transform infrared spectroscopy was used to determine the presence of functional groups on the synthesized polymers (Agilent Cary 600 series). The sample was analyzed using the attenuated total reflection (ATR) mode on a PIKE Technologies GladiATR setup. The samples were scanned with the number of runs set at 16. Wavenumbers of the range 400 cm^{-1} to 4000 cm^{-1} were employed.

Zeta potential

Zeta potential of the polymers before and after the pH change was determined using a Malvern Zetasizer (Nanoseries Nano-ZS). The polymer solutions were all made of the same concentration of 15 mg/mL in deionized water. The zeta potentials were measured at 25 ºC.

3.2.4 Preparation of polymer solution for flocculation

A 15 mg/mL (1.5 wt%)solution of polymer in deionized water was prepared by taking suitable quantity of polymer and deionized water and was mixed for at least 12 hours to ensure homogeneity.

3.2.5 Characterization of mature fine tailings

Dean-Stark analysis

Dean-Stark analysis was performed to determine water, solids and bitumen composition of MFT (Veillet et al., 2010). The equipment setup is shown in Figure 3.2.

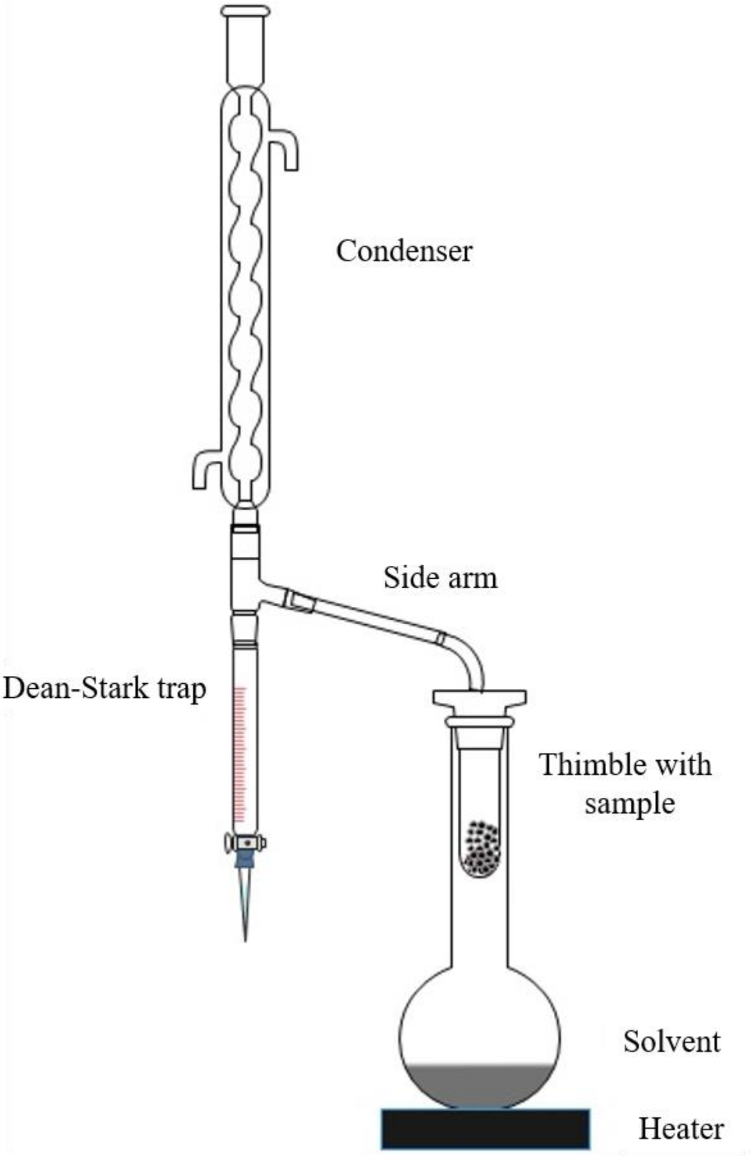

Figure 3.2. Schematic diagram of Dean-Stark apparatus.

The round bottom flask is placed on a heater and filled with toluene, which is used for bitumen extraction. A condenser is provided to recover the volatile material, which is collected in a Dean-Stark trap, where the condensed liquid separates into a layer of water and another of toluene. The side arm of the trap is attached to an arrangement that holds the sample.

Approximately 120 g of the sample is placed in the thimble which is suspended from the lower arm of the trap into the glass cylinder. The round bottom flask is heated, generating vapors of water and toluene. The water collects at the bottom of the trap, and is periodically transferred into a measuring cylinder to determine the volume of water collected. Toluene, which forms the upper layer, flows down the side arm and into the thimble to dissolve the bitumen in the oil sands tailings sample. The bitumen-rich toluene flows to the bottom of the apparatus into the toluene filled round bottom flask. This cycle is repeated for 12 to 14 hours, after which majority of the bitumen is recovered from the oil sands tailings sample.

The thimble is weighed before and after the Dean-Stark analysis to determine the solids content of the sample. The water collected is weighed to give the water composition and the mass of bitumen is determined by vaporizing the toluene from the toluene bitumen solution.

Moisture Analysis

The MFT sample was analyzed for its water and solids composition using a moisture analyzer MB45 Moisture Analyzer. As the human error in calculating the solid composition was lesser compared to the Dean-Stark analysis, the solid compositions from the moisture analyzer were used for calculations.

Atomic Absorption Spectroscopy (AAS)

Atomic absorption spectroscopy was used to detect the concentration of metal ions in the mature fine tailings sample. The instrument used was VARIAN 220 FS atomic absorption spectrophotometer with air-acetylene flame for the detection of sodium, potassium, magnesium and calcium. A hollow cathode lamp was used as a light source for each element.

3.2.6 Flocculation studies

The MFT flocculation performance of the polymers made in this investigation was studied by comparing initial settling rate, turbidity, and capillary suction time. The experiments for each polymer, for each dosage, and for each parameter were performed three times to check for consistency.

Preparation of MFT suspensions

Mature fine tailings suspensions for the flocculation studies were prepared by diluting them from 35.35% solids to 5% solids using deionized water.

Polymer dosage

The polymer dosage was expressed based on the solids content of the MFT sample. The weight of the polymer required for each dosage is tabulated in Table 3.4.

Table 3.4. Polymer dosages for copolymers and pDMAEMA homopolymers.

Dosage (ppm)	Mass of polymer (mg)	Volume of polymer solution (mL)
2000	10	0.67
4000	20	1.33
6000	30	2.00
8000	40	2.67
10000	50	3.33

The mass of polymers required for each dosage were calculated as follows. Consider a polymer dosage of 2000 ppm (~2000 g/t) for 100 g of diluted MFT (5% by weight) sample,

$$2000 \times 10^{-6} = \frac{mass\ of\ polymer\ (g)}{5\ g\ of\ MFT\ solids}$$

$$mass\ of\ polymer = 10^{-2}\ g\ of\ polymer = 10\ mg\ polymer$$

Polymer solutions were prepared in concentrations of 15 mg/ml. Hence, the volume of polymer solution required to obtain 2000 ppm of polymer is:

$$15\frac{mg}{ml} = \frac{10\,mg}{V\,ml}$$

$$V = 0.666\,mL = 666.67\ \mu L$$

The flocculation studies for pNIPAM homopolymers were performed at dosages from 500 to 2000 ppm, as preliminary tests have shown poor flocculation performance for these polymers at dosages higher than 2000 ppm. These values are tabulated in Table 3.5.

Table 3.5. Polymer dosages for pNIPAM homopolymers.

Dosage (ppm)	**Weight of polymer (mg)**	**Volume of polymer solution (µL)**
500	2.50	166.67
750	3.75	250.00
1000	5.00	333.33
1500	7.50	500.00
2000	10.00	666.67

Mixing parameters

Agitation of the polymer-MFT mixture is an important parameter that enables polymer adsorption on the surface of the MFT solids. Mixing conditions similar to those used in literature were employed for this work (Reis et al., 2016). The mixing conditions that were employed (immediately after injecting the polymer) were 600 rpm for 2 minutes, followed by 8 minutes of mixing at 290 rpm. A propeller shape three-blade impeller (5 cm diameter) fixed to a digital mixer (Vajihinejad et al., 2017)and used for this work as shown in Figure 3.3.

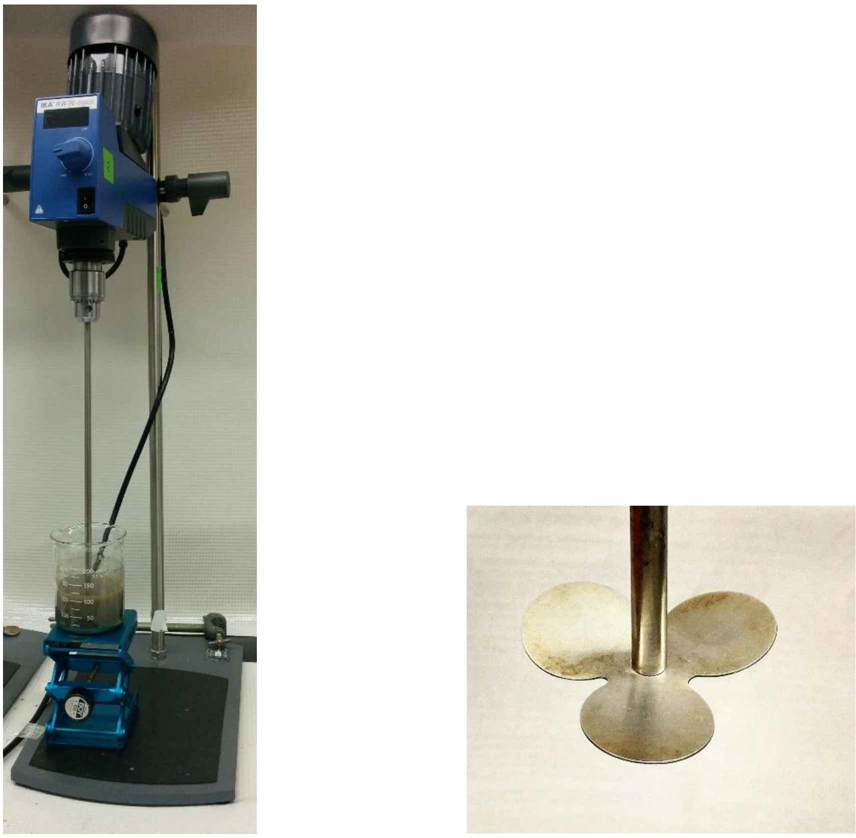

Figure 3.3. Digital mixer and impeller used for flocculation.

Carbon dioxide introduction

The pH of the 5% by weight MFT solution was determined to be in the range of 7.2-7.8. Four different CO_2 introduction strategies where compared, with the pH being lowered to about 5, as illustrated in Figure 3.4.

In the first case, no CO_2 was added to the system. This case was used as a blank experiment to quantify the effect of CO_2 addition on flocculation performance. The polymer was added directly to the 5% by weight MFT suspension and mixed under the condition described earlier. As pNIPAM is not sensitive to pH changes, NIPAM homopolymers were tested for this case only.

In the second case, the polymer (DMAEMA homo- and co-polymers) solution was initially bubbled with CO_2 until the solution was saturated (approximately 30 minutes). Once the polymer solution was saturated with CO_2, the same procedure described for Case 1 above was followed.

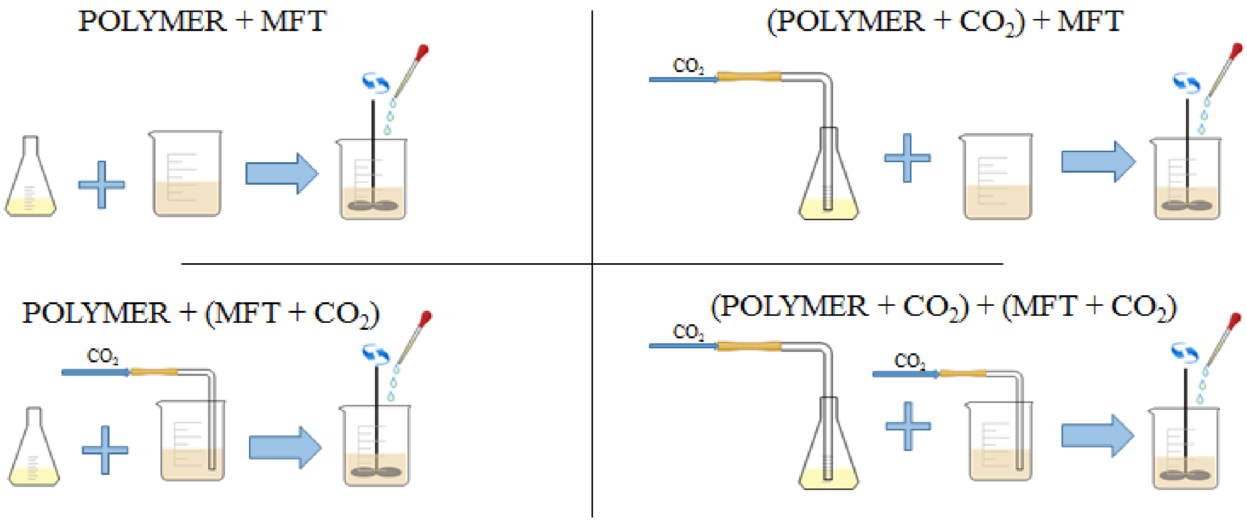

Figure 3.4. CO_2 introduction strategies P + MFT, (P+CO_2) + MFT, P + (MFT+ CO_2) and (P+ CO_2) + (MFT+ CO_2) in a clockwise manner.

In the third case, CO_2 was bubbled into the MFT suspension for 15 minutes to ensure saturation with CO_2, prior to polymer addition. Then, the polymer solution was mixed with the CO_2-saturated MFT suspension.

Finally, in the fourth case, CO_2 was bubble in both polymer solution and 5% MFT suspension before they were mixed.

Two controls were used in the study: 1) 5% by weight MFT suspension untreated with CO_2 or polymer, and 2) 5% by weight MFT suspension treated with only CO_2. These control experiments were done to isolate the effect brought about by the polymer on the flocculation performance.

Initial settling rate (ISR)

The settling rate was determined by the measuring the rate of descent of the solid-liquid interface (mudline). The mudline height was recorded every 30 seconds for the first 7 minutes, and then recorded every 1 minute over a 25 minute period. The ISR was determined by plotting a tangent on the settling curve for the first 10 minutes, and hence noting down readings beyond 25 minutes would be redundant. The data was then plotted as h/H versus time where h is the height of the mudline, and H is the total height of the MFT solution at the beginning of the flocculation experiment. Finally, the ISR is calculated in meters/hour (m/h) as,

$$ISR = slope \text{ x } H$$

where the slope of the h/H x t curve was calculated using the points collected for the first 10 minutes of flocculation.

Turbidity

Turbidity measurements determine the efficacy of the polymer in producing a supernatant with a maximum water clarity. Turbidity measurements of the supernatant were recorded after 24 hours from the start of each settling test, by pipetting roughly 35-50 ml from the supernatant present in the measuring cylinders, as shown in Figure 3.5.

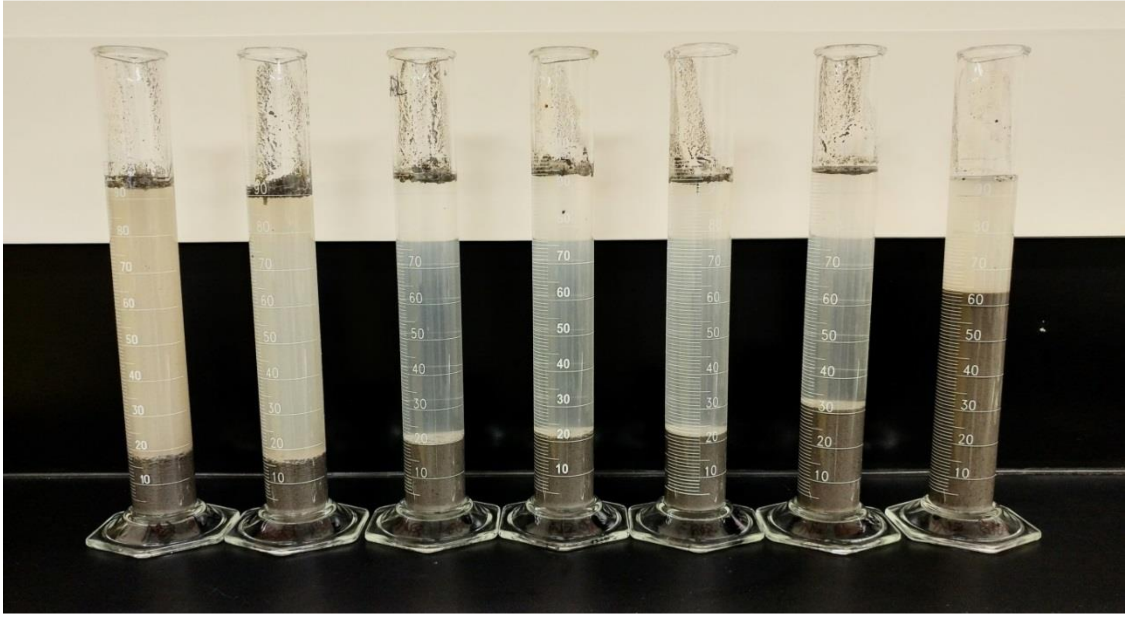

Figure 3.5. Samples for turbidity measurements.

Turbidity measurements were performed using 2100 AN turbidimeter from Hach. The functioning of a turbidimeter, or a nephlometer, is based on the principle of light scattering. As shown in Figure 3.6 (Hach Company, 2012a), light from an LED source flashes on the sample placed in the sample cell.

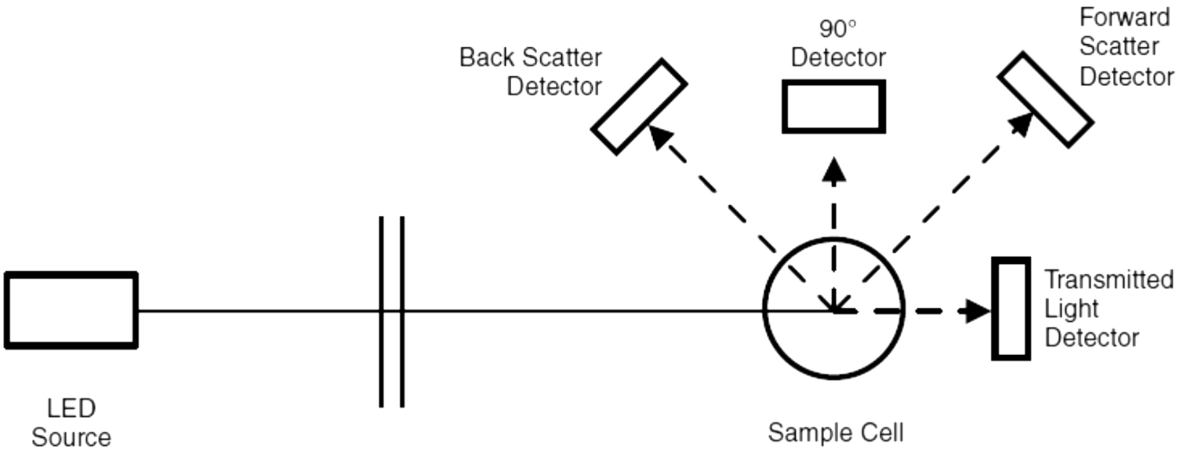

Figure 3.6. Schematic of the internals of a turbidimeter (adapted from Hach Company, 2012).

The scattered light is collected at a 90° detector, a back scatter detector, and a forward scatter detector. The remaining unscattered light is detected at the transmitted light detector. The turbidity of the samples are plotted to obtain a graph of turbidity versus dosage.

Capillary suction time

Capillary suction time (CST) determines how fast a sample can be dewatered. Measurement of capillary suction time is an important parameter in determining the sludge characteristics (Smollen, 1986; Sawalha et al., 2010).The equipment used for CST measurements was a Triton Type 319 Multi CST which is shown in Figure 3.7.

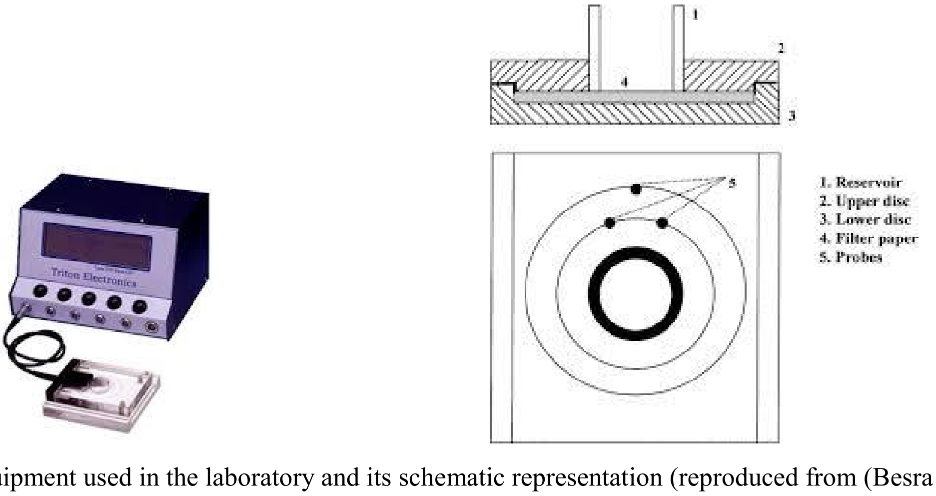

Figure 3.7. CST equipment used in the laboratory and its schematic representation (reproduced from (Besra et al., 2005) and http://www.tritonel.com/product/type-319-multi-purpose-cst_2/).

It consists of a unit, fitted with a screen, to which are attached five probes. Each node comprises of an assembly of a lower and upper disc at the center of which, rests a reservoir. The upper disc has a circular opening in which rests the cylindrical vessel, the reservoir. The reservoir holds the sample which is to be analyzed. The upper disc comprises of two concentric circular grooves fitted with sensors. The lower disc holds the absorbent filter paper on which the water from the sample spreads uniformly. The time taken by the water to reach the outer sensor from the inner is reported as the CST of the sample.

The CST of the samples at the very start of the settling test (just after agitating the mixture) and that of the sediment bed formed after a period of 24 hours, were recorded. These two parameters help in determining the dewatering characteristic of the sample and its change with time. A high CST indicates a sludge with inferior characteristics (Smollen, 1986).

4. RESULTS AND DISCUSSION

4.1 Polymer Characterization

Figure 4.1 shows how the zeta potential, changes when CO_2 was added to the aqueous solutions of cationic polymers (DMAEMA homo- and copolymers). The more positive the zeta potential, the greater is the cationicity of the polymer solution. The pH decreases with CO_2 addition, and the zeta potentials of the polymer solutions increase, indicating that the polymer chains became positively charged due to the protonation of the tertiary amide groups of the DMAEMA units.

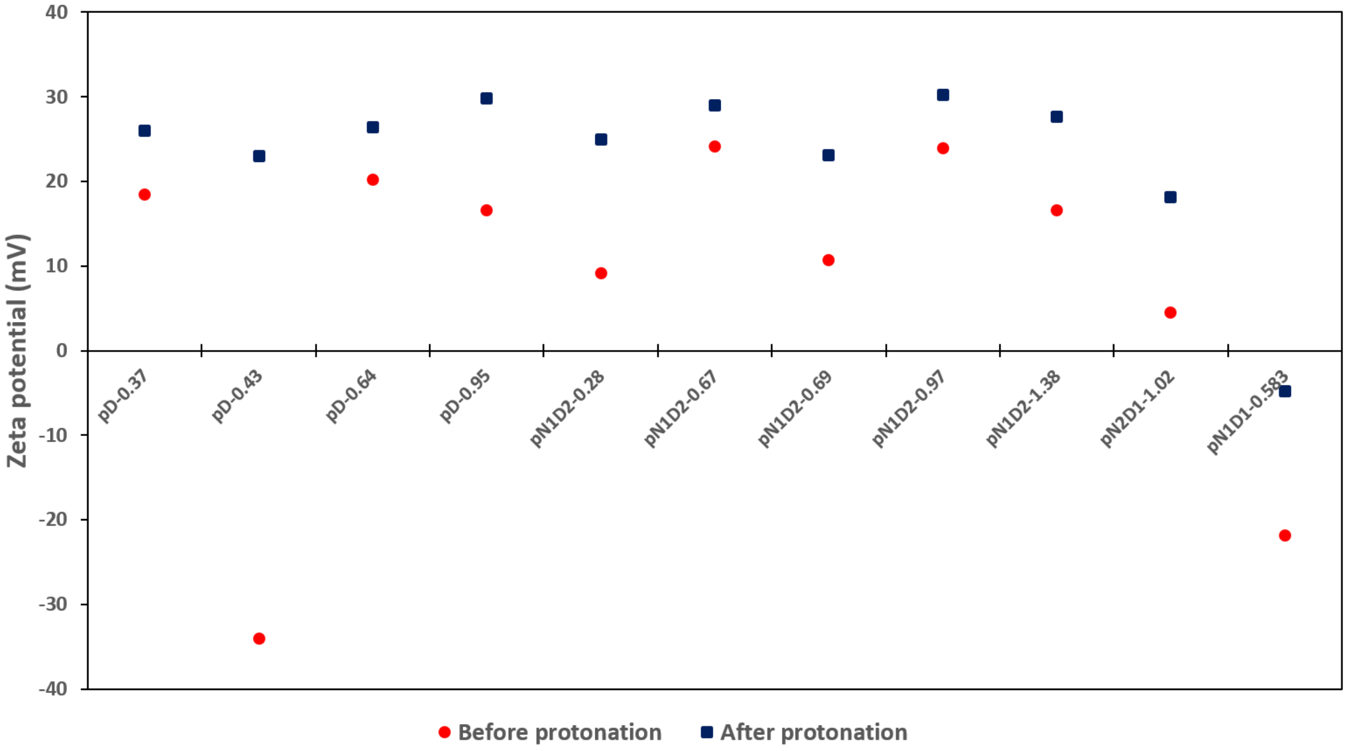

Figure 4.1. Zeta potential measurements of the cationic polymers before and after CO_2 introduction.

It was observed that the zeta potential remains approximately constant after protonation for most polymers. A near constant zeta potential is expected because the concentrations of the polymer solutions were kept very low (15 mg/mL); therefore, the concentration of CO_2 in all polymer solutions was about the same (determined by the solubility of CO_2 in pure water), causing the zeta potential to remain approximately the same. From the data presented in Figure 4.1, no definite trend relating polymer type or molecular weight to zeta potential was observed.

The weight average molecular weight (M_w) and comonomer percentages of the four types of polymers investigated in this thesis are listed in Table 4.1.

Table 4.1. Polymer weight average molecular weights and feed comonomer percentages.

Polymer	Comonomer percentage (weight %)		M_w (Daltons)	PDI
	NIPAM	DMAEMA		
pN-1.27	100	0	1,270,510	1.7
pN-1.85	100	0	1,848,000	1.5
pN-1.90	100	0	1,900,000	1.4
pN-2.07	100	0	2,067,000	1.5
pN-2.16	100	0	2,160,000	1.3
pN-2.57	100	0	2,565,000	1.5
pD-0.37	0	100	370,000	2.8
pD-0.43	0	100	428,758	1.7
pD-0.64	0	100	638,000	3.0
pD-0.95	0	100	950,000	2.2
pN1D2-0.28[+]	33.33	66.67	276,944	2.8
pN1D2-0.67[+]	33.33	66.67	671,585	2.3
pN1D2-0.69[+]	33.33	66.67	689,262	2.2
pN1D2-0.97[+]	33.33	66.67	972,825	1.6
pN1D2-1.38[+]	33.33	66.67	1,377,714	1.9
pN1D1-1.03[+]	50	50	583,039	1.4
pN2D1-0.58[+]	66.67	33.33	1,853,043	1.5

[+] p(NIPAM-*co*-DMAEMA)

The FTIR spectra of DMAEMA and NIPAM copolymers have been reported in literature (Meléndez-Ortiz et al., 2008), and the main peak assignments are listed in Table 4.2.

Table 4.2. Characteristic wavelengths of the functional groups in DMAEMA and NIPAM.

Functional group	Wavenumber (cm^{-1})
C-COO- group in DMAEMA	1157
C=O bond in DMAEMA	1715
-CH$_2$ asymmetrical stretching in DMAEMA	2825
–CH$_2$ symmetrical stretching of in DMAEMA	2920
C=O bond of the amide group in NIPAM	1655
N-H group stretching vibration in NIPAM	3271
N-H group bending vibration in NIPAM	1541

The FTIR spectrum of pN1D1-1.03 is shown in Figure 4.2, which is representative of the spectra of the other NIPAM-DMAEMA copolymers. The presence of DMAEMA and NIPAM groups in the copolymer is confirmed by the peaks depicted at 1643 cm^{-1} for carbonyl stretching, at 3284 cm^{-1} for the stretching vibration of the N-H group, at 1535 cm^{-1} for the bending vibration of the N-H group of NIPAM, and at 1149 cm^{-1} and 1726 cm^{-1} for the carboxyl and carbonyl groups of DMAEMA, respectively. Symmetrical and asymmetrical stretching of –CH$_2$ groups of DMAEMA were observed at 2970 cm^{-1} and 2821 cm^{-1}, respectively.

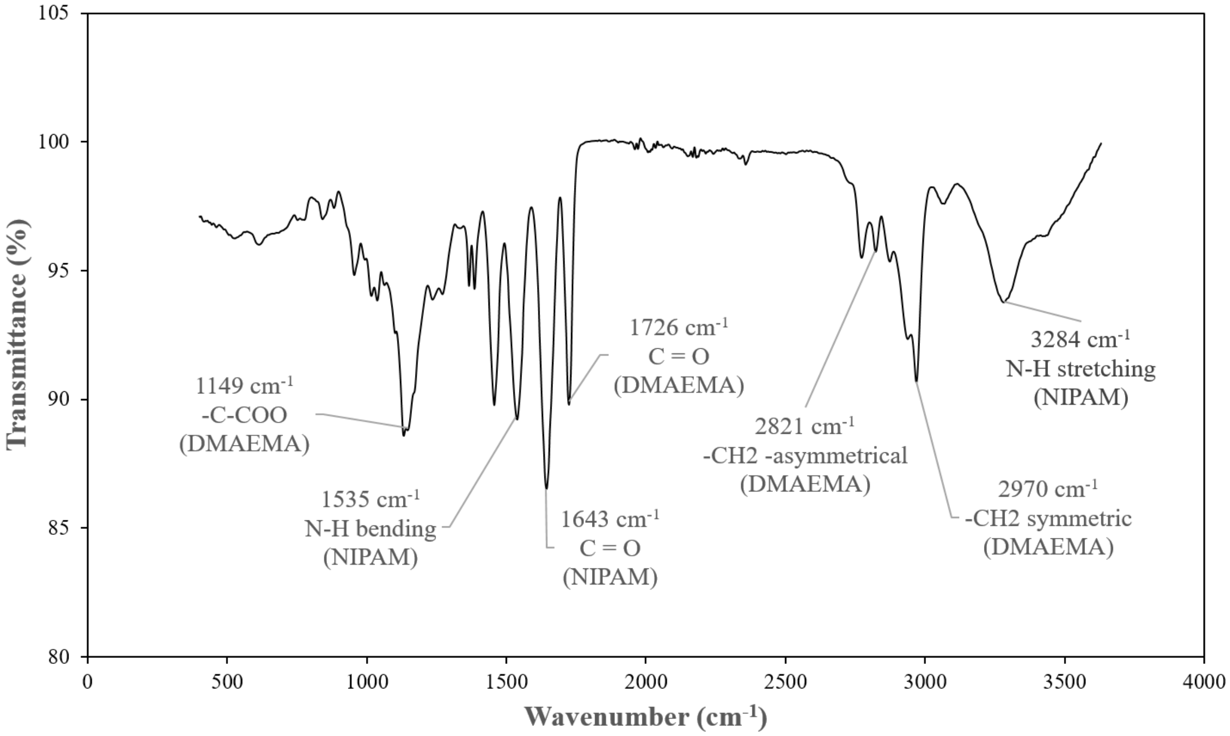

Figure 4.2. FTIR spectrum of pN1D1-1.03.

The FTIR spectrum of the pDMAEMA homopolymer pD-0.43 is shown in Figure 4.3. The spectra of the other DMAEMA homopolymers are similar to the one shown in Figure 4.3. Characteristic bands at 1144 cm^{-1} and 1726 cm^{-1} for the carboxyl and carbonyl groups of DMAEMA respectively, were observed. Symmetrical and asymmetrical stretching of $–CH_2$ groups were observed at 2937 cm^{-1} and 2821 cm^{-1} respectively.

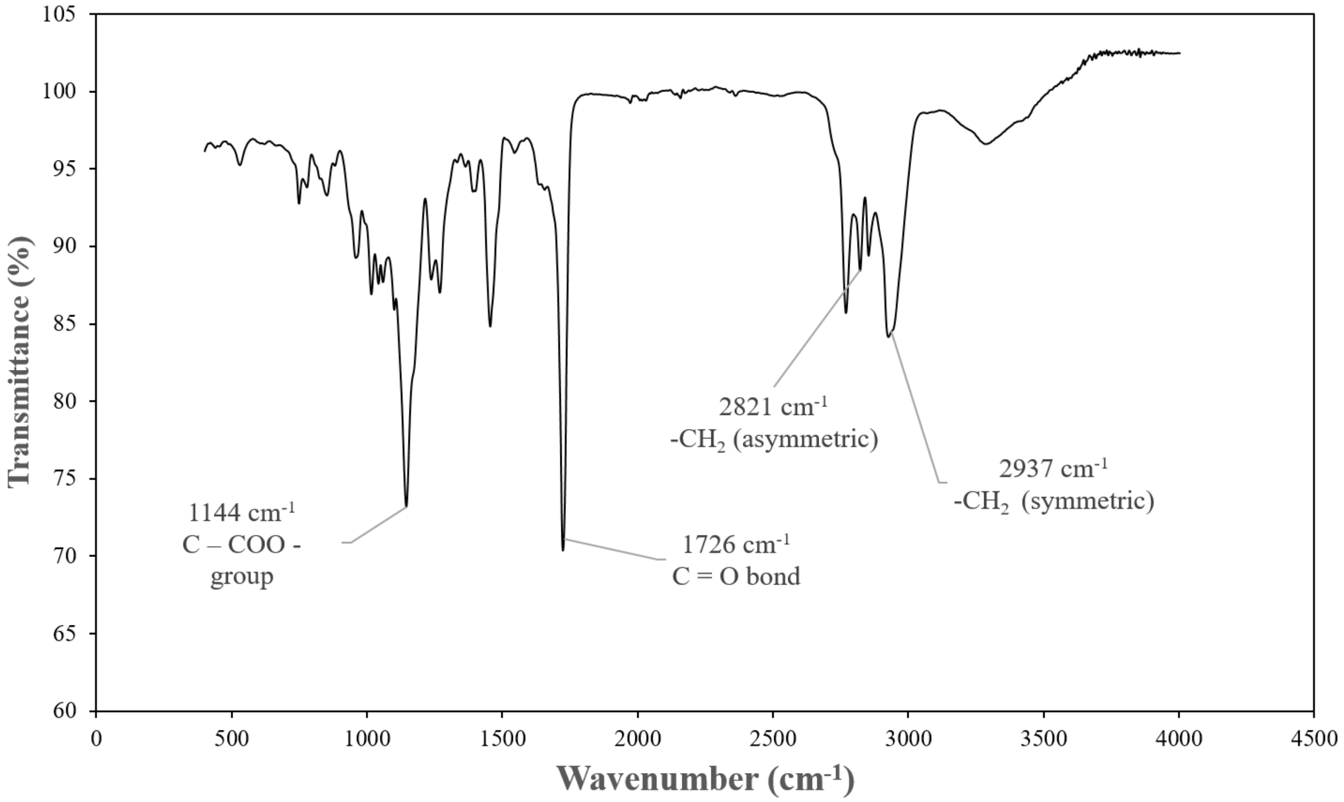

Figure 4.3. FTIR spectrum of pD-0.43.

The FTIR spectrum of the pNIPAM homopolymer pN-1.9 is shown in Figure 4.4, and it is representative of the spectra of the other NIPAM homopolymers. Characteristic bands at 1635 cm^{-1} for C = O bond of the amide group was observed. Stretching and bending vibrations of N-H group was observed at 3290 cm^{-1} and 1527 cm^{-1} respectively.

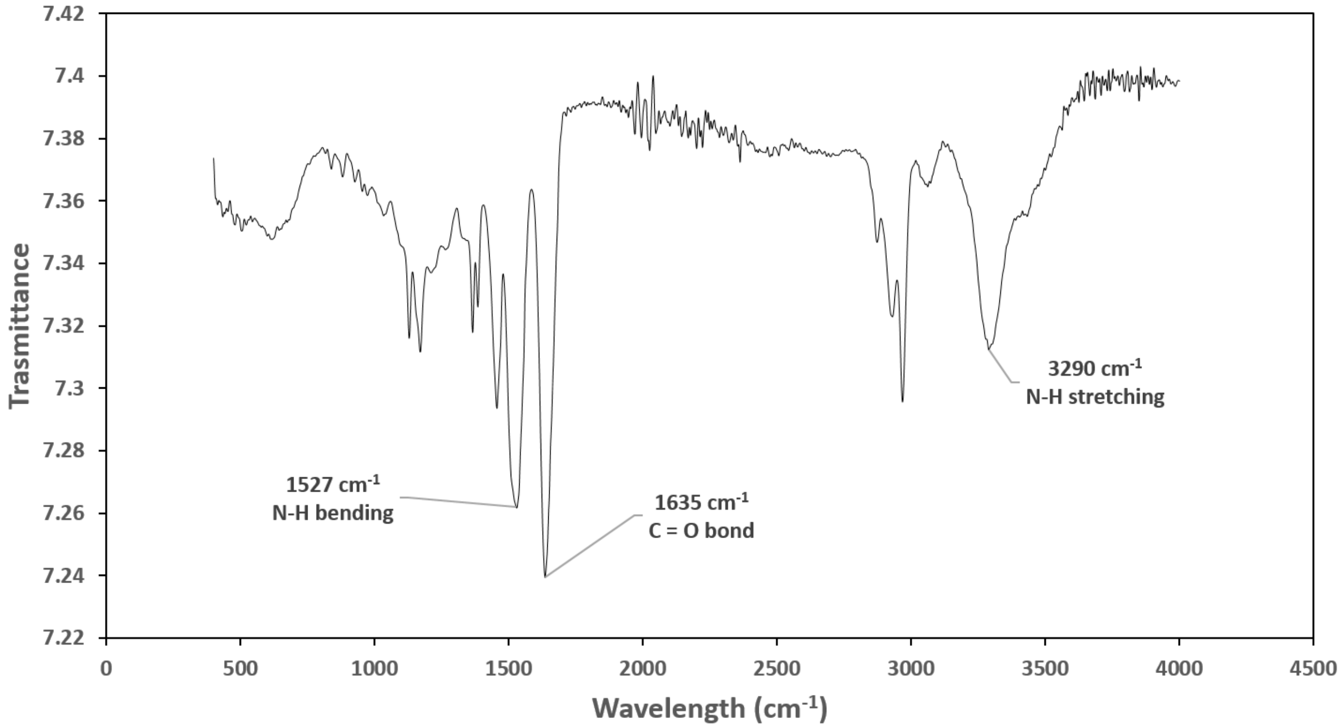

Figure 4.4. FTIR spectrum of pN-1.9.

4.2 Mature Fine Tailings Characterization

Table 4.3 shows the results from the Dean Stark analysis of the MFT used in this research.

Table 4.3. Dean stark analysis of the MFT.

Component	Weight %
Solids	33
Water	62
Bitumen	4
Total	99

Table 4.4 shows the moisture analysis of the MFT sample using the moisture analyzer.

Table 4.4. Moisture analysis of the MFT.

Component	Weight %
Solids	35
Water	65

As the error in calculating the solid composition with the moisture analyzer was lower than that with the Dean Stark analysis, the solids composition from the moisture analyzer was used in subsequent calculations.

The MFT sample was also analyzed by atomic absorption spectroscopy to determine the concentration of individual ions present in the sample. Table 4.5 contains the concentrations of the ionic constituents of the MFT sample prior to dilution.

Table 4.5. Ion composition of the MFT.

Ion	Composition (ppm)
Sodium	90.1
Potassium	11.3
Magnesium	21.7
Calcium	8.2

4.3 Flocculation Studies

Three variables were investigated systematically in this study:

1. Polymer type: pNIPAM, pDMAEMA or p(NIPAM-*co*-DMAEMA) of different molecular weight averages and compositions.
2. Polymer dosage (2000 to 10,000 ppm for DMAEMA homo- and copolymers, and 500 to 2000 ppm for pNIPAM).
3. CO_2 injection methods
   3.1. **[P + MFT]**: Polymer + MFT
   3.2. **[(P+CO_2) + MFT]**: (Polymer + CO_2) + MFT
   3.3. **[P + (MFT+CO_2)]**: Polymer + (MFT + CO_2)
   3.4. **[(P+CO_2) + (MFT+CO_2)]**: (Polymer + CO_2) + (MFT + CO_2)

Two control runs were devised to test the performance of the synthesized polymer flocculants: Control I measured initial settling rate (ISR), turbidity (NTU), and capillary suction time (CST) of the diluted MFT solution without adding polymer or CO_2; Control II measured the same performance parameters for the MFT solution but in the presence of CO_2. Table 4.6 summarizes these results.

Table 4.6. Flocculation parameters for the control experiments.

Parameter	Control I 5% MFT	Control II 5% MFT + CO_2
Initial settling rate (ISR) (m/h)	0	0.03
Turbidity (NTU)	>10000	83
Capillary suction time (CST) at t = 0 (s)	189.4	92.1
Capillary suction time (CST) at t = 24 h (s)	170.5	222.4

No settling of the diluted MFT was observed in the first 30 minutes for either control experiment (ISR = 0). The turbidity could not be measured (NTU > 10000) for Control I, but adding CO_2 (Control II) decreased turbidity substantially, and lowered CST by about 45%.

4.3.1 Initial settling rate (ISR)

Figure 4.5 compares the ISR of NIPAM homopolymers listed in Table 4.1 at dosages from 500 ppm to 2000 ppm.

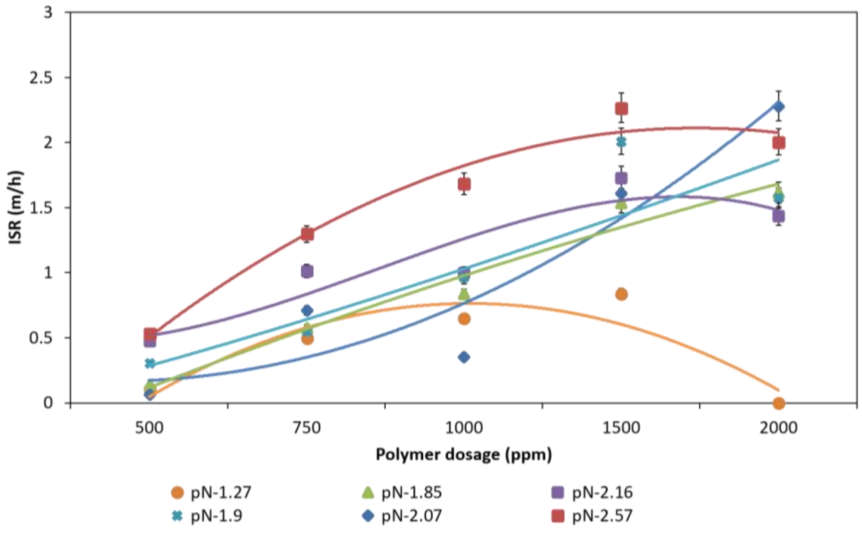

Figure 4.5. Initial settling rate (ISR) as a function of polymer dosage, for pNIPAM homopolymers.

The NIPAM homopolymers exhibited the typical behavior of a polymeric flocculant which was described earlier in Chapter 2. To recap this discussion; the ISR of NIPAM homopolmyers increased with dosage up to the optimum dosage where the highest ISR was recorded. As the dosage is increased beyond the optimum dosage, the ISR begins to decrease. A larger quantity of polymer exists in the solution which covers more than half of the surface area of the solid particle, due to which adsorption of polymer particles on the solid particles gets difficult (Bolt, 2007). As a result the ISR drops beyond this dosage.

Figure 4.6 compares the ISR of DMAEMA homopolymers listed in Table 4.1 at dosages from 2000 ppm to 10000 ppm.

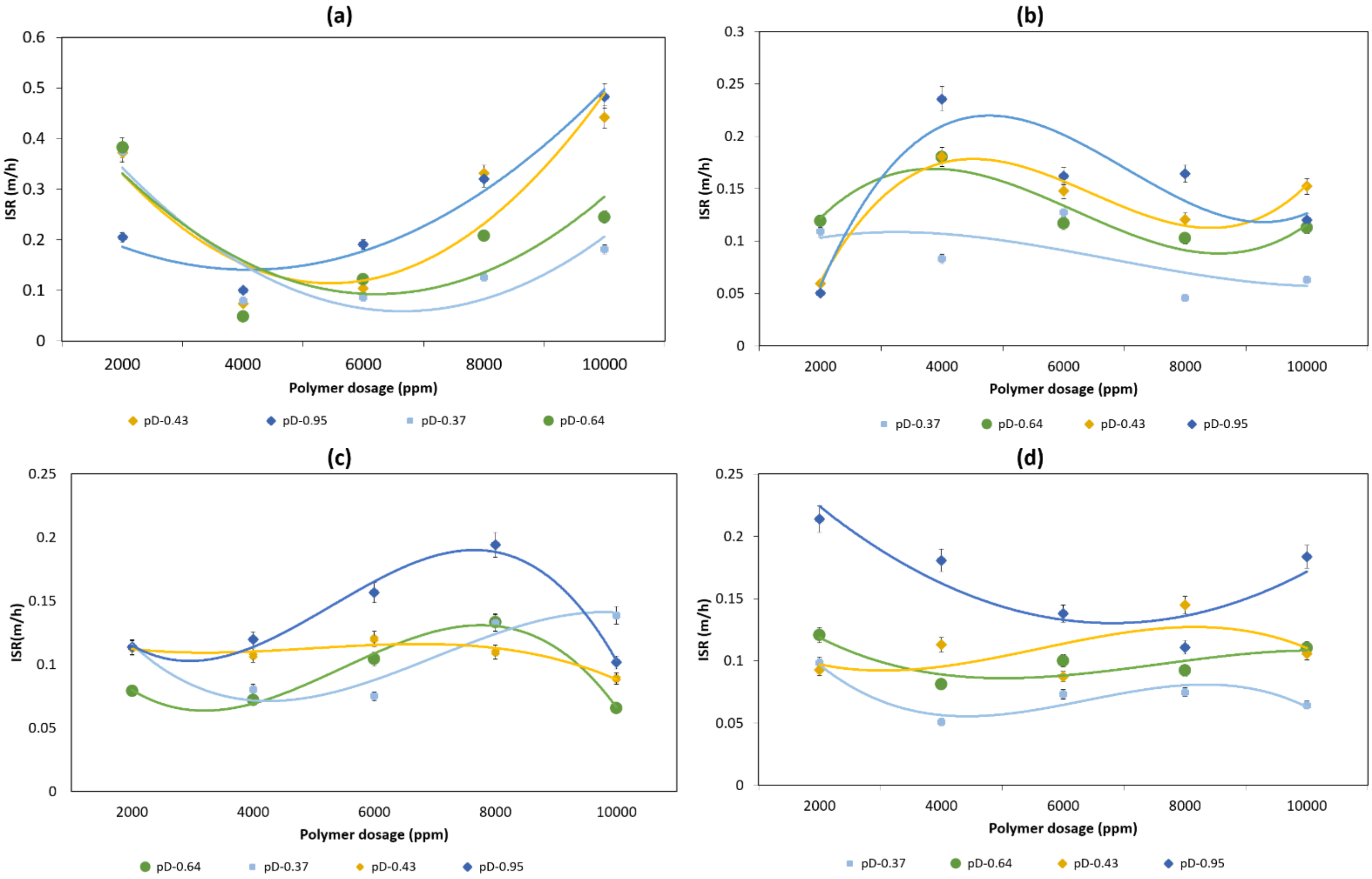

Figure 4.6. Initial settling rate (ISR) of pDMAEMA homopolymers as a function of polymer dosage, under different conditions of CO_2 introduction: **a)** P + MFT **b)** (P+CO_2) + MFT **c)** P + (MFT+CO_2) and **d)** (P+CO_2) + (MFT+CO_2).

The trend of ISR observed for DMAEMA homopolymers is not as prominent as the NIPAM homopolymers. However, it can be noticed that in the Figure 4.6 (a), there is no peak or an optimum dosage observed, which implies the optimum dosage does not lie in the dosage range of 2000 ppm to 10000ppm. As CO_2 is introduced in the system in (b) and (c), it is expected to enhance the flocculation characteristic of the polymer. This lowers the optimum dosage to a value lower than that in (a), which makes the peak visible in the employed dosage range. This confirms the effect of charged species. However, in (d), due to the high concentration of CO_2 in the system, flocculation is comparatively better than in (a), (b) and (c) and hence the optimum dosage is probably lower than 2000 ppm, which is outside of the dosage range chosen. One can notice the fact that the changes in ISR for DMAEMA homopolymers are lower than and not as significant as those obtained for NIPAM homoplymers (take note of the scale on y axis)

Figure 4.7 compares the ISR of DMAEMA and NIPAM copolymers listed in Table 4.1 at dosages from 2000 ppm to 10000 ppm.

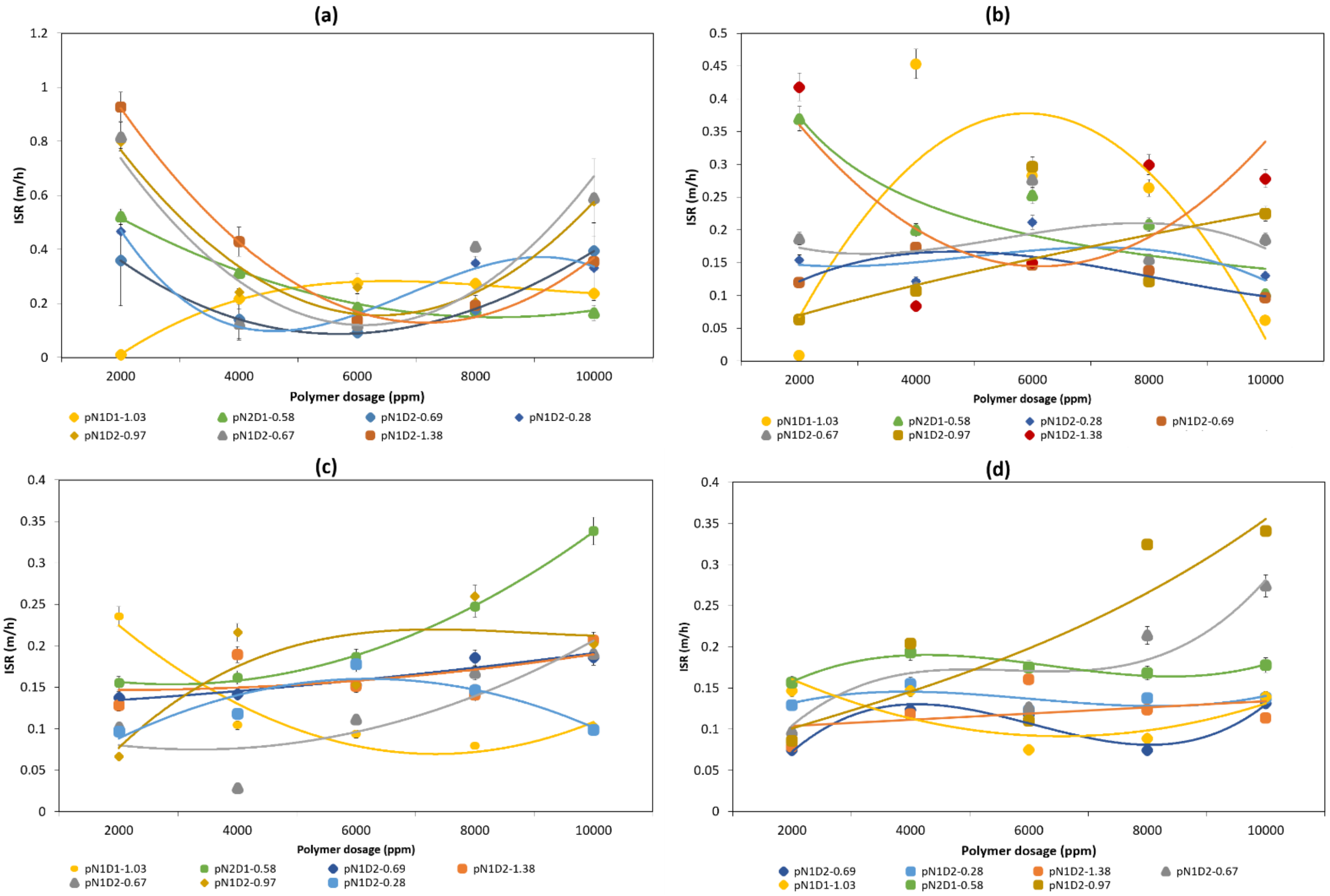

Figure 4.7. Initial settling rate (ISR) of DMAEMA and NIPAM copolymers as a function of polymer dosage, under different conditions of CO_2 introduction: **a)** P + MFT **b)** (P+CO_2) + MFT **c)** P + (MFT+CO_2) and **d)** (P+CO_2) + (MFT+CO_2).

Trends observed in Figure 4.7 resemble those obtained in Figure 4.6, however, these trends are not as uniform. This could be attributed to compositional differences of the copolymers with the homopolymers.

The drop in ISR for both, the homopolymers of DMAEMA and its copolymers, may be due to a case of hindered settling caused due to the presence of CO_2 bubbles in the system, in addition to the stabilization being caused by the presence of excess charges (explained in detail with the next figure). Figure 4.7 (c) and (d) cases had a negligible difference with both having nearly the same ISR, as the introduction of CO_2 through the MFT had a greater influence than polymer dosage on ISR.

Figure 4.8 compares ISR for all polymers listed in Table 4.1 at the dosages they performed the best, that is, had the highest ISR.

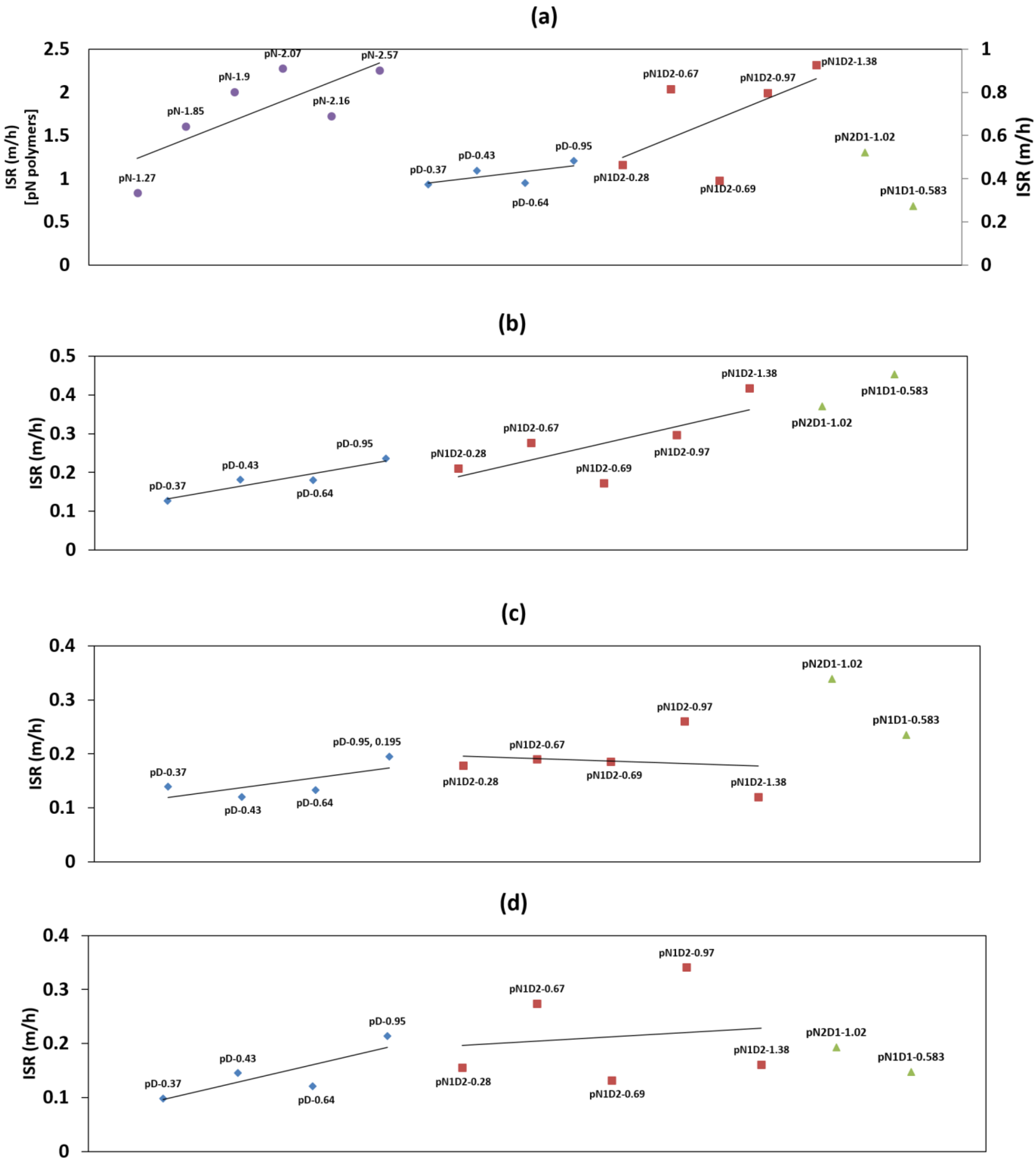

Figure 4.8. Highest values of initial settling rate (ISR) under different conditions of CO_2 introduction: **a)** P + MFT **b)** (P+CO_2) + MFT **c)** P + (MFT+CO_2) and **d)** (P+CO_2) + (MFT+CO_2).

The dosage which generated the best ISR for each polymer, is shown in Appendix A. Each plot in Figure 4.7 refers to a particular mode of CO_2 addition, as described in Section 3.2.6. The polymers are arranged in order of increasing molecular weights of their respective families (pNIPAMs, pDMAEMAs and NIPAM/DMAEMA copolymers).

Consider first, the case when CO_2 was not added to the system (P+MFT). The values of ISR increase with increasing polymer molecular weight for pNIPAM, pDMAEMA, and pN1D2, with the effect being more pronounced for the series of NIPAM homopolymers. This shows that these polymers behave similar to the neutral polymers like PAM: their ISR increases with polymer molecular weight, since longer polymer chains can adsorb onto a larger number of solid particles, forming heavier flocs that settle faster.

Interestingly, when CO_2 is introduced, the highest values for ISR of all DMAEMA polymers decrease (note change in the y-scale). This indicates that adding CO_2 to these systems will slow down the sedimentation rate of the formed flocs. When CO_2 is added only to the polymer solution, (P+CO_2) + MFT, CO_2 is present in the system in a much lower quantity (maximum of 3.33 mL for a 10,000 ppm polymer dosage; refer Chapter 3 for calculations) than when CO_2 was introduced in the MFT (100 mL). Due to which, in P + (MFT+CO_2) and (P+CO_2) + (MFT+CO_2) cases, the MFT get coagulated before the flocculation begins. This can be confirmed by referring to Table 4.6 where CO_2 achieved dewatering of MFT. This shows that with CO_2 in the system, the treatment of MFT was initiated prior to polymer introduction. This resulted in a better performance as a coagulated MFT system was provided for the polymer to flocculate. In this case, the polymer flocculates through bridging and charge neutralization caused by the protonation of the tertiary amide group of DMAEMA at low pH (achieved using CO_2). The protonation was confirmed using zeta potential measurements (refer Table 4.2). Figure 4.8 (c) and (d) produced nearly the same ISRs. Introduction of CO_2 through the MFT seemed to play a dominant role in achieving settling (that is, there was no significant effect of the protonated polymer solution introduced in (d)).

Molecular weight of the polymer played a role in achieving the highest ISRs for each family. The best value for each polymer in each family increased with molecular weight of the polymer as observed in Figure 4.8 (a). The effect was more prominent for NIPAM homopolymers and slightly lesser for the cationic polymers.

One can observe the same effects of molecular weight on the ISR in the presence of CO_2, shown in Figure 4.8 (b), (c) and (d). However, it is not as pronounced, due to the dominance of CO_2.

Among the cationic homopolymers, pD-0.95 had the best ISR of 0.195 m/h at 4000 ppm, and the copolymer pN1D2-0.97 of 0.339 m/h at 2000 ppm, among the copolymers which is low as compared to the 2.26 m/h ISR of pN-2.56 NIPAM homopolymer.

Figure 4.9 shows the highest ISR achieved in each family. The figure is more comprehensible to understand the effects of different polymer types on ISR and the effect CO_2 had on them.

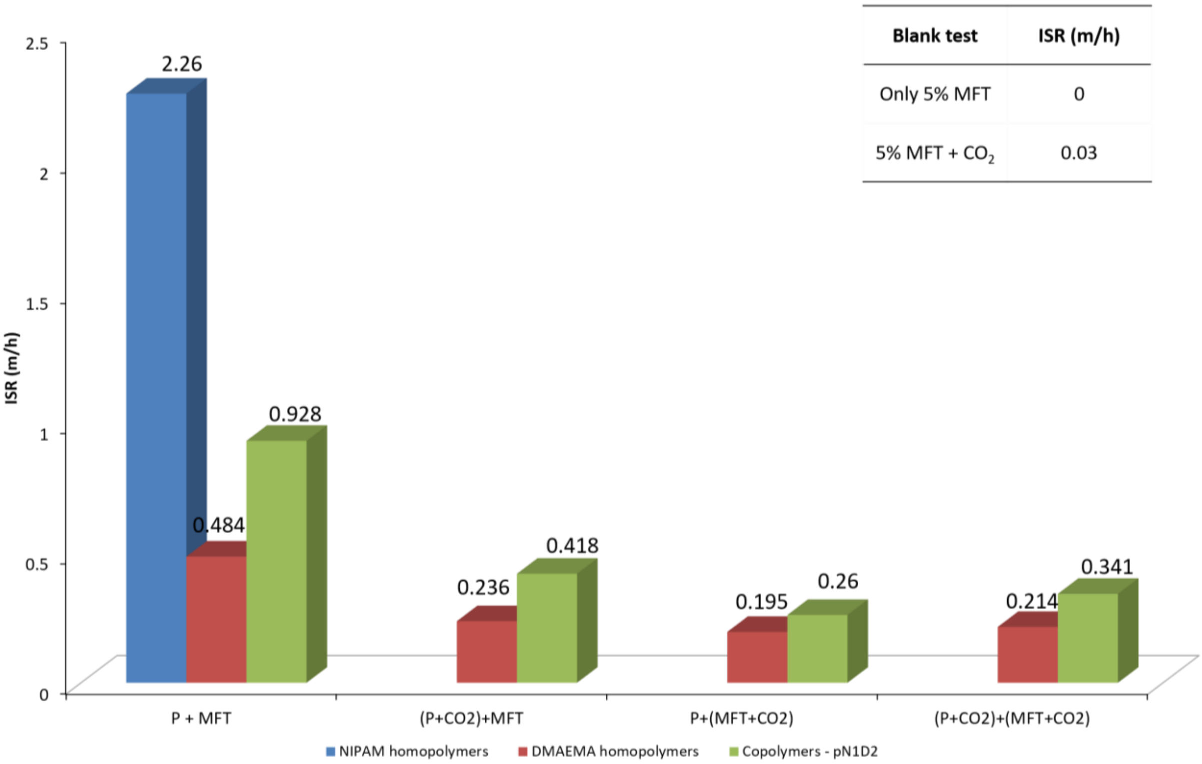

Blank test	ISR (m/h)
Only 5% MFT	0
5% MFT + CO_2	0.03

Figure 4.9. Highest initial settling rates observed for pNIPAM, pDMAEMA and copolymers at different modes of CO_2 introduction.

NIPAM homopolymers had the highest ISRs for P+MFT condition. DMAEMA homopolymers and copolymers showed lower ISR values as compared to NIPAM homoplymers. A probable reason could be the influence of charges, which was explained earlier. However, combining these two monomers as copolymers produced a better performance than just the DMAEMA homopolymers. Compositional advantage of a higher NIPAM percentages could be the reason for better polymer performance. The drop in ISR values with CO_2 introduction is clearly visible in this figure.

From these observations, we can conclude that pNIPAM achieved better settling rates for MFT suspensions in the absence of CO_2. Introduction of CO_2 in the MFT solution resulted in the lowest ISR values due to hindered settling and molecular weight had a significant effect on the ISR.

4.3.2 Capillary suction time (CST)

Figure 4.10 compares the CST at $t = 0$ of NIPAM homopolymers listed in Table 4.1 at dosages from 500 ppm to 2000 ppm.

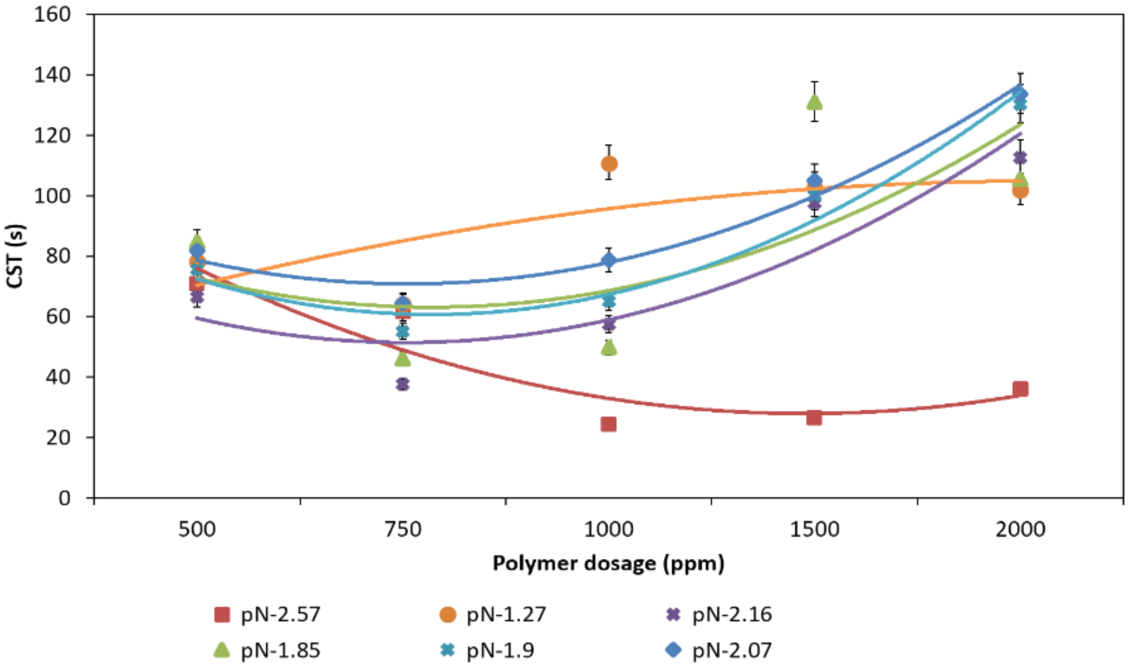

Figure 4.10. Capillary suction time (CST) at $t = 0$ as a function of polymer dosage, for pNIPAM homopolymers.

Majority of the NIPAM homopolymers showed a slightly decreasing trend before an increase in their CST values. With an increase in dosage, more polymer is available to bring the solids together. This creates more compact flocs due to which the dewatering capability increase, thus showing a fall in CST. As the dosages move towards the higher end, the CST increases due to the same reason as explained for ISR; increase in polymer dosage causes a larger surface area of the solid particles to be covered with polymer. This reduced the possibility of polymer-solid collisions that leads to adsorption, due to which flocculation could not take place effectively.

Compact floc formation was affected due to high polymer dosage and resulting in bad dewatering characteristics, which was reflected as high CST values.

Figure 4.11 compares the CST at *t* = 0 of DMAEMA and NIPAM copolymers listed in Table 4.1 at dosages from 2000 ppm to 10000 ppm.

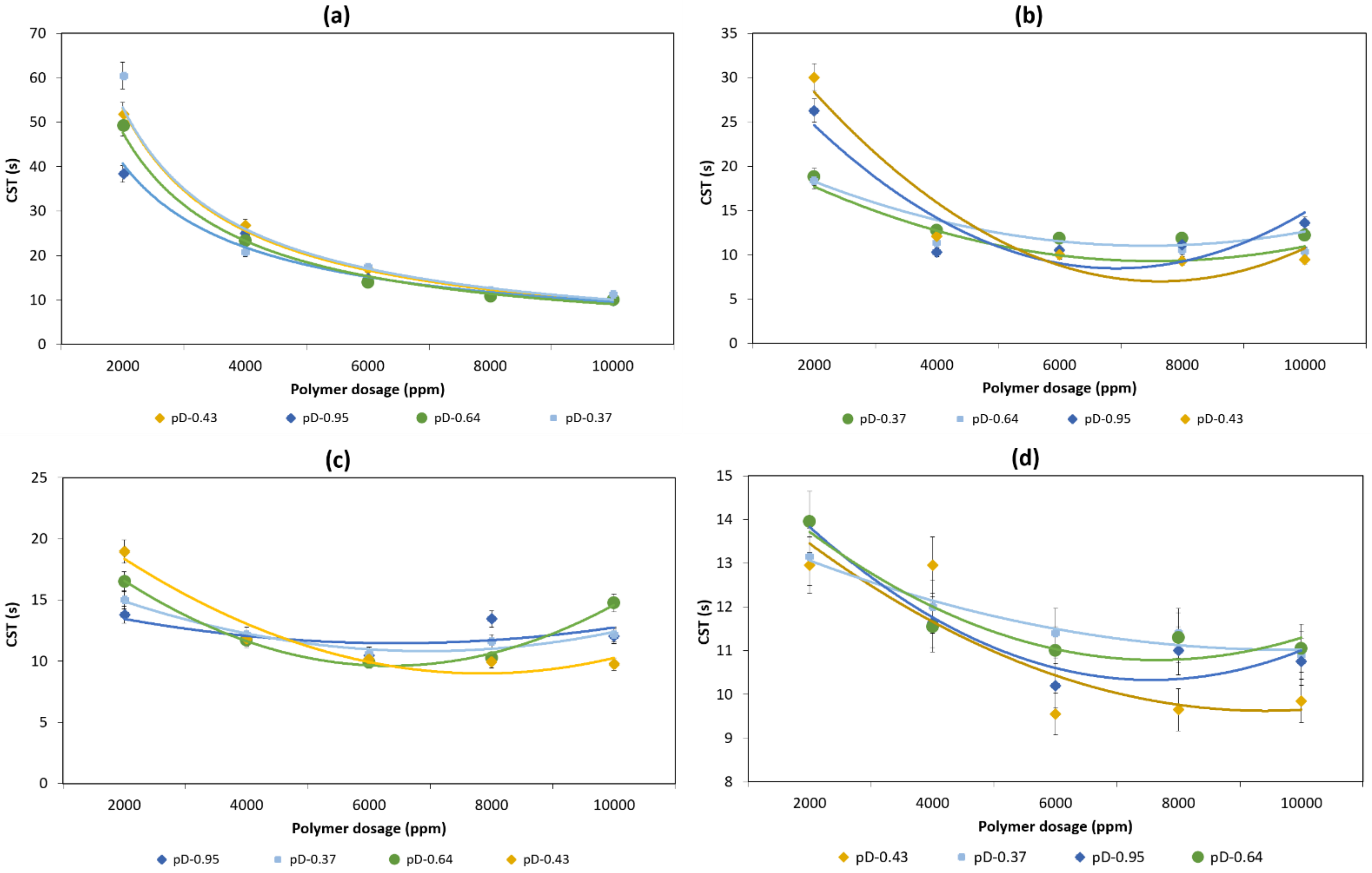

Figure 4.11. Capillary suction time (CST) at *t* = 0 of pDMAEMA homopolymers as a function of polymer dosage, under different conditions of CO_2 introduction: **a)** P + MFT **b)** (P+CO_2) + MFT **c)** P + (MFT+CO_2) and **d)** (P+CO_2) + (MFT+CO_2).

The CSTs of DMAEMA homopolymers are much lower than that of NIPAM. The general CST versus dosage trend was a decrease in CST until a plateau was reached with an increase in polymer dosage, which was similar to the trend observed for NIPAM homopolymers. However, the trends in Figure 4.11, show a clear decrease and a plateau indicating the dosage ranges chosen for these polymers contain the optimum dosage value for all polymers in this family. Homopolymers of DMAEMA yielded lower CSTs due to charge neutralization, in addition to the bridging mechanism, that produced more compact flocs than the NIPAM homopolymers.

Introduction of CO_2, enhanced the flocculation performance to achieve low CSTs at lower dosages. A surplus of charges in the system affects the polymer performance as repulsive forces between the polymer-covered fines become dominant. These interactions could lead to water entrapment in flocs that are not as compact or tight, thus giving poor dewatering polymer performances. As a result, at higher polymer concentration resulted in plateaued or elevated trends, as observed for dosages beyond 6000 ppm for (b), (c) and (d) in Figure 4.11.

Figure 4.12 compares the CST at *t* = 0 of DMAEMA and NIPAM copolymers listed in Table 4.1 at dosages from 2000 ppm to 10000 ppm.

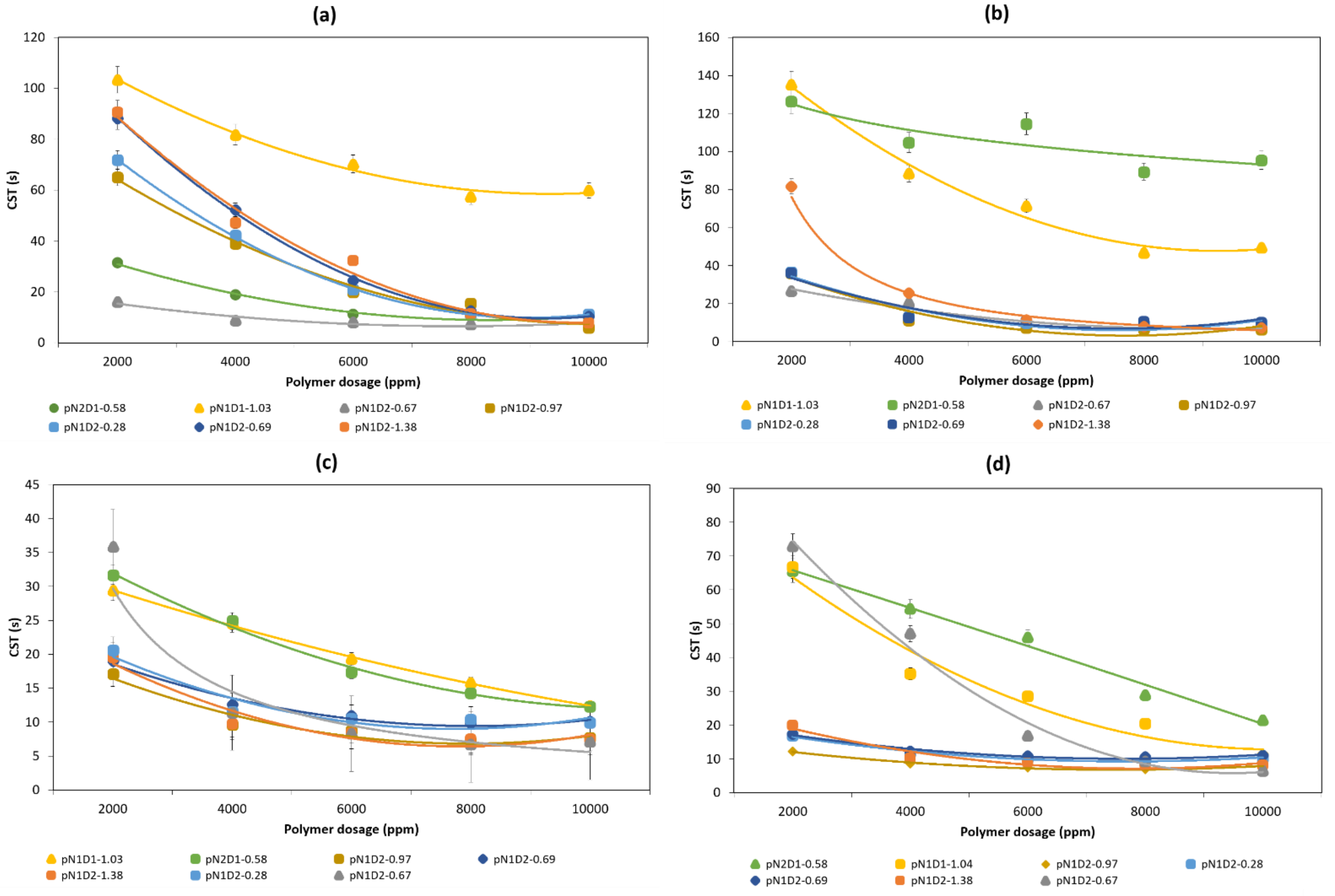

Figure 4.12. Capillary suction time (CST) at *t* = 0 of DMAEMA and NIPAM copolymers as a function of polymer dosage, under different conditions of CO_2 introduction: **a)** P + MFT **b)** (P+CO_2) + MFT **c)** P + (MFT+CO_2) and **d)** (P+CO_2) + (MFT+CO_2).

Copolymers had decreasing CSTs with increase in dosage, with majority of the polymers converging at a similar value for high dosages, like the DMAEMA homopolymers. However, DMAEMA homopolymers performed better than the copolymers in achieving low CSTs at lower dosages than the copolymers, due to the compositional difference of a higher percentage of NIPAM in the copolymers' polymer chain. Copolymers having a higher NIPAM compositions; pN2D1-0.58 and pN1D1-1.03, had higher CSTs with CO_2 introduction as these polymers are influenced by CO_2 to a lesser extent compared to those with higher DMAEMA composition. With the introduction of CO_2, more uniform trends were obtained, and in cases having higher CO_2 quantities, (c) and (d), a narrower range of CST values for the dosages was generated as more compact flocs formed due to higher number of charges.

Figure 4.13 compares CST at $t = 0$ for all polymers listed in Table 4.1 at the dosages they performed the best (that is, had the lowest CST). As mentioned earlier for ISR, each plot in Figure 4.13 refers to a particular mode of CO_2 addition, as described in Section 3.2.6, and the polymers are arranged in order of increasing molecular weights in their respective families (pNIPAMs, pDMAEMAs and copolymers). The best dosage for individual polymers at different modes of CO_2 introductions are shown in Appendix B.

Consider first the P+MFT case where no CO_2 was used, in Figure 4.13 (a). Homopolymers of DMAEMA performed better than those of NIPAM, but their CST did not depend nearly as strongly on polymer molecular weight as those of pNIPAM did. Copolymers of NIPAM and DMAEMA in 1:2 ratio achieved the lowest CST values, but those with 2:1 or 1:1 ratio did not perform nearly as well. From Figure 4.13, it is clear that the decrease in CST for pNIPAM polymers with molecular weight, was more prominent than for the cationic polymers. One may propose that charge neutralization helps make sediments with lower CSTs, without a strong influence of the molecular weight of the flocculant. As a result, the CST x polymer molecular weight dependency for these polymers remains nearly flat and the same was observed for (b), (c) and (d), with the best value for NIPAM homopolymers being 24.45 seconds, DMAEMA homopolymers being approximately 9.5 seconds and for copolymers, around 6 seconds.

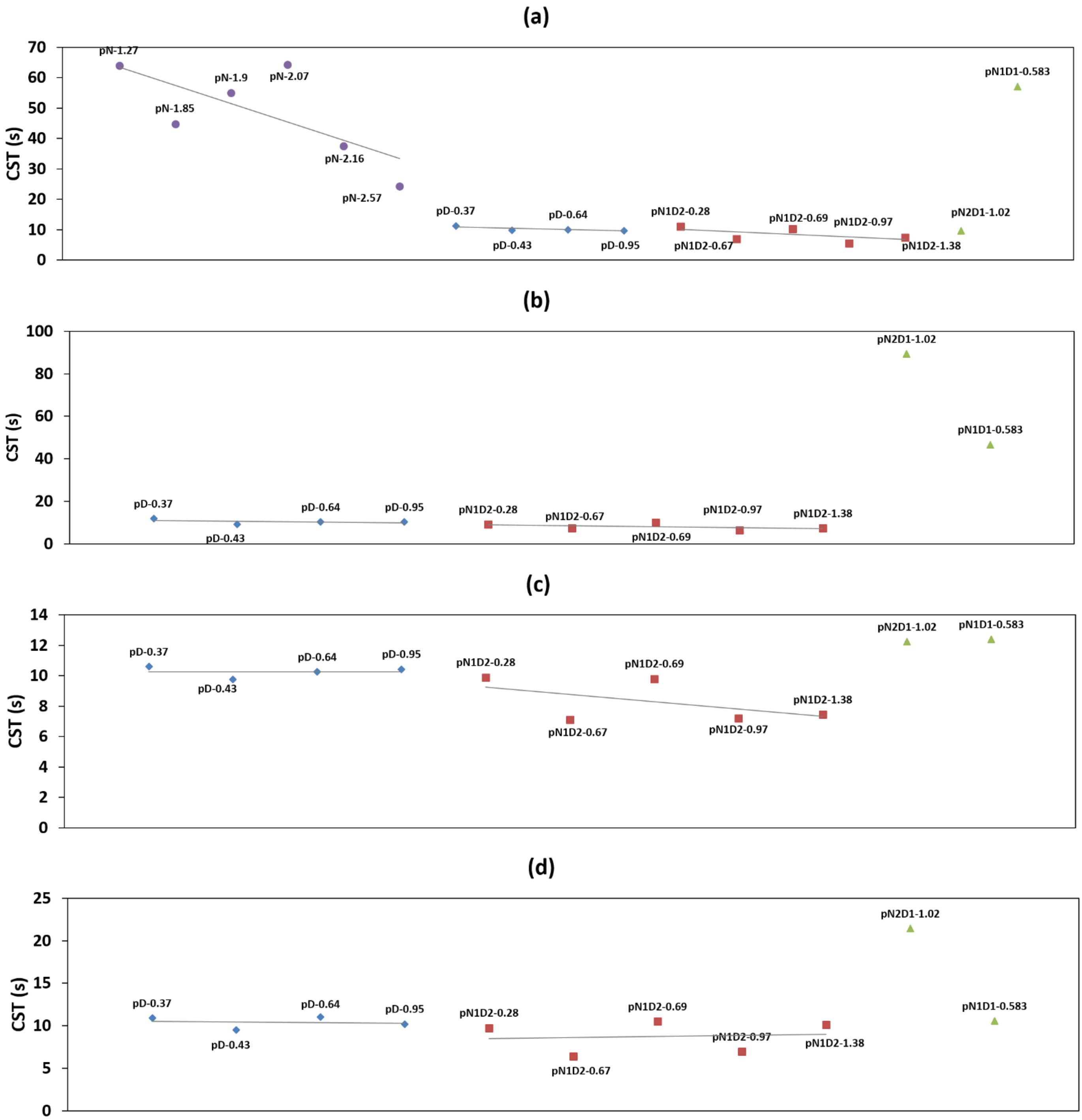

Figure 4.13. Lowest values of CST at $t = 0$ under different conditions of CO_2 introduction: **a)** P+ MFT **b)** (P+CO_2) + MFT **c)** P + (MFT+CO_2) and **d)** (P+CO_2) + (MFT+CO_2).

Figure 4.14 shows the lowest CST at $t = 0$ achieved in each family. The figure is more comprehensible to understand the effects of different polymer types on CST at $t = 0$ and the effect CO_2 had on them.

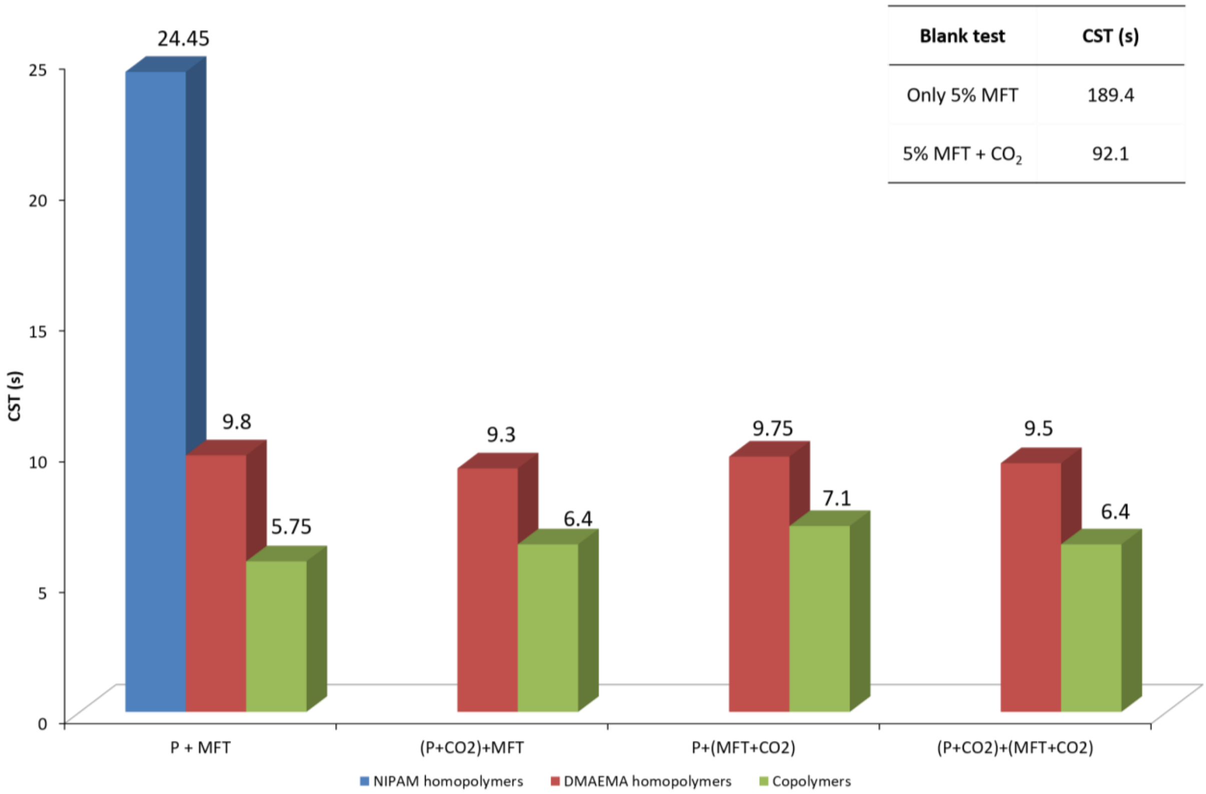

Blank test	**CST (s)**
Only 5% MFT	189.4
5% MFT + CO_2	92.1

Figure 4.14. Lowest CST *t* = 0 values observed for pNIPAM, pDMAEMA and copolymers at different modes of CO_2 introduction.

The polymers were capable of producing CSTs lower than 25 seconds, which is significantly higher that of the blank (180 seconds). NIPAM homopolymers were not as effective as the cationic polymers when it came to producing effective CSTs at *t* = 0. pDMAEMA homopolymers performed better than pNIPAM polymers, however, the copolymers of NIPAM and DMAEMA performed the best. There was no significant difference between the CSTs observed for the DMAEMA polymers at different cases of CO_2 introduction. On further analysis, it was noted that the optimum dosage showed a slight shift from 10000 ppm from 8000 ppm, with the introduction of CO_2 (refer Appendix B).

Figure 4.15 compares the CST after *t* = 24 h of NIPAM homopolymers listed in Table 4.1 at dosages from 500 ppm to 2000 ppm.

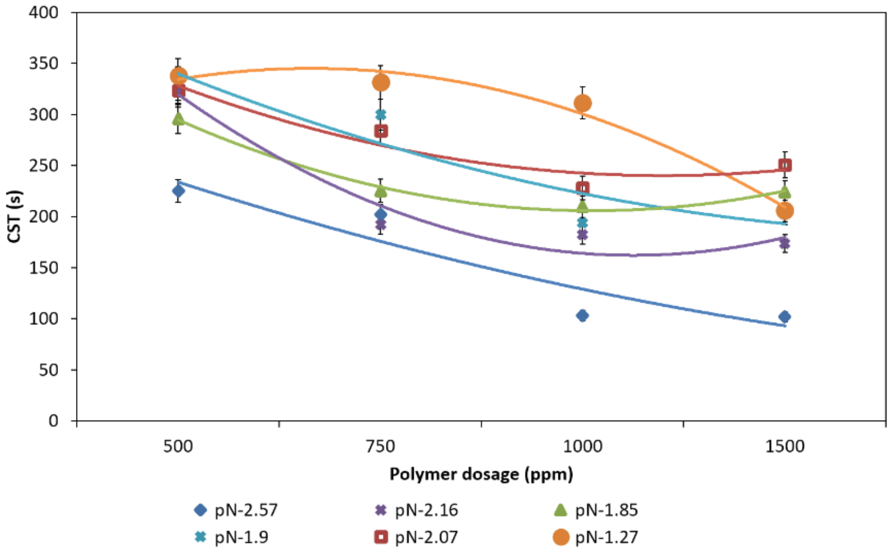

Figure 4.15. Capillary suction time (CST) at *t* = 24 h as a function of polymer dosage, for pNIPAM homopolymers.

The CST values after a period of 24 hours showed a more decreasing trend compared to Figure 4.10 for NIPAM homopolymers.

A typical CST value after 24 hours is higher than that at the start of settling, as part of water is expelled from the sediment cake into the supernatant layer. This leads to a lesser quantity of water in the sample due to which a higher CST reading is obtained. The nature of the graphs for CST at *t* = 24 h are quite similar and in fact, much more uniform as compared to those of CST at *t* = 0. The trends remain similar to the CSTs observed at *t* = 0. CST *t* = 24 h shows that with time, CST values increase, due to lesser quantity of water being expelled. It was because of this reason that a steeper drop in CSTs for *t* = 24 h was observed as compared to CST at *t* = 0. The trends and explanations provided for the trends remain the same as that for CST at *t* = 0.

Figure 4.16 compares the CST at *t* = 24 h of DMAEMA homopolymers listed in Table 4.1 at dosages from 2000 ppm to 10000 ppm. The CST values showed a more uniform decreasing trend as compared to CST at *t* = 0.

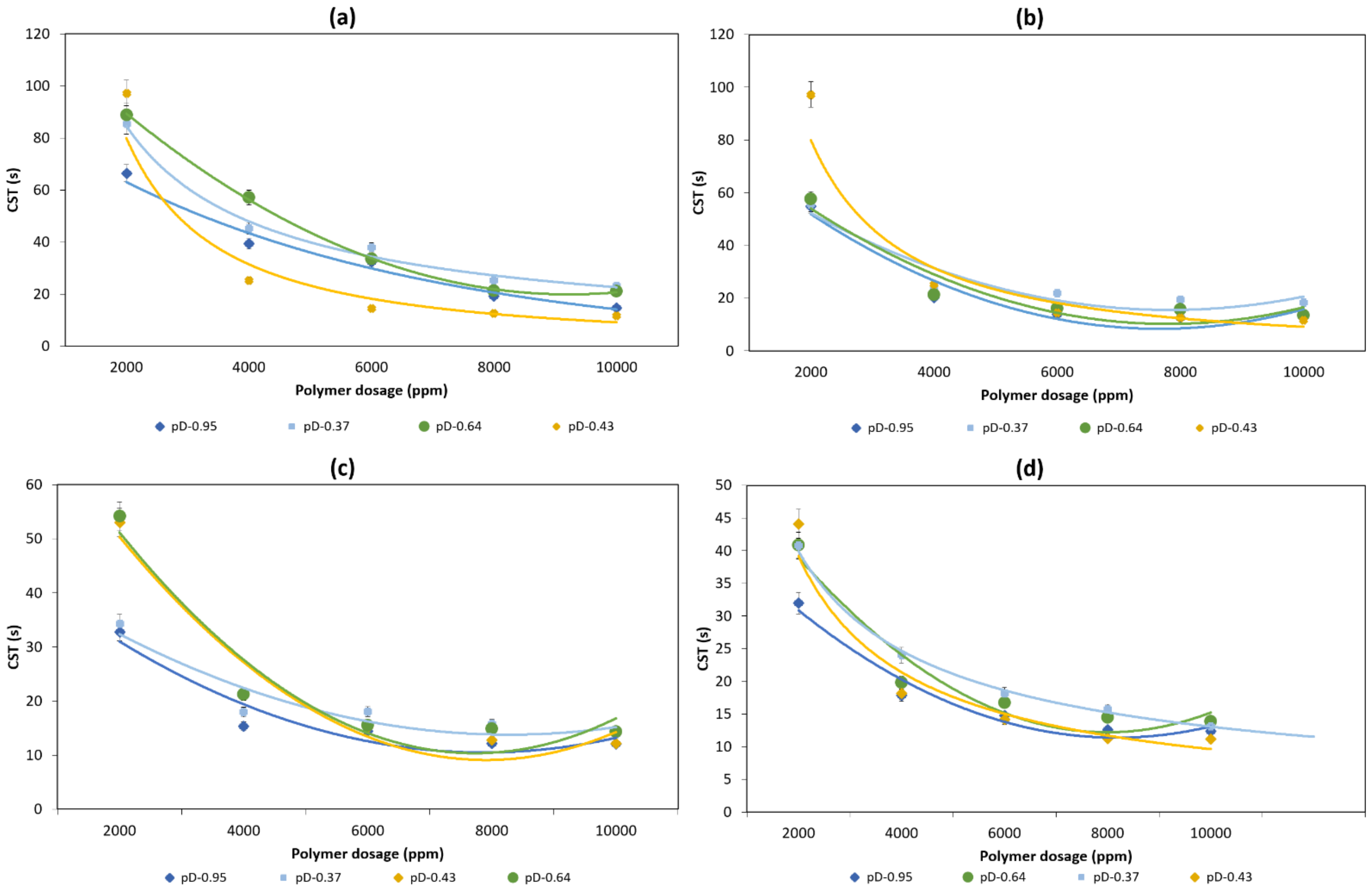

Figure 4.16. Capillary suction time (CST) at *t* = 24 h curves of DMAEMA homopolymers with polymer dosage, under different conditions of CO_2 introduction: **a)** P + MFT **b)** (P+CO_2) + MFT **c)** P + (MFT+CO_2) and **d)** (P+CO_2) + (MFT+CO_2).

Figure 4.17 compares the CST after *t* = 24 h of DMAEMA and NIPAM copolymers listed in Table 4.1 at dosages from 2000 ppm to 10000 ppm.

The cationic polymers followed the same general trend as for CST *t* = 0. With increase in polymer dosage, better dewatering characteristics were observed. In addition, the copolymers with higher NIPAM composition showed higher CSTs due compositional effects. As observed for CST at *t* = 0, the copolymers with a higher composition of NIPAM showed higher CSTs with CO_2 introduction as they are less sensitive to pH changes, which was explained earlier in this section.

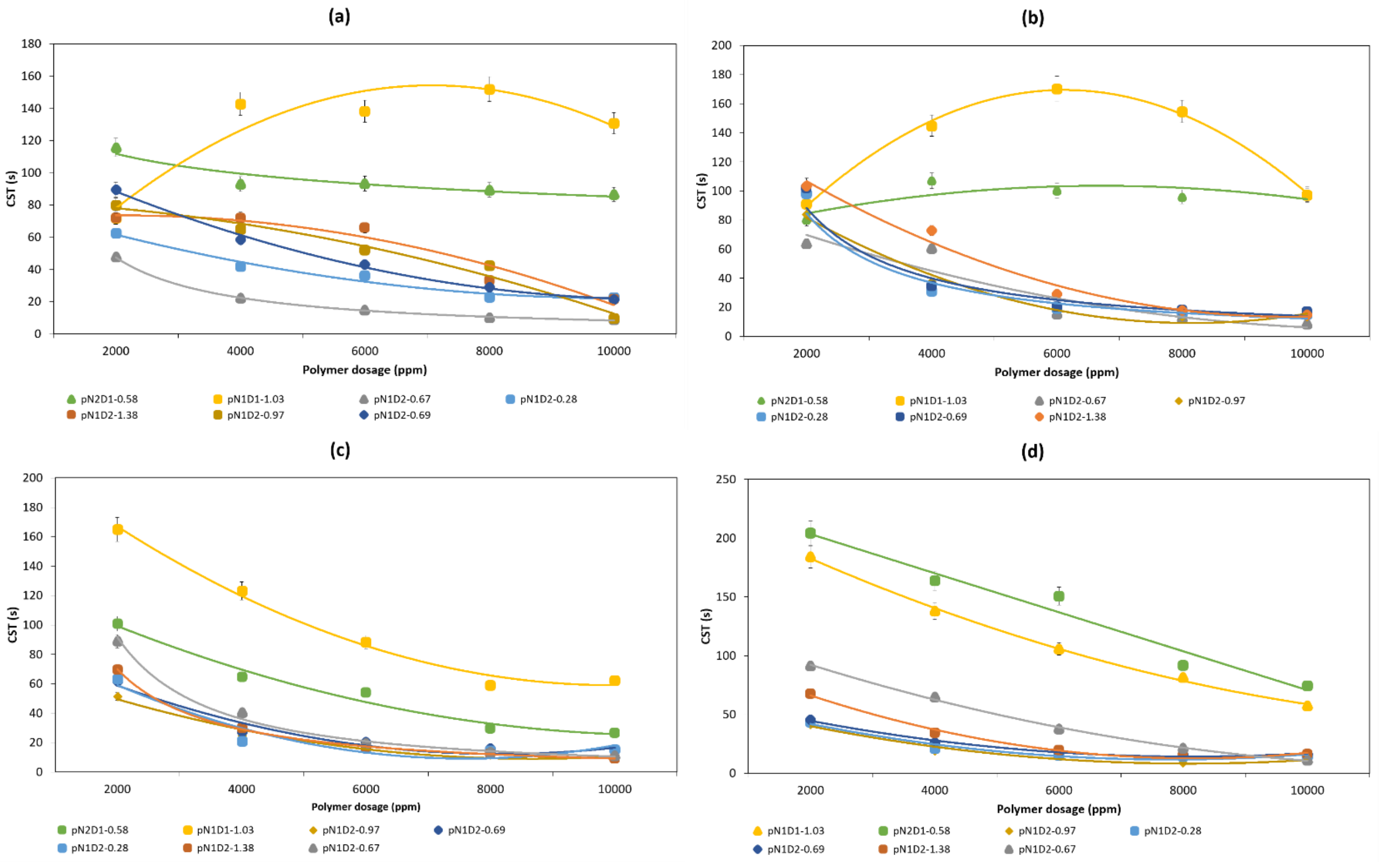

Figure 4.17. Capillary suction time (CST) at *t* =24 h curves of DMAEMA and NIPAM copolymers with polymer dosage, under different conditions of CO_2 introduction: **a)** P + MFT **b)** (P+CO_2) + MFT **c)** P + (MFT+CO_2) and **d)** (P+CO_2) + (MFT+CO_2).

Figure 4.18 compares CST at *t* = 24 h for all polymers listed in Table 4.1 at the dosages they performed the best (that is, had the lowest CST). As mentioned earlier for ISR, each plot in Figure 4.18 refers to a particular mode of CO_2 addition, as described in Section 3.2.6, and the polymers are arranged in order of increasing molecular weights in their respective families (pNIPAMs, pDMAEMAs and copolymers). The best dosage for individual polymers at different modes of CO_2 introductions are shown in Appendix C.

Similar to CST at *t* = 0, the NIPAM homopolymers had a more pronounced dependence on molecular weight as compared to the cationic polymers. The DMAEMA polymers showed very little or no dependence on polymer molecular weight.

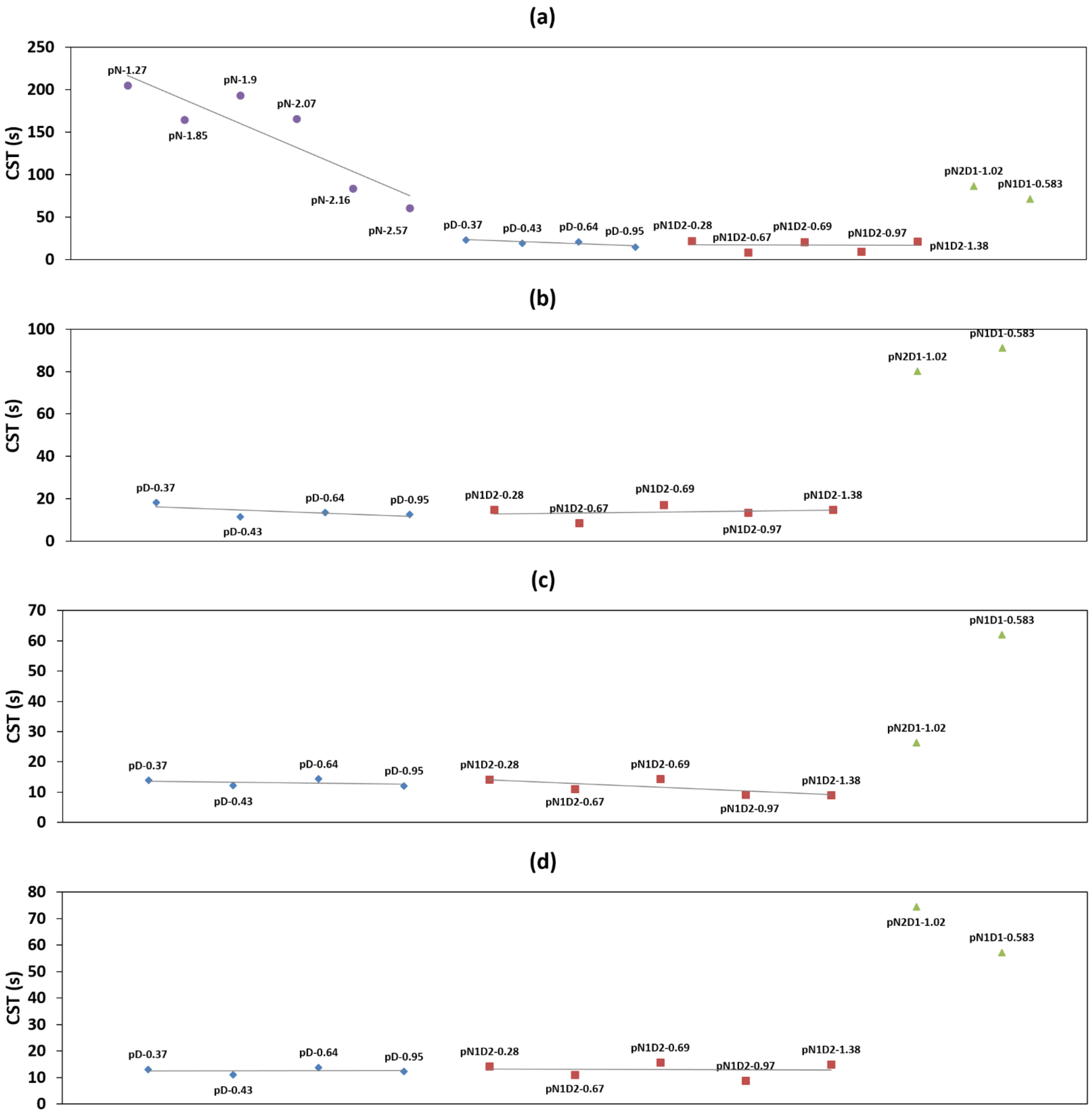

Figure 4.18. Lowest values of CST at *t* = 24 hours and dosage curves under different conditions of CO_2 introduction: **a)** P + MFT **b)** (P+CO_2) + MFT **c)** P + (MFT+CO_2) and **d)** (P+CO_2) + (MFT+CO_2).

Figure 4.19 shows the lowest CST at *t* = 24 h achieved in each family. The figure is more comprehensible to understand the effects of different polymer types on CST at *t* = 24 h and the effect CO_2 had on them.

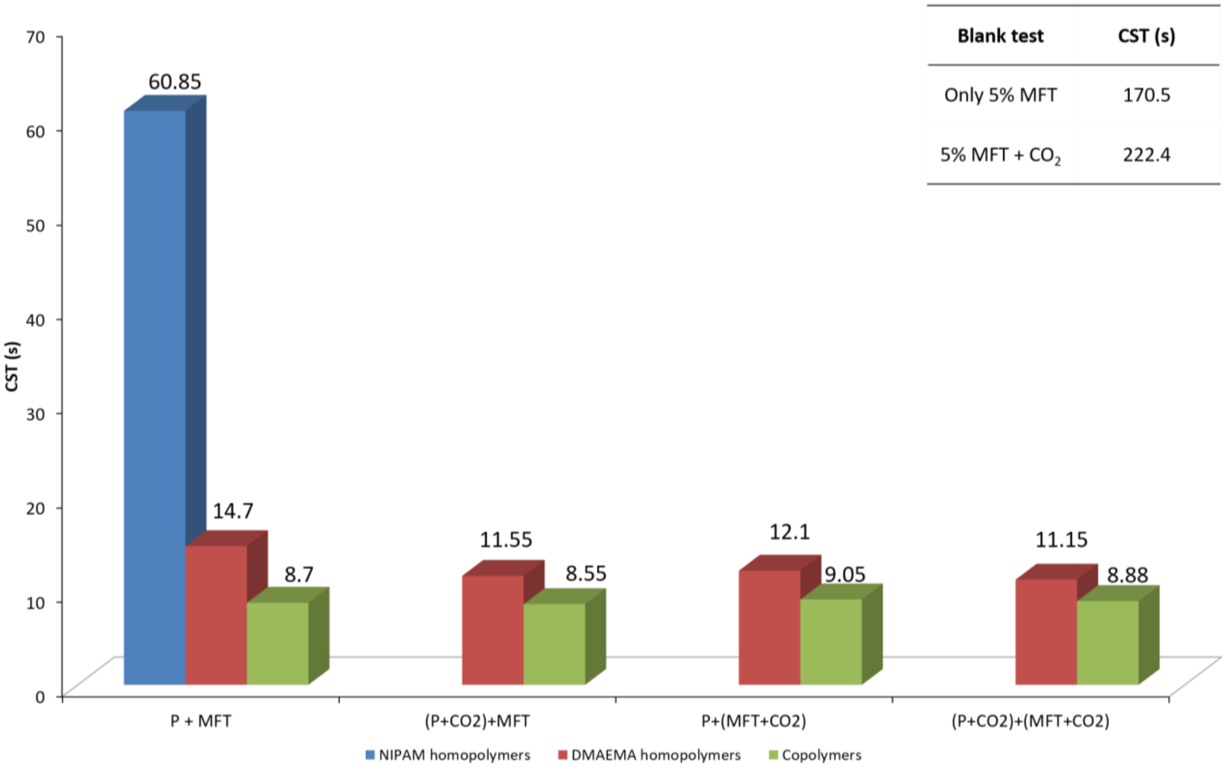

Blank test	CST (s)
Only 5% MFT	170.5
5% MFT + CO_2	222.4

Figure 4.19. Lowest CST at *t* = 24 h values observed for pNIPAM, pDMAEMA and copolymers for different modes of CO_2 introduction.

NIPAM homopolymers were not as effective as the cationic polymers in achieving low CST readings at *t* = 0. The same can be observed for CST at *t* = 24 h. Homopolymers of pDMAEMA has a higher CST compared to the copolymers.

Among all polymer flocculants, pD-0.43 had lowest CST value among the homopolymers, possibly due to its high charge density as pD-0.43 performed better than any other polymer at *t* = 0. Among the copolymers, pN1D2-0.67 produced better results than the rest. Overall, CST at *t* = 24 h have higher values than CSTs at *t* = 0.

4.3.3 Turbidity

Figure 4.20 compares the supernatant turbidity after *t* = 24 h of NIPAM homopolymers listed in Table 4.1 at dosages from 500 ppm to 2000 ppm.

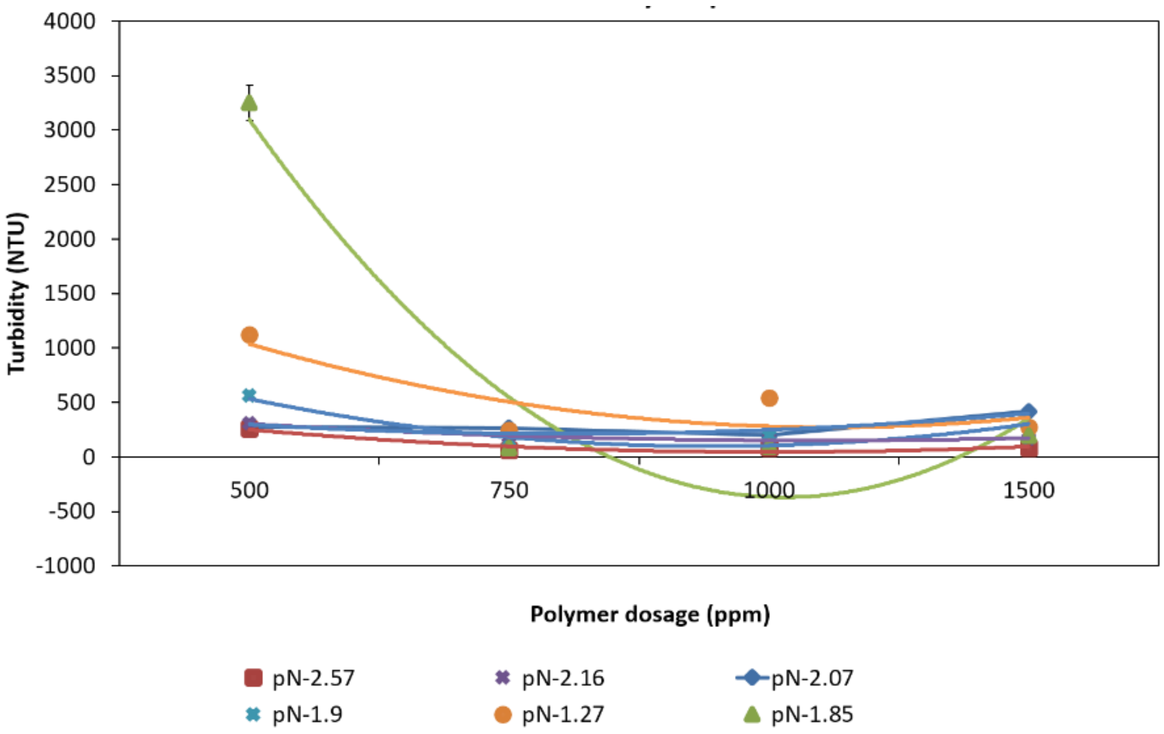

Figure 4.20. Supernatant turbidity after *t* = 24 h as a function of polymer dosage, for pNIPAM homopolymers.

The polymers exhibit a general decreasing trend with increase in dosage for P+M scenario. As the dosage increases, a larger number of polymer particles are involved in the flocculation of the solid particles, bringing them together. However, beyond an optimum dosage, the turbidity increases with polymer dosage. As mentioned for CST parameter, increase in surface area coverage of the solid particle by polymers decreases the probability of polymer chain to collide with a solid particle. This reduces polymer adsorption on the particle surface, thereby leaving the solid particle suspended in the supernatant. This increases the supernatant turbidity, which is observed as a slight elevation of the trend-line.

Figure 4.21 compares the supernatant turbidity after *t* = 24 h of DMAEMA homopolymers listed in Table 4.1 at dosages from 2000 ppm to 10000 ppm.

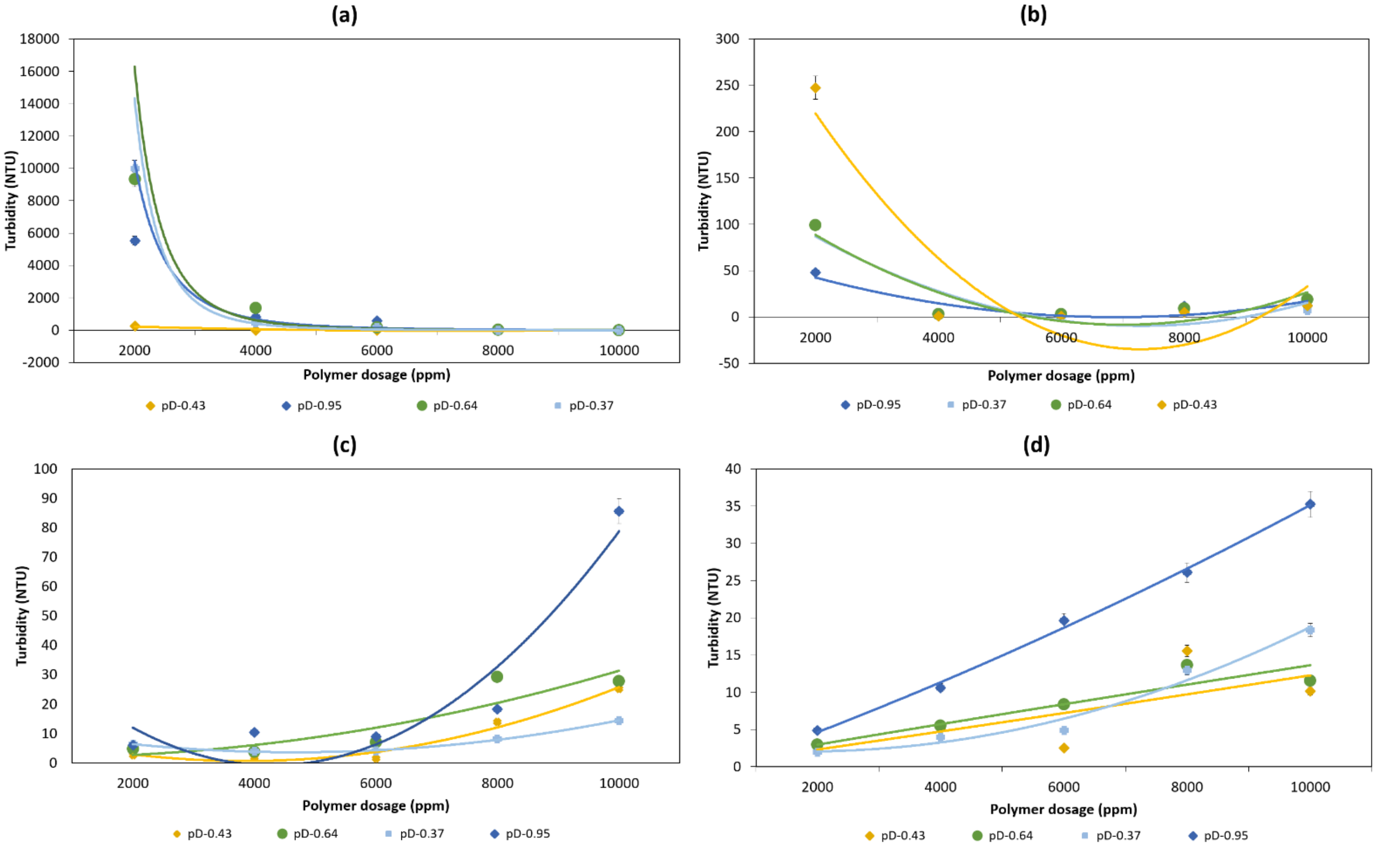

Figure 4.21. Supernatant turbidity after *t* = 24 h as a function of polymer dosage, for DMAEMA homopolymers under different conditions of CO_2 introduction: **a)** P + MFT **b)** (P+CO_2) + MFT **c)** P + (MFT+CO_2) and **d)** (P+CO_2) + (MFT+CO_2).

Flocculation with pDMAEMA generated supernatants with lower turbidities than those obtained with pNIPAM, most likely because pDMAEMA can flocculate fines through charge neutralization and bridging. On comparing the NIPAM and DMAEMA homopolymers, DMAEMA homopolymers showed a much steeper rise in the turbidity values at higher dosages. This is due to effect of surplus charges in addition to the effect of excess particle surface being covered with polymer. Higher polymer dosage leads to a greater surface area of the particle being covered, which gives rise to repulsive forces between the particles. This could prevent formation of heavier flocs as the repulsive forces minimize the probability of collisions between particles thus reducing adsorption of polymer onto the solid particle surface. This is evident with the introduction of CO_2 and using polymers at high dosages (Figure 4.21 (c) and (d)). Referring to the two figures (Figure 4.21 (c) and (d)), introduction of CO_2 tends to coagulate the system due to which the “best” turbidity value was achieved at lower dosages. However, an increase in polymer dosage would increase the turbidity due to the above mentioned reason. The lowest (and hence, the best) turbidity is achieved at the lowest polymer dosage of 2000 ppm after which, it increases.

Figure 4.22 compares the supernatant turbidity after t = 24 h of DMAEMA and NIPAM copolymers listed in Table 4.1 at dosages from 2000 ppm to 10000 ppm.

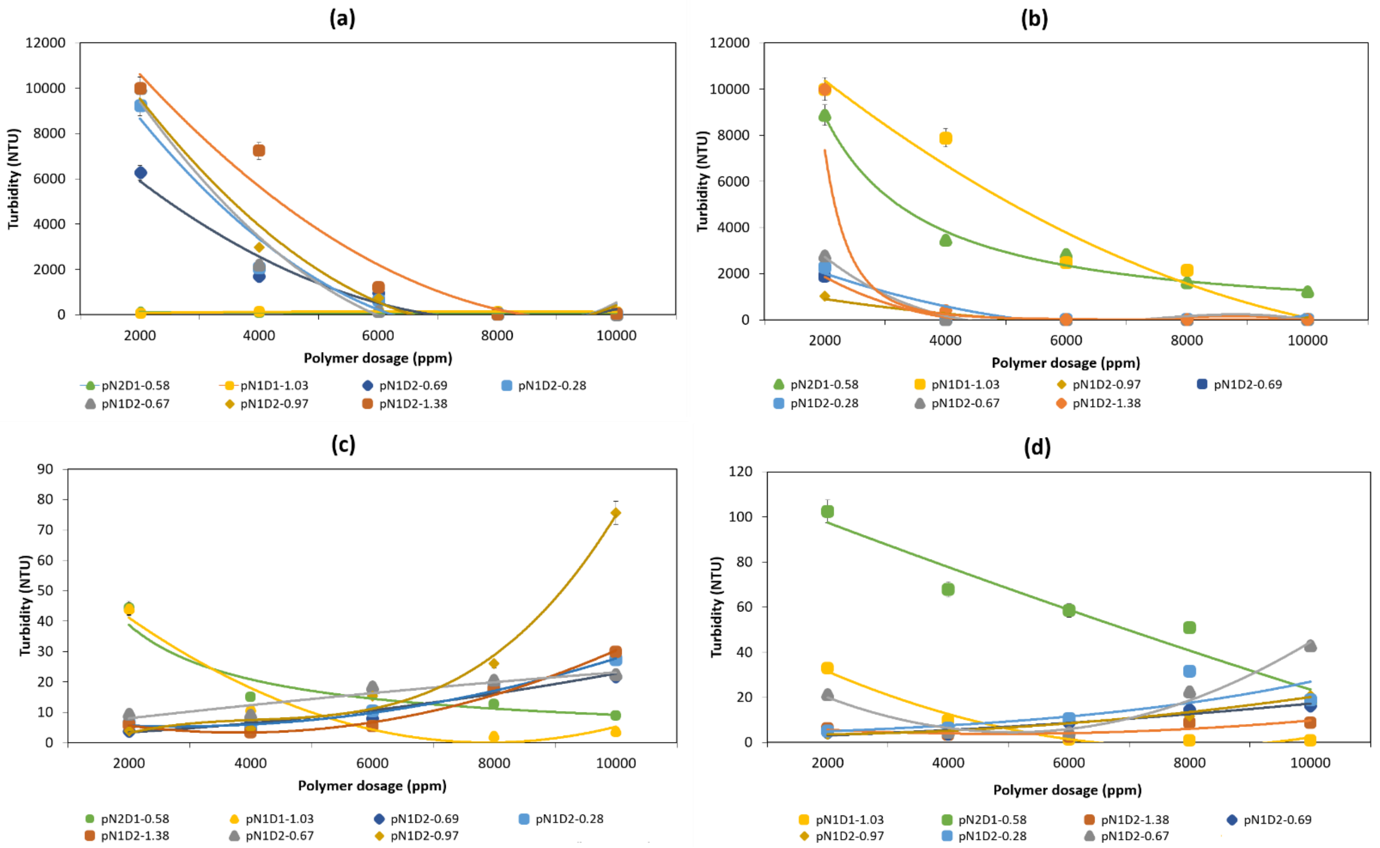

Figure 4.22. Supernatant turbidity after t = 24 h as a function of polymer dosage, for DMAEMA and NIPAM copolymers, under different conditions of CO_2 introduction: **a)** P + MFT **b)** (P+CO_2) + MFT **c)** P + (MFT+CO_2) and **d)** (P+CO_2) + (MFT+CO_2).

The same effects were observed for the case of copolymers as were for the DMAEMA homopolymers. Due to the compositional difference, the copolymers hold over the homopolymers, the increase in the turbidities was not as severe with the copolymers. This meant that the optimum dosage for majority of the polymers would be achieved at a higher dosage than 2000 ppm, because of which a drop, plateau and a rise were observed.

Figure 4.23 compares supernatant turbidity at t =24 h for all polymers listed in Table 4.1 at the dosages they performed the best. Each plot in Figure 4.23 refers to a particular mode of CO_2 addition, as described in Section 3.2.6.

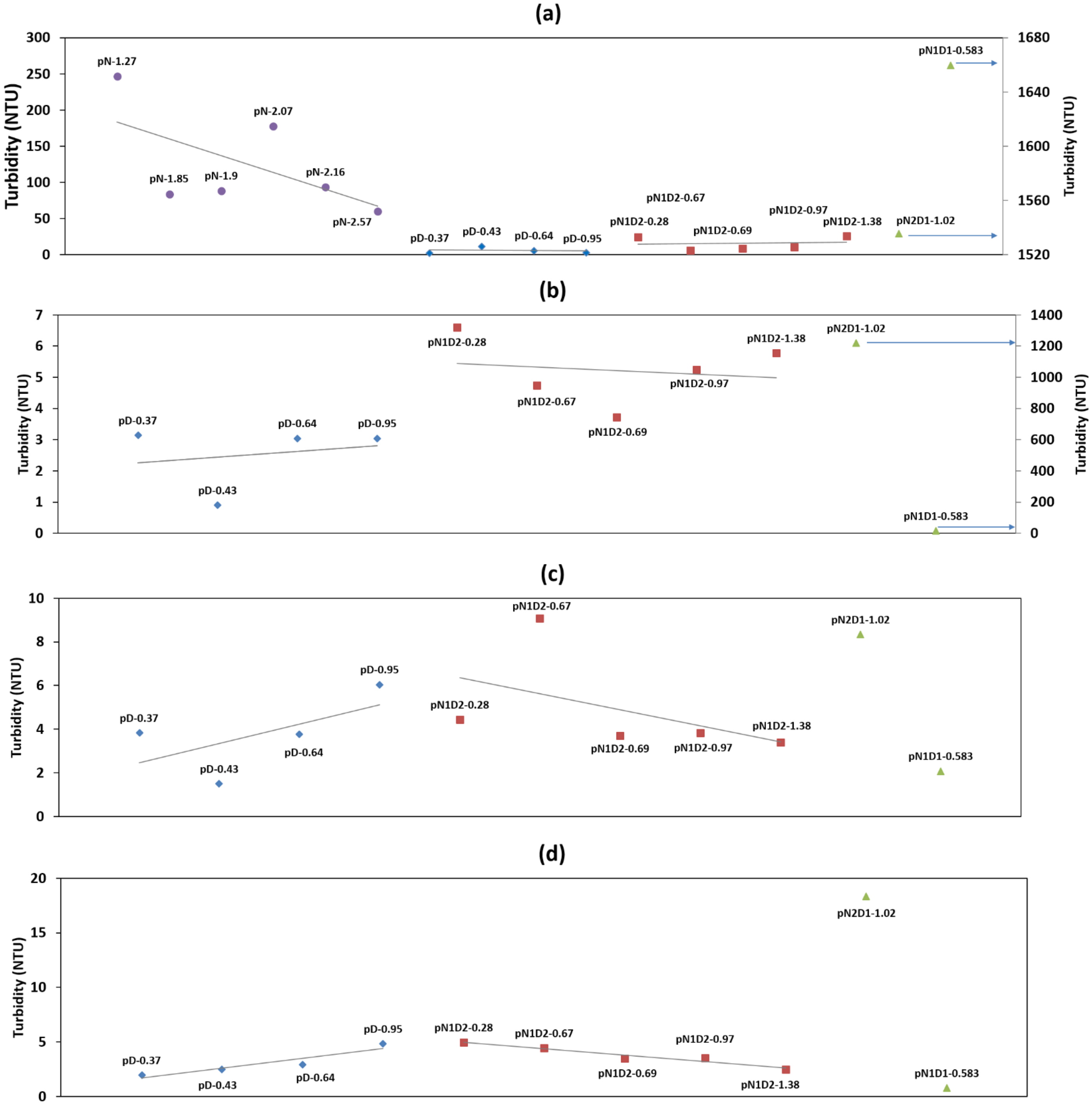

Figure 4.23. Lowest values of supernatant turbidity after $t = 24$ h, under different conditions of CO_2 introduction: **a)** P + MFT **b)** (P+CO_2) + MFT **c)** P + (MFT+CO_2) and **d)** (P+CO_2) + (MFT+CO_2).

The polymers are arranged in order of increasing molecular weights of their respective families. The best dosage for individual polymers at different modes of CO_2 introductions can be found in Appendix D.

Let us consider Figure 4.23 (a), where no CO_2 was used. The polymer with the highest molecular weight, pN-2.57 had the least supernatant turbidity of 60.5 NTU among the NIPAM homopolymers. A significant molecular weight dependence of the turbidity was observed only for NIPAM homopolymers. Molecular weight had a very slight impact for the cationic polymers. With the introduction of CO_2, the changes brought about by molecular weight became negligible (note the change in the scale of Y axis).

Figure 4.24 shows the lowest supernatant turbidity after *t* = 24 h, achieved in each family. The figure is more comprehensible to understand the effects of different polymer types on supernatant turbidity and the effect CO_2 had on them.

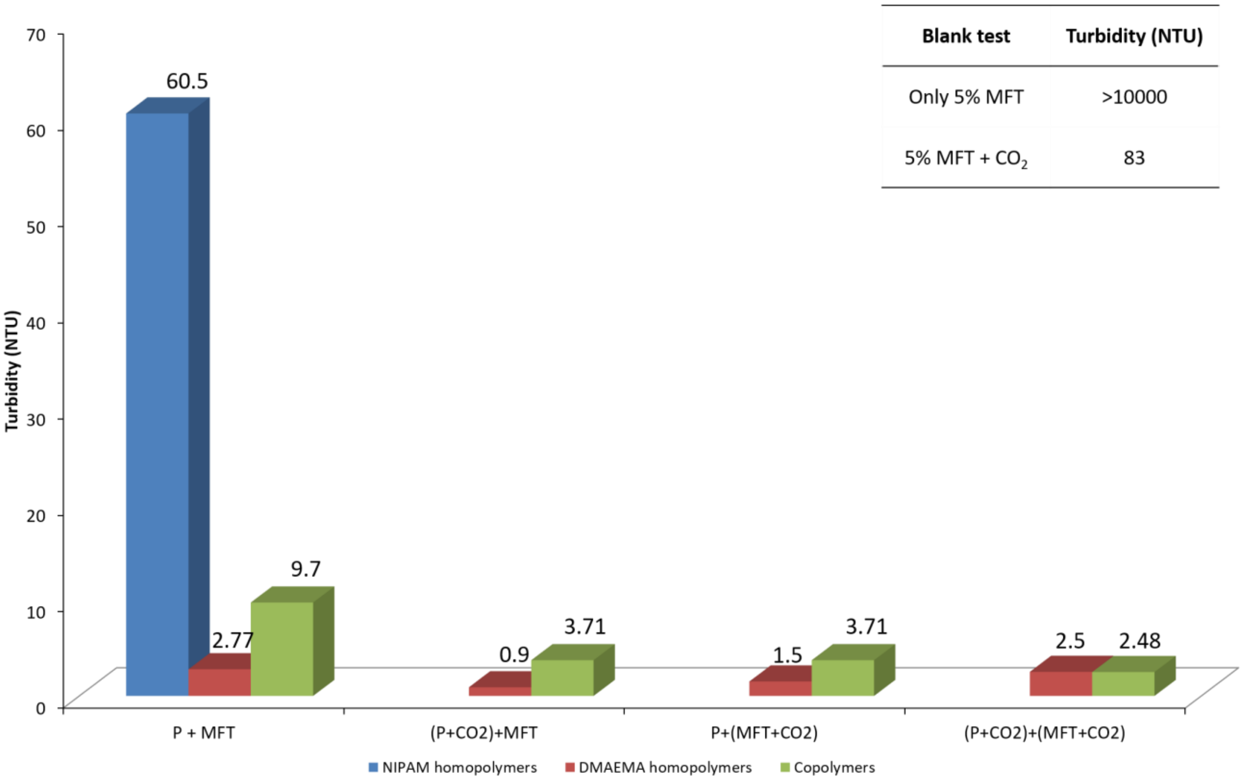

Blank test	Turbidity (NTU)
Only 5% MFT	>10000
5% MFT + CO_2	83

Figure 4.24. Lowest supernatant turbidity *t* = 24 h values observed for pNIPAM, pDMAEMA and copolymers for different modes of CO_2 introduction.

DMAEMA polymer showed a lower turbidity than the NIPAM homopolymer due to the combined effect of bridging and charge neutralization mechanisms that operate DMAEMA polymers' flocculation mechanism. Copolymers with higher NIPAM composition hence had higher supernatant turbidity as compared to pDMAEMA homoplymers. As observed for other flocculation parameters, lower turbidities were achieved with the introduction of CO_2 as compared to the blank (83 NTU). In addition, the dosage required to achieve low values (less than 20 NTU) decreased (refer Appendix D) with the mode of CO_2 introduction.

4.3.4 Effect of CO_2 on flocculation parameters

Figure 4.25 represents the changes in flocculation parameters with different modes of CO_2 introduction, at polymer dosages of 2000 ppm, for the polymers of different families.

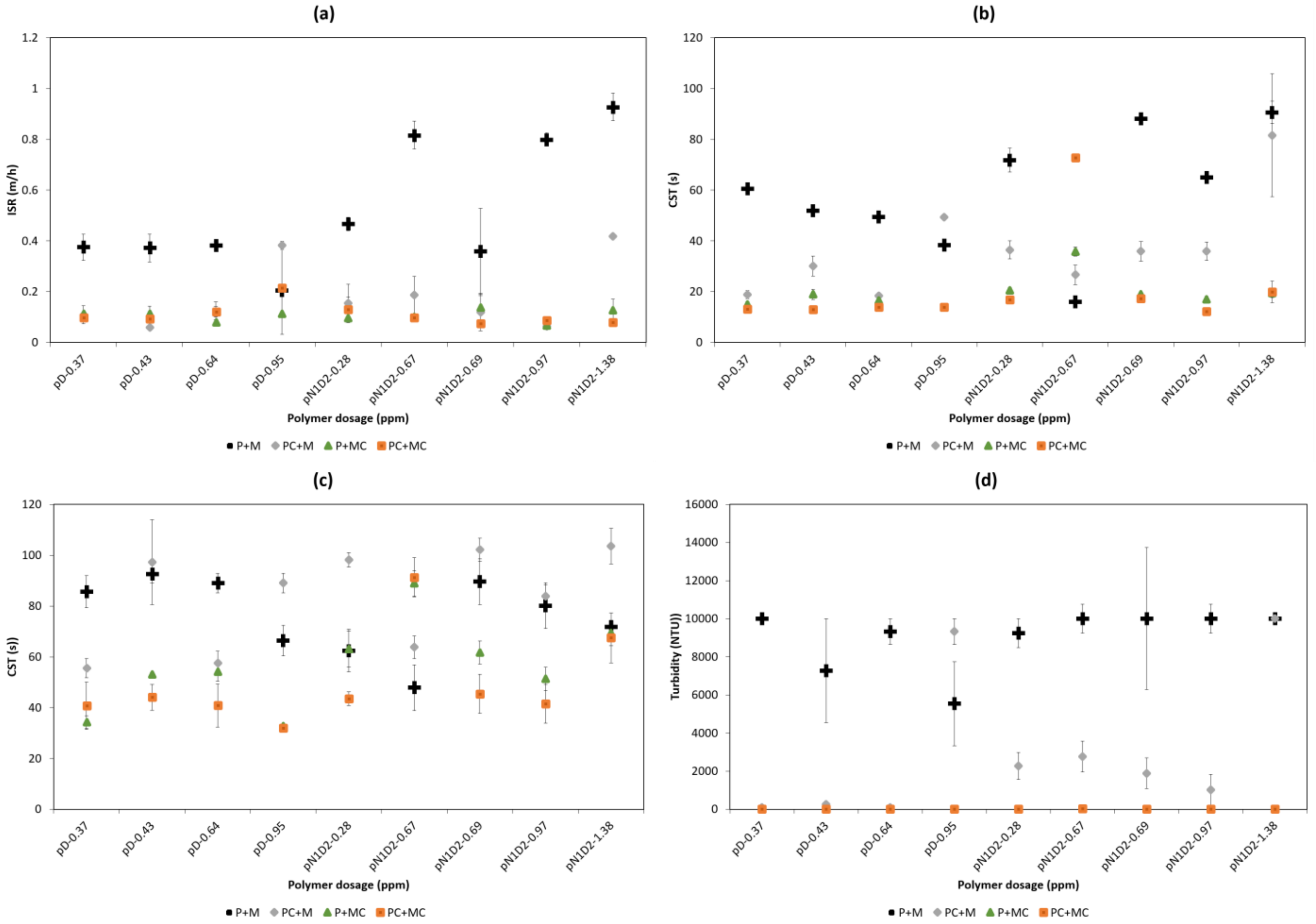

Figure 4.25. Effect of CO_2 on flocculation parameters: **a)** Initial settling rate (ISR) **b)** Capillary suction time (CST) at $t = 0$ **c)** Capillary suction time (CST) at $t = 24$ h **d)** Supernatant turbidity, at a polymer dosage of 2000 ppm.

The trends observed in Figure 4.25 shows a drop for all flocculation parameters: ISR, CST at $t = 0$, CST at $t = 24$ h and supernatant turbidity for majority of the polymers with the introduction of CO_2. Lower CST and turbidity values are desirable for good flocculation performance which were achieved with the introduction of CO_2. However, a low ISR is not a desirable characteristic of a good flocculant. This is one of the disadvantages of using CO_2 as it lowered the ISR for all the cationic polymers.

Figure 4.26 represents the changes in flocculation parameters with different modes of CO_2 introduction, at polymer dosages of 10000 ppm, for the polymers of different families.

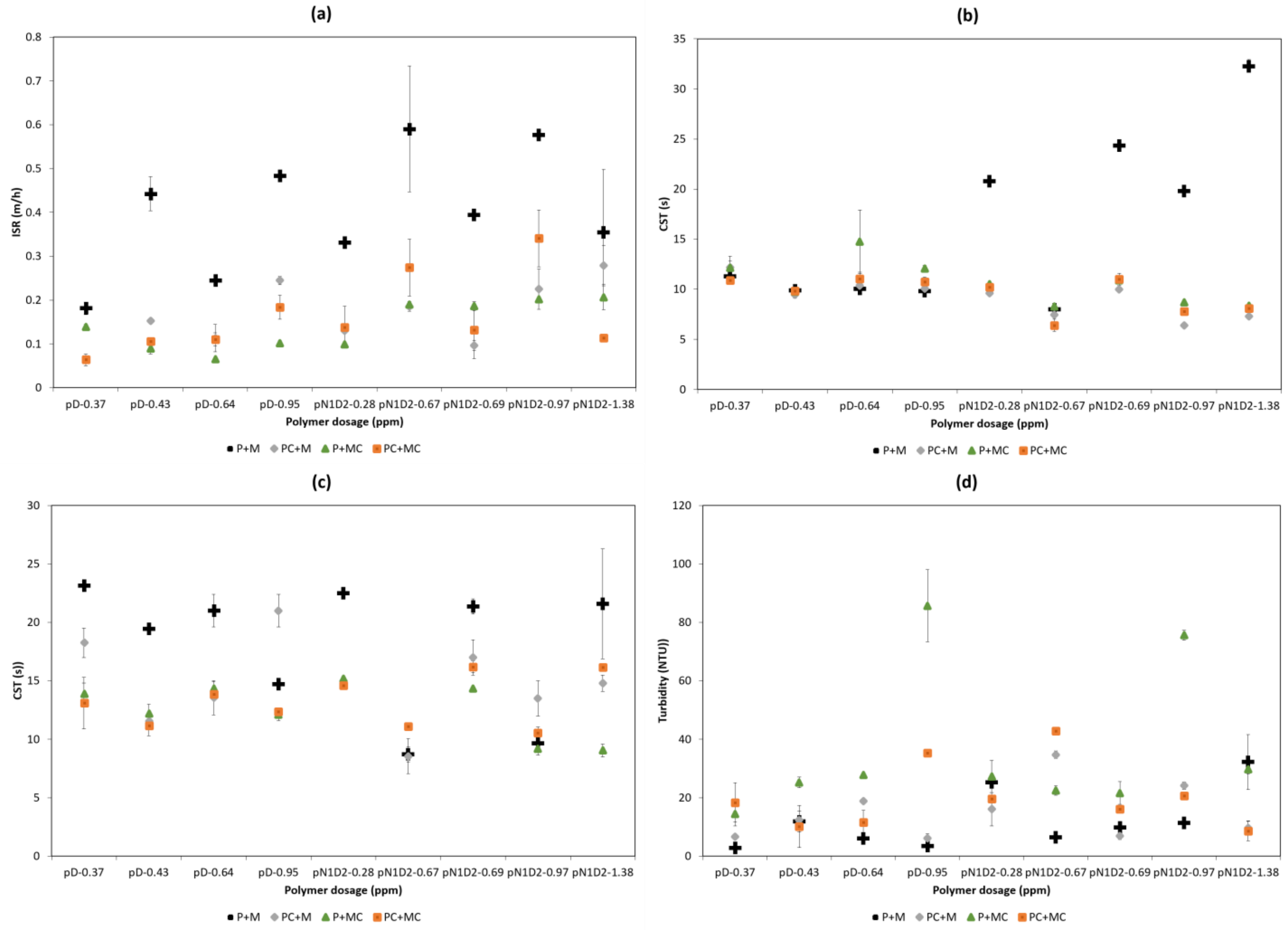

Figure 4.26. Effect of CO_2 on flocculation parameters: **a)** Initial settling rate (ISR) **b)** Capillary suction time (CST) at *t* = 0 **c)** Capillary suction time (CST) at *t* = 24 h **d)** Supernatant turbidity, at a polymer dosage of 10000 ppm for all polymers.

Different observations were made when the polymer dosage was increased to 10000 ppm (Figure 4.26). The difference in between the values of the flocculation parameters were not as wide as in Figure 4.25. The influence of CO_2 on polymer performance got worse for some polymers. For example, majority of the copolymers exhibited the same CST at *t* = 0 values in the presence and absence of CO_2. DMAEMA homopolymers generated CST values of the P+MFT case no different from the cases having CO_2. Polymers pN1D2-0.69 and pN1D2-0.67, among others, showed higher supernatant turbidities with CO_2 introduction. ISR values did not show a significant change with CO_2 addition.

From these observations, it can be concluded that CO_2 at high polymer dosage does not enhance the flocculation characteristics of the polymer by a large extend, and in some cases makes it worse. Lower polymer dosages are to be used in order to tap the benefits of CO_2 to obtain a desirable polymer flocculation performance.

In order to understand this more clearly, consider the figures below. Figure 4.27 shows the effect of CO_2 on the flocculation parameters at low (2000 ppm) and high dosages (10000 ppm) of polymer pD-0.43.

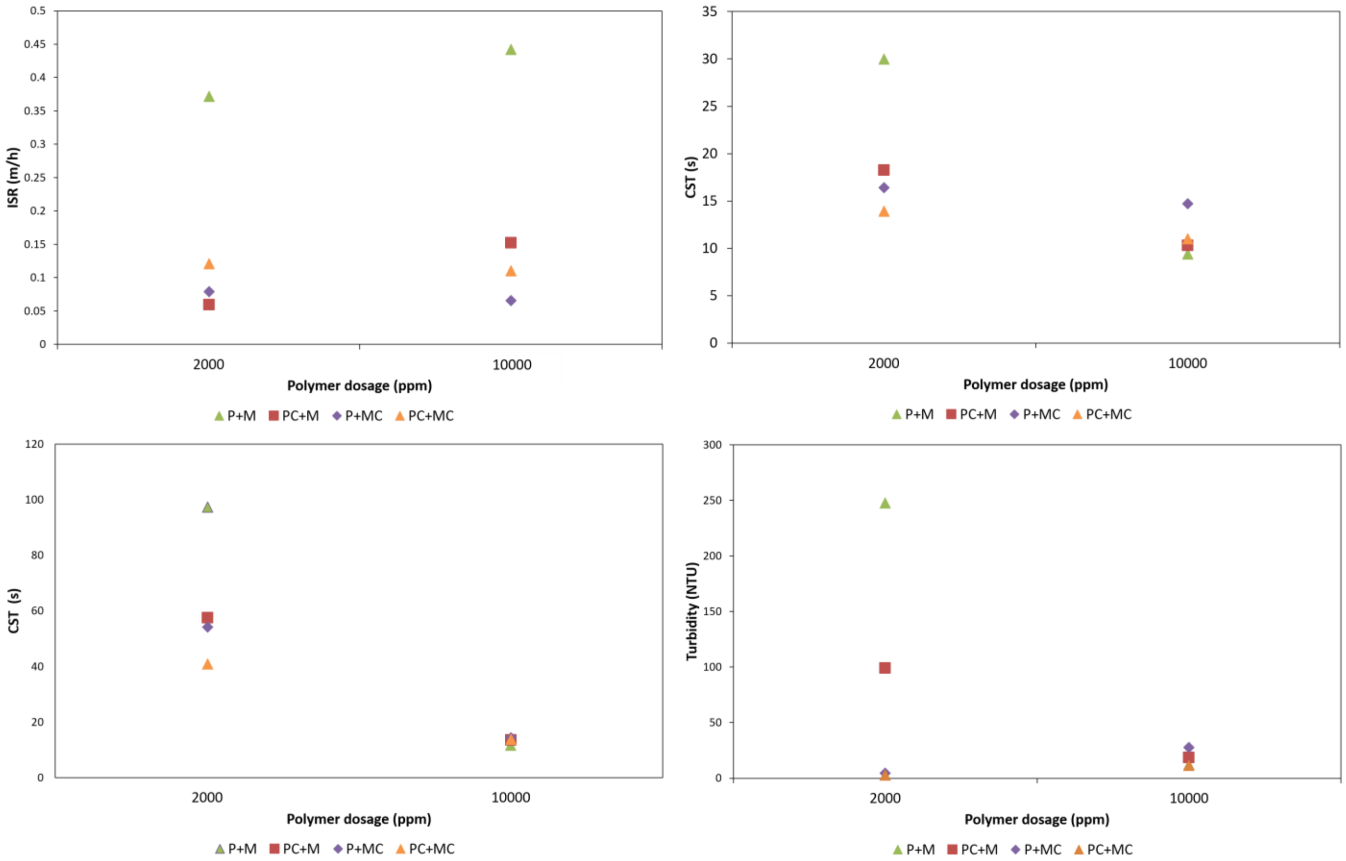

Figure 4.27. Effect of CO_2 on flocculation parameters: **a)** Initial settling rate (ISR) **b)** Capillary suction time (CST) at *t* = 0 **c)** Capillary suction time (CST) at *t* = 24 h **d)** Supernatant turbidity, at 2000 ppm and 10000 ppm polymer dosage of pD-0.43.

With the introduction of CO_2, the ISR falls by a considerable margin (approximately 0.28 m/h). The ISR at low and high dosages of 2000 ppm and 10000ppm respectively, experienced a drop by a similar range. The effect brought about by CO_2 introduction was not very different at low and high dosages for ISR.

However, the CSTs exhibited a different behavior. The effect of CO_2 on these parameters was much more pronounced at lower dosages, compared to higher dosages. The CST values dropped approximately 15 seconds at low dosages whereas, at high dosages, all the four cases had CSTs in close proximity with each other. This effect was more pronounced with CST t = 24 hr. The drop was approximately 40 seconds at low dosages and at high dosages, all the cases' CSTs were nearly the same value. The same was observed for supernatant turbidity.

This can be confirmed with Figure 4.28 which shows the effect of CO_2 on the flocculation parameters at low (2000 ppm) and high dosages (10000 ppm) of polymer pN1D2-0.67.

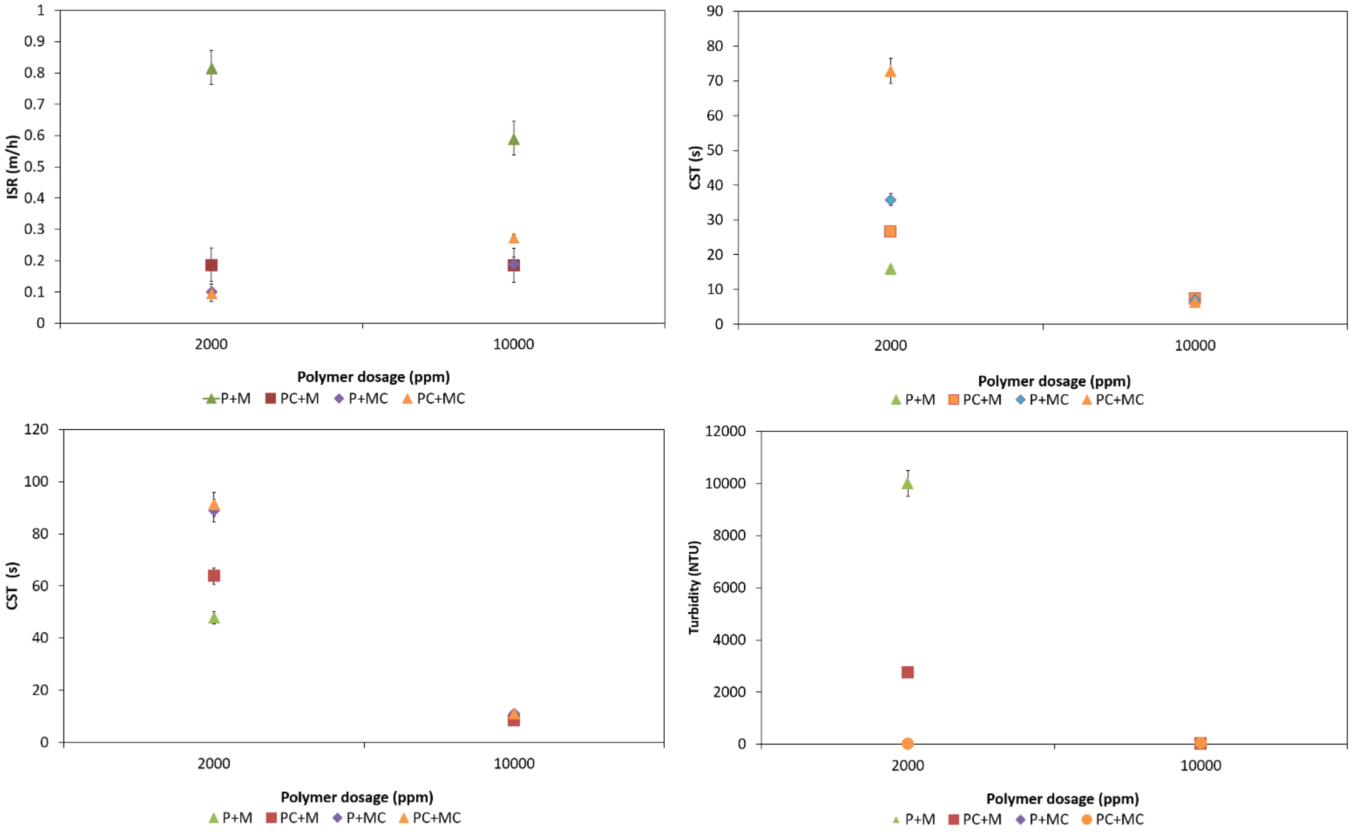

Figure 4.28. Effect of CO_2 on flocculation parameters: **a)** Initial settling rate (ISR) **b)** Capillary suction time (CST) at t = 0 **c)** Capillary suction time (CST) at t = 24 h **d)** Supernatant turbidity, at 2000 ppm and 10000 ppm polymer dosage of pN1D2-0.67.

These two polymers were chosen as they had the best performance as flocculants (explained later, in Section 4.3.6). Introduction of CO_2 at low dosages gave rise to a wider range in ISR, CST and turbidity, as observed in the Figure 4.22. This shows that low dosage seem more advantageous than high dosages when it comes to tapping the benefits of using CO_2.

4.3.5 Polymer blends

Table 4.7 lists the polymers that had the best performance for the different flocculation parameters in this work. These polymer were chosen on the values each of them generated, under different conditions of CO_2 introduction, for the flocculation parameter: ISR, CST at t = 0, CST at t = 24 h and supernatant turbidity.

Table 4.7. List of the best performing polymers.

	pNIPAM	**pDMAEMA**	**NIPAM/DMAEMA Copolymers**
ISR	pN-2.07/pN-2.57	pD-0.95	pN1D2-1.38/pN1D2-0.97
CST t=0	pN-2.57	pD-0.43	pN1D2-0.67/pN1D2-0.97
CST t=24	pN-2.57	pD-0.43	pN1D2-0.67
Turbidity	pN-2.57	pD-0.43	pN1D2-1.38/pN1D1-1.03

The polymers that produced the best value (highest ISR and least CST and turbidity) among all the four cases of CO_2 introduction, were considered as the best polymers in their respective families. The solids content was determined for pD-0.43 at 10000 ppm to achieve a value of 51%. This preliminary test showed that some compaction was achieved which led to usage of these polymers in other forms, such as blends.

Among the homopolymers, pN-2.57 and pD-0.43 were the better performers, while pN1D2-0.67 and pN1D2-0.97 were selected as the best copolymers. However, comparing the performance of pN1D2-0.67 and pN1D2-0.97, pN1D2-0.67 achieved values in close proximity for majority of the flocculation parameters at different dosages. This implies that similar (desirable) results can be achieved at lower dosages using this polymer. Due to this reason, pN1D2-0.67 was declared the better performing polymer among the two. Comparing the performance of the DMAEMA homopolymers with the copolymers, the copolymers produced better numbers for ISR and CST as compared to the homopolymers.

The best mode of CO_2 addition was P + (MFT+CO_2), where CO_2 was contacted directly with MFT but not the polymer solution. This mode generated lower CSTs and supernatant turbidities. The "best" dosage was selected as 6000 ppm, since increasing it to 10,000 did not substantially affect the performance of these flocculants.

The flocculation performance of polymer blends are tabulated in Table 4.8.

Table 4.8. Performance of polymer blends versus their individual components

	pN-2.57	**pD-0.43**	**pN1D2-0.67**	**pN-2.57/ pD-0.43 blend**	**pN-2.57/ pN1D2-0.67 blend**
ISR	2.26	0.12	0.11	4.59	6.22
(m/h)	(1500 ppm)	(6000 ppm)	(6000 ppm)	(80/ 20)	(40/ 60)
CST t=0	24.45	10.15	8.30	9.90	10.40
(s)	(1000 ppm)	(6000 ppm)	(6000 ppm)	(40/ 60)	(20/ 80)
CST t=24	60.80	15.00	19.35	7.30	6.70
(s)	(2000 ppm)	(6000 ppm)	(6000 ppm)	(60/ 40)	(40/ 60)
Turbidity	60.80	1.50	18.30	8.20	29.20
(NTU)	(750ppm)	(6000 ppm)	(6000 ppm)	(40/ 60)	(80/ 20)

Polymer blends of pN-2.57 + pD-0.43 and of pN-2.57 + pN1D2-0.67 were prepared at different ratios to obtain a final polymer dosage of 6000 ppm, which was added to the MFT after bubbling it with CO_2.

The MFT was mixed with the polymers at 300 rpm for 1 minute as this was sufficient to notice a visible formation of flocs. The values for ISR, CST at $t = 0$, CST at $t = 24$ h, and turbidity of the blends were measured and compared with those of individual components at the same dosage and conditions. There was a significant increase in the ISR for the polymer blends, which was higher than for the individual components, indicating a synergistic effect. The CST for the blends also improved, but to a much lower extent than for ISR. Finally, the turbidity obtained with the blends, while still acceptable, was not improved as much, and in some cases was worse than for some of the blend constituents. It may be concluded, however that the polymer blends overall performed better than their individual components. In addition, the condition employed for mixing these polymers with MFT, P + (MFT+CO_2), is similar to the one practiced by CNRL, which make this approach attractive for scaling up to industrial conditions.

5. CONCLUSIONS

The synthesized polymers were tested under different methods of CO_2 introduction. Under these different conditions, the polymers were tested on mature fine tailings (5% solids) to study flocculation parameters such as initial settling rate (ISR), capillary suction time (CST) and turbidity of the supernatant.

Initial settling rate (ISR) increased with an increase in dosage up until an “optimum dosage” beyond which they began to drop. Capillary suction time (CST) decreased with increase in polymer dosage and began to increase with an increase in dosage beyond an optimum value. The same was observed in case of supernatant turbidity.

NIPAM homopolymer had the highest ISR whereas better CST and turbidity readings were achieved by the cationic polymers. DMAEMA homopolymer had the lowest turbidities due to their cationic nature at low pH. Among the cationic polymers, the copolymers had a higher settling rate than the homopolymer due to compositional advantage of having NIPAM in their polymer chain. DMAEMA homopolymers had the lowest turbidities among the other polymers.

From the study, a change in polymer performance was observed, thus indicating the polymers were responsive to pH changes brought about by CO_2. It was observed that introduction of CO_2 helped in achieving lower CST and turbidity values. However, introduction of CO_2 lowered the ISR, among which, introduction of CO_2 through the MFT solution showed better results for ISR, CST and turbidity measurements than when CO_2 being introduced through the polymer solution (or without any CO_2 introduction at all).

Molecular weight dependence of the flocculation parameters was investigated in this study. Molecular weight had a significant impact on all the flocculation parameters for NIPAM homopolymers. There was significant rise in ISR and drop in CST and turbidity readings with molecular weight when NIPAM homopolymers were used as flocculant. However, molecular weight had a significant impact only on the ISR for the DMAEMA homopolymers and copolymers. ISR increased with increase in molecular weight for the cationic polymers although not as significantly as for NIPAM homopolymers. Molecular weight had a negligible impact on the CST and supernatant turbidity for the cationic polymers. These molecular weight dependencies were observed for a miniature molecular weight range of approximately 1 million Daltons.

Polymer blends of the homopolymers performed better than the copolymers in terms of ISR and CST measurements. These polymers were achieved a 175% increase in ISR and 65.4% in CST measurements. A higher increase was observed when the homopolymers were used as blends with the copolymers. However, the turbidity of the supernatant did not show a substantial increase in its value but was within acceptable limits.

These polymers showed better results as compared to the controls used and functioned even better when used as blends.

Through this study these polymers may find applications as effective flocculants for oil sands tailings treatment along with other applications that require a pH change.

6. FUTURE WORK

There are many aspects to this project that can be studied further:

Only one stimuli was studied (pH sensitivity using CO_2) but literature states that dual stimuli responsive polymers function better (Han, Tong, & Zhao, 2012) than single stimuli responsive polymer. This was the main reason for finalizing thermosensitive monomers as temperature sensitivity and pH sensitivity can work hand in hand. Keeping this in mind, flocculation performance of the copolymer can be studied by altering both, the pH and the temperature, to obtain an optimized performance.

The pH sensitivity of the polymers can be studied by altering the quantity of CO_2 in the system. Through this study, charge densities of the polymers can be controlled by determining the extent to which the polymer gets protonated.

The polymers synthesized can be synthesized in a more controlled manner using techniques such as atom transfer reversible polymerization (ATRP) or Reversible addition fragmentation chain-transfer polymerization (RAFT) to obtain well defined polymers in terms of composition and molecular weight.

Using these highly controlled polymerization techniques, novel polymers with the desired characteristics (for example, uniform molecular weight distributions and biodegradable polymers) can be synthesized.

Polymer dosages were studied from a range of 2000 ppm to 10,000 ppm in intervals of 2000 ppm. Intermediate or lower dosages can be studied to determine finer trends of the parameters that were measured.

The MFT samples that were used were diluted to 5% solids. The solids content can be increased to study the effect of dilution on flocculation parameters.

7. BIBLIOGRAPHY

Adin, A., Soffer, Y., & Aim, R. Ben. (1998). Effluent pretreatment by iron coagulation applying various dose-pH combinations for optimum particle separation. *Water Science and Technology*. https://doi.org/10.1016/S0273-1223(98)00564-2

Alamgir, A., Harbottle, D., Masliyah, J., & Xu, Z. (2012). Al-PAM assisted filtration system for abatement of mature fine tailings. *Chemical Engineering Science*, *80*, 91–99. https://doi.org/10.1016/j.ces.2012.06.010

Alberta Energy Regulator. (2015). ST98-2015: Alberta's Energy Reserves 2014 and Supply/Demand Outlook 2015-2024. *Alberta's Energy Reserves 2014 and Supply/Demand Outlook*, 299.

Alberta Government. (2009). Environmental management of Alberta's oil sands, 1–26. Retrieved from http://www.environment.gov.ab.ca/info/library/8042.pdf

Allen, E. W. (2008). Process water treatment in Canada's oil sands industry: II. A review of emerging technologies. *Journal of Environmental Engineering and Science*, *7*(5), 499–524. https://doi.org/10.1139/S08-020

Baines, F. L., Billingham, N. C., & Armes, S. P. (1996). Synthesis and Solution Properties of Water-Soluble Hydrophilic-Hydrophobic Block Copolymers. *Macromolecules*, *29*(2 mL), 3416–3420. https://doi.org/10.1021/ma951699+

Besra, L., Sengupta, D. K., Singh, B. P., & Bhattacharjee, S. (2005). A novel method based on Capillary Suction Time (CST) for assessment of dispersion characteristics of suspensions. *Journal of the American Ceramic Society*, *88*(1), 109–113. https://doi.org/10.1111/j.1551-2916.2004.00008.x

BGC Engineering Inc. (2010). Oil Sands Tailings Technology Review. *Oil Sands Research and Information Network*, *OSRIN Repo*(July), OSRIN Report No. TR-1. 136 . https://doi.org/OSRIN Report No. TR-1

Bogoeva-Gaceva, G., & Andonova, A. (1993). Synthesis and properties of polyelectrolytes based on dimethylaminoethyl methacrylate quaternary salt. *Polymer*, *34*(18), 3934–3939. https://doi.org/10.1016/0032-3861(93)90523-D

Bolto, B., & Gregory, J. (2007). Organic polyelectrolytes in water treatment. *Water Research*, *41*(11), 2301–2324. https://doi.org/10.1016/j.watres.2007.03.012

Botha, L., & Soares, J. B. P. (2015). The Influence of Tailings Composition on Flocculation. *Canadian Journal of Chemical Engineering*, *93*(9), 1514–1523. https://doi.org/10.1002/cjce.22241

Buscall, R., & Corner, T. (1982). The phase-separation behaviour of aqueous solutions of polyacrylic acid and its partial sodium salts in the presence of sodium chloride. *European Polymer Journal*, *18*(11), 967–974. https://doi.org/10.1016/0014-3057(82)90084-2

Chécot, F., Lecommandoux, S., Gnanou, Y., & Klok, H. A. (2002). Water-soluble stimuli-responsive vesicles from peptide-based diblock copolymers. *Angewandte Chemie - International Edition*, *41*(8), 1339–1343. https://doi.org/10.1002/1521-3773(20020415)41:8<1339::AID-ANIE1339>3.0.CO;2-N

Chalaturnyk, R. J., Don Scott, J., & Özüm, B. (2002). Management of Oil Sands Tailings. *Petroleum Science and Technology*, *20*(9–10), 1025–1046. https://doi.org/10.1081/LFT-120003695

Chen, D., P, K. J., Kory, M. M., & Ely, D. L. (1989). Amphiphilic networks : II. Biocompatibility and controlled drug release of. *Journal of Biomedical Materials Research*, *23*, 1327–1342.

Cherng, J. Y., Van De Wetering, P., Talsma, H., Crommelin, D. J. a, & Hennink, W. E. (1996). Effect of size and serum proteins on transfection efficiency of poly ((2-dimethylamino) ethyl methacrylate)-plasmid nanoparticles. *Pharmaceutical Research*. Retrieved from http://www.springerlink.com/index/U56H778170368K3W.pdf

Clark, E. A., & Lipson, J. E. G. (2012). LCST and UCST behavior in polymer solutions and blends. *Polymer*, *53*(2), 536–545. https://doi.org/10.1016/j.polymer.2011.11.045

Creutz, S., Teyssié, P., & Jérôme, R. (1997). Living anionic homo- and block copolymerization of 2-(tert-butylamino) ethyl methacrylate. *Journal of Polymer Science Part A: Polymer Chemistry*, *35*(10), 2035–2040. https://doi.org/DOI: 10.1002/(SICI)1099-0518(19970730)35:10<2035::AID-POLA18>3.0.CO;2-H

Dai, S., Ravi, P., & Tam, K. C. (2008). pH-Responsive polymers: synthesis, properties and applications. *Soft Matter*, *4*(3), 435. https://doi.org/10.1039/b714741d

Dentel, S. K. (1991). Coagulant control in water treatment. *Critical Reviews in Environmental Control*, *21*(1), 41–135. https://doi.org/10.1080/10643389109388409

Fong, N., Ng, S., Chung, K. H., Tu, Y., Li, Z., Sparks, B. D., & Kotlyar, L. S. (2004). Bitumen recovery from model systems using a warm slurry extraction process: Effects of oilsands components and process water chemistry. *Fuel*, *83*(14–15 SPEC. ISS.), 1865–1880. https://doi.org/10.1016/j.fuel.2003.09.025

Froment, G. F. (1989). Methane Steam Reforming, Methanation and Water-Gas Shift : 1 . Intrinsic Kinetics, *35*(1), 88–96.

Guangyue, L., Shangqi, L. I. U., Pingping, S., Yang, L. I. U., & Yanyan, L. U. O. (2016). A new optimization method for steam-liquid level intelligent control model in oil sands steam-assisted gravity drainage (SAGD) process, *43*(2), 301–307.

Guo, J. (2015). Design, synthesis, characterization of a new pH-responsive copolymer and its application in oil sands tailings treatment. https://doi.org/10.1007/s13398-014-0173-7.2

Hach Company. (2012a). Model 2100AN Laboratory Turbidimeter: Instrument Manual, 2000–2006. Retrieved from http://download.sechang.com/pds/inventory/785/785_1643.pdf

Hach Company. (2012b). Model 2100AN Laboratory Turbidimeter: Instrument Manual, 2000–2006.

Han, D., Tong, X., Boissiere, O., & Zhao, Y. (2012). General strategy for making CO2-switchable polymers. *ACS Macro Lett.*, *1*(Copyright (C) 2012 American Chemical Society (ACS). All Rights Reserved.), 57–61. https://doi.org/10.1021/mz2000175

Han, D., Tong, X., & Zhao, Y. (2012). Block copolymer micelles with a dual-stimuli-responsive core for fast or slow degradation. *Langmuir*, *28*(5), 2327–2331. https://doi.org/10.1021/la204930n

Henderson, J. M., & Wheatley, A. D. (1987). Factors Affecting the Efficient Flocculation of Tailings By Polyacrylamides. *Coal Preparation*, *4*(1–2), 1–49. https://doi.org/10.1080/07349348708945525

Hinrichs, W. L. J., Wetering, P. Van De, & Hennink, W. E. (1999). Thermosensitive polymers as carriers for DNA delivery, *60*, 249–259.

Kammer, H.-W., Inoue, T., & Ougizawa, T. (1989). Upper and lower critical solution temperature behaviour in polymer blends and its thermodynamic interpretation. *Polymer*, *30*(5), 888–892. https://doi.org/10.1016/0032-3861(89)90187-0

Kasongo, T., Zhou, Z., Xu, Z., & Masliyah, J. (2000). Effect of clays and calcium ions on bitumen extraction from Athabasca oil sands using flotation. *Can. J. Chem. Eng.*, *78*(August), 674–681. https://doi.org/10.1002/cjce.5450780409

Konan, K. L., Peyratout, C., Bonnet, J. P., Smith, A., Jacquet, A., Magnoux, P., & Ayrault, P. (2007). Surface properties of kaolin and illite suspensions in concentrated calcium hydroxide medium. *Journal of Colloid and Interface Science*, *307*(1), 101–108. https://doi.org/10.1016/j.jcis.2006.10.085

Li, H., Long, J., Xu, Z., & Masliyah, J. H. (2005). Synergetic Role of Polymer Flocculant in Low-Temperature Bitumen Extraction and Tailings Treatment, (6), 936–943.

Li, H., Long, J., Xu, Z., & Masliyah, J. H. (2007). Flocculation of Kaolinite Clay Suspensions Using a Temperature-Sensitive Polymer, *53*(2), 479–488. https://doi.org/10.1002/aic

Liu, F., & Eisenberg, A. (2003). Preparation and pH triggered inversion of vesicles from poly (acrylic acid)-b lock-polystyrene-b lock-Poly (4-vinyl pyridine). *Journal of the American Chemical Society*, *125*(49), 15059–15064.

Liu, Q., Yu, Z., & Ni, P. (2004). Micellization and applications of narrow-distribution poly[2-(dimethylamino)ethyl methacrylate]. *Colloid and Polymer Science*, *282*(4), 387–393. https://doi.org/10.1007/s00396-003-0956-4

Long, J., Li, H., Xu, Z., & Masliyah, J. H. (2006). Role of Colloidal Interactions in Oil Sand Tailings Treatment, *52*(1), 371–383. https://doi.org/10.1002/aic.10603

Long, J., Li, H., Xu, Z., & Masliyah, J. H. (2011). Improving oil sands processability using a temperature-sensitive polymer. *Energy and Fuels*, *25*(2), 701–707. https://doi.org/10.1021/ef1012819

MacKinnon, Matthews, Shaw, & Cuddy. (2001). Water Quality Issues Associated With

Composite Tailings (CT) Technology for Managing Oil Sands Tailings. *International Journal of Surface Mining, Reclamation and Environment*, *15*(4), 235–256. https://doi.org/10.1076/ijsm.15.4.235.7416

Masliyah, J. H, Xu, Z., Czarnecki, J. A, & Dabros, M. (2011). *Handbook on theory and practice of bitumen recovery from Athabasca Oil Sands*.

Meewes, M., Ricka, J., De Silva, M., Nyffenegger, R., & Binkert, T. (1991). Coil-globule transition of poly(N-isopropylacrylamide): a study of surfactant effects by light scattering. *Macromolecules*, *24*(21), 5811–5816. https://doi.org/10.1021/ma00021a014

Meléndez-Ortiz, H. I., & Bucio, E. (2008). Radiation synthesis of a thermo-pH responsive binary graft copolymer (PP-g-DMAEMA)-g-NIPAAm by a two step method. *Polymer Bulletin*, *61*(5), 619–629. https://doi.org/10.1007/s00289-008-0982-y

Mpofu, P., Addai-Mensah, J., & Ralston, J. (2004). Flocculation and dewatering behaviour of smectite dispersions: Effect of polymer structure type. *Minerals Engineering*, *17*(3), 411–423. https://doi.org/10.1016/j.mineng.2003.11.010

O'Shea, J. P., Qiao, G. G., & Franks, G. V. (2010). Solid-liquid separations with a temperature-responsive polymeric flocculant: Effect of temperature and molecular weight on polymer adsorption and deposition. *Journal of Colloid and Interface Science*, *348*(1), 9–23. https://doi.org/10.1016/j.jcis.2010.04.063

Oh, J., Lee, H., Shim, H., & Choi, S. (1994). Synthesis and surface activity of novel ABA type triblock cationic amphiphiles. *Polymer Bulletin*, 32, 149–154.

Orakdogen, N. (2011). PH-responsive swelling behavior, elasticity and molecular characteristics of poly(N,N-dimethylaminoethyl methacrylate) gels at various initial monomer concentrations. *Polymer Bulletin*, *67*(7), 1347–1366. https://doi.org/10.1007/s00289-011-0559-z

Parviainen, H., Hiltunen, M., & Maunu, S. L. (2014). Preparation and Flocculation Behavior of Cellulose-g-PMOTAC Copolymer, *40448*, 1–7. https://doi.org/10.1002/app.40448

Proskin, S., Sego, D., & Alostaz, M. (2010). Cold Regions Science and Technology Freeze – thaw and consolidation tests on Suncor mature fi ne tailings (MFT). *Cold Regions Science* *and Technology*, *63*(3), 110–120. https://doi.org/10.1016/j.coldregions.2010.05.007

Reis, L. G., Oliveira, R. S., Palhares, T. N., Spinelli, L. S., Lucas, E. F., Vedoy, D. R. L., … Soares, J. B. P. (2016). Using acrylamide/propylene oxide copolymers to dewater and densify mature fine tailings. *Minerals Engineering*, *95*, 29–39. https://doi.org/10.1016/j.mineng.2016.06.005

Saidi-Mehrabad, A., He, Z., Tamas, I., Sharp, C. E., Brady, A. L., Rochman, F. F., … Dunfield, P. F. (2013). Methanotrophic bacteria in oilsands tailings ponds of northern Alberta. *The ISME Journal*, *7*(5), 908–21. https://doi.org/10.1038/ismej.2012.163

Sakohara, S., Kawachi, T., Gotoh, T., & Iizawa, T. (2013). Consolidation of suspended particles by using dual ionic thermosensitive polymers with incorporated a hydrophobic component. *Separation and Purification Technology*, *106*, 90–96. https://doi.org/10.1016/j.seppur.2012.12.030

Sawalha, O., & Scholz, M. (2010). Modeling the Relationship between Capillary Suction Time and Specific Resistance to Filtration. *Journal of Environmental Engineering*, *136*(9), 983–991. https://doi.org/10.1061/(ASCE)EE.1943-7870.0000223

Scardina, Paolo; Edwards, M. (1999). Prediction And Measurement Of Bubble Formation In Water Treatment. *New York*, *125*(December), 1149–1159.

Schild, H. G. (1992). Poly (N-Isopropylacrylamide): Experiment, Theory and Application. *Prog. Polym. Sci.*, *17*, 163–249. https://doi.org/10.1016/0079-6700(92)90023-R

Seuring, J., & Agarwal, S. (2012a). 14. *Macromolecular Rapid Communications*, *33*(22), 1898–1920. https://doi.org/10.1002/marc.201200433

Seuring, J., & Agarwal, S. (2012b). Polymers with upper critical solution temperature in aqueous solution. *Macromol. Rapid Commun.*, *33*(22), 1898–1920. https://doi.org/10.1002/marc.201200433

Sevimli, S., Sagnella, S., Kavallaris, M., Bulmus, V., & Davis, T. P. (2012). Synthesis, self-assembly and stimuli responsive properties of cholesterol conjugated polymers. *Polymer Chemistry*, *3*(8), 2057. https://doi.org/10.1039/c2py20112g

Shen, C. (2013). *SAGD for Heavy Oil Recovery. Enhanced Oil Recovery Field Case Studies*

(First Edit). Elsevier Inc. https://doi.org/10.1016/B978-0-12-386545-8.00017-8

Shen, H., Zhang, L., & Eisenberg, A. (1999). Multiple pH-Induced Morphological Changes in Aggregates of Polystyrene- block -poly(4-vinylpyridine) in DMF/H_2O Mixtures. *Journal of the American Chemical Society*, *121*(12), 2728–2740. https://doi.org/10.1021/ja983712m

Smith, W. V, & Ewart, R. H. (1948). Kinetics of Emulsion Polymerization Kinetics of Emulsion Polymerization. *The Journal of Chemical Physics*, *16*(4), 592. https://doi.org/10.1063/1.1746951

Smollen, M. (1986). Dewaterability of municipal sludges - a comparitive study of specific resistance to filtration and capillary suction time as dewaterability parameters. *Water SA*.

Sworska, A., Laskowski, J. S., & Cymerman, G. (2000). Flocculation of the Syncrude fine tailings Part I. Effect of pH, polymer dosage and Mg^{2+}, 143–152.

Timoney, K. P., & Lee, P. (2009). Does the Alberta Tar Sands Industry Pollute? The Scientific Evidence. *The Open Conservation Biology Journal*, *3*, 65–81. https://doi.org/10.2174/1874839200903010065

Vajihinejad, V., Guillermo, R., & Soares, B. P. (2017). Dewatering Oil Sands Mature Fine Tailings (MFTs) with Poly(acrylamide- co -diallyldimethylammonium chloride): Effect of Average Molecular Weight and Copolymer Composition. https://doi.org/10.1021/acs.iecr.6b04348

Van De Wetering, P., Cherng, J. Y., Talsma, H., Crommelin, D. J. A., & Hennink, W. E. (1998). 2-(Dimethylamino)Ethyl Methacrylate Based (Co)Polymers As Gene Transfer Agents. *Journal of Controlled Release*, *53*(1–3), 145–153. https://doi.org/10.1016/S0168-3659(97)00248-4

Van Durme, K., Van Assche, G., Nies, E., & Van Mele, B. (2007). Phase transformations in aqueous low molar mass poly(vinyl methyl ether) solutions: Theoretical prediction and experimental validation of the peculiar solvent melting line, bimodal LCST, and (adjacent) UCST miscibility gaps. *Journal of Physical Chemistry B*, *111*(6), 1288–1295. https://doi.org/10.1021/jp063322j

Vedoy, D. R. L., & Soares, J. B. P. (2015). Water-soluble polymers for oil sands tailing treatment: A Review. *Canadian Journal of Chemical Engineering*, *93*(5), 888–904.

https://doi.org/10.1002/cjce.22129

Veillet, S., Tomao, V., Ruiz, K., & Chemat, F. (2010). Green procedure using limonene in the Dean-Stark apparatus for moisture determination in food products. *Analytica Chimica Acta*, *674*(1), 49–52. https://doi.org/10.1016/j.aca.2010.06.009

Wang, C., Harbottle, D., Liu, Q., & Xu, Z. (2014). Current state of fine mineral tailings treatment: A critical review on theory and practice. *Minerals Engineering*, *58*, 113–131. https://doi.org/10.1016/j.mineng.2014.01.018

Wang, X. T., Feng, X., Xu, Z., & Masliyah, J. H. (2010). Polymer Aids for Settling and Filtration of oil Sands Tailings, *88*(JUNE), 403–410. https://doi.org/10.1002/cjce.20283

Ward, M. A., & Georgiou, T. K. (2011). Thermoresponsive polymers for biomedical applications. *Polymers*, *3*(3), 1215–1242. https://doi.org/10.3390/polym3031215

Yan, Q., Zhou, R., Fu, C., Zhang, H., Yin, Y., & Yuan, J. (2011). CO_2-responsive polymeric vesicles that breathe. *Angewandte Chemie - International Edition*, *50*(21), 4923–4927. https://doi.org/10.1002/anie.201100708

Yang, J. M., Jong, Y. J., & Hsu, K. Y. (1997). Preparation and properties of SBS-g-DMAEMA copolymer membrane by ultraviolet radiation. *Journal of Biomedical Materials Research*, *35*(2), 175–180. https://doi.org/10.1002/(SICI)1097-4636(199705)35:2<175::AID-JBM5>3.0.CO;2-K

Yoshimitsu, H., Kanazawa, A., Kanaoka, S., & Aoshima, S. (2012). Well-defined polymeric ionic liquids with an upper critical solution temperature in water. *Macromolecules*, *45*(23), 9427–9434. https://doi.org/10.1021/ma301746u

Zhang, L., Barlow, R. J., & Eisenberg, A. (1995). Scaling relations and coronal dimensions in aqueous block polyelectrolyte micelles. *Macromolecules*, *28*(18), 6055–6066. https://doi.org/10.1021/ma00122a010

Zhang, Q., Schattling, P., Theato, P., & Hoogenboom, R. (2015). UV-tunable upper critical solution temperature behavior of azobenzene containing poly(methyl methacrylate) in aqueous ethanol. *European Polymer Journal*, *62*(6), 435–441. https://doi.org/10.1016/j.eurpolymj.2014.06.029

Zhu, R., Liu, Q., Xu, Z., Masliyah, J. H., & Khan, A. (2011). Role of dissolving carbon dioxide in densification of oil sands tailings. *Energy and Fuels*, *25*(5), 2049–2057. https://doi.org/10.1021/ef200203f

Zırıh, T., & Orakdogen, N. (2016). Evaluation of pH / temperature double responsivity of copolymerized methacrylate-based networks : Solvent diffusion analysis with adjustable swelling kinetics. *European Polymer Journal*, *75*, 371–387. https://doi.org/10.1016/j.eurpolymj.2016.01.011

APPENDIX A: DOSAGES FOR BEST ISR VALUES

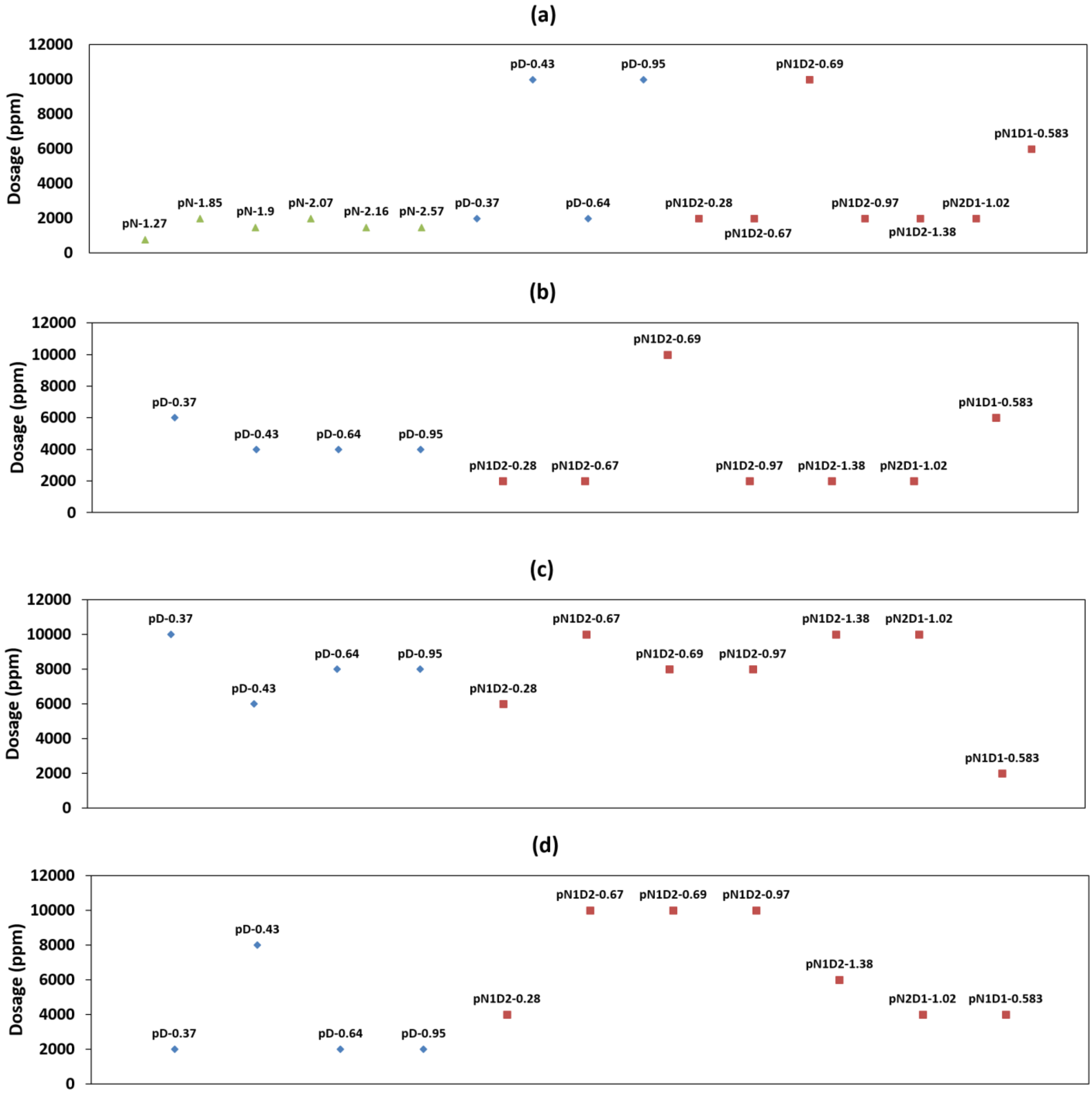

Figure A.0.1. Dosage values for best ISR for all polymers different modes CO_2 introduction: **a)** P + MFT **b)** (P+CO_2) + MFT **c)** P + (MFT+CO_2) and **d)** (P+CO_2) + (MFT+CO_2).

APPENDIX B: DOSAGES FOR BEST CST *t* = 0 VALUES

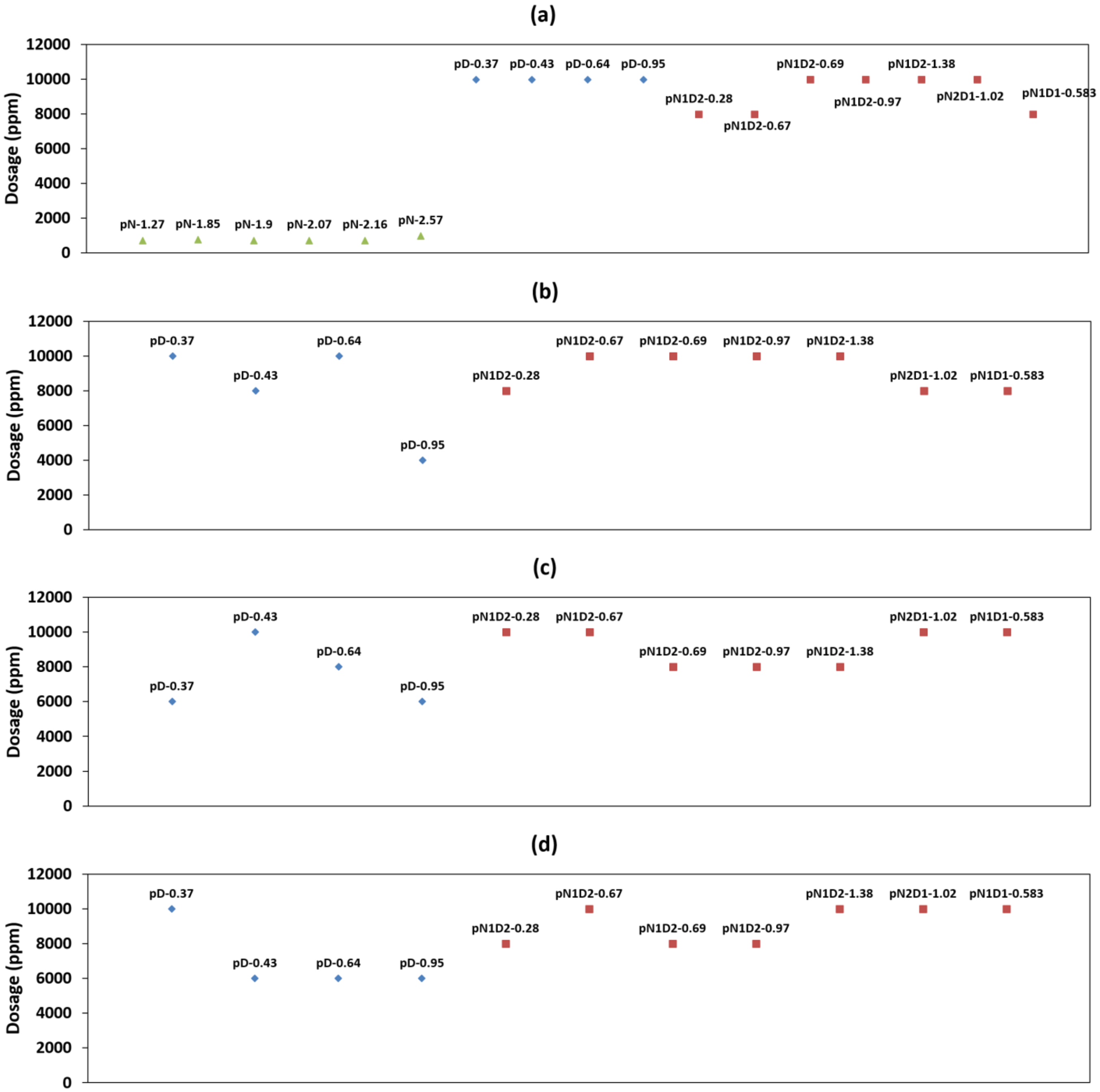

Figure B.0.1. Dosage values for best CST *t* = 0 for all polymers different modes CO_2 introduction: **a)** P + MFT **b)** (P+CO_2) + MFT **c)** P + (MFT+CO_2) and **d)** (P+CO_2) + (MFT+CO_2).

APPENDIX C: DOSAGES FOR BEST CST *t* = 24 h VALUES

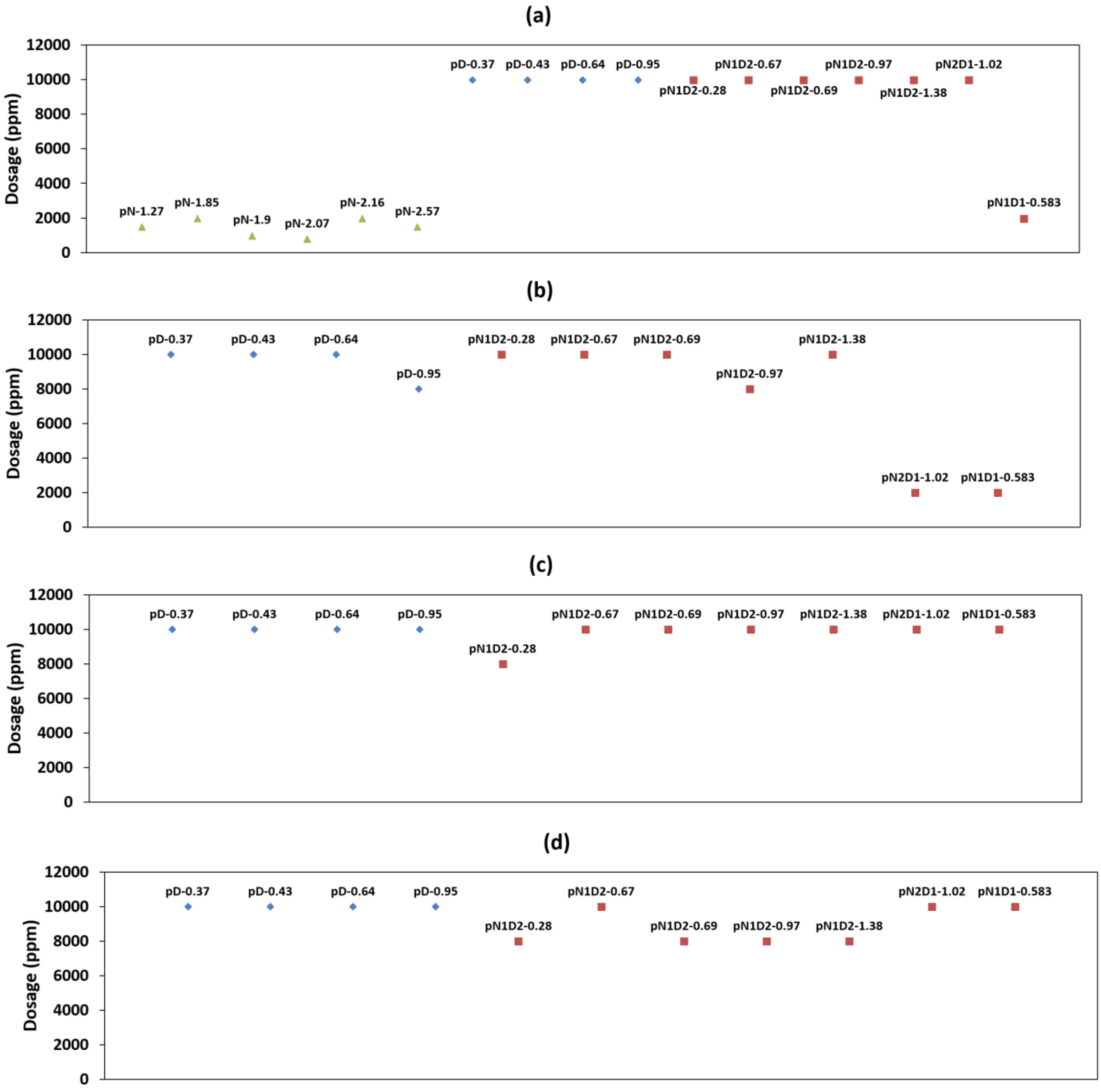

Figure C.0.1. Dosage values for best CST at *t* = 24 h for all polymers different modes CO_2 introduction: **a)** P + MFT **b)** (P+CO_2) + MFT **c)** P + (MFT+CO_2) and **d)** (P+CO_2) + (MFT+CO_2).

APPENDIX D: DOSAGES FOR BEST TURBIDITY VALUES

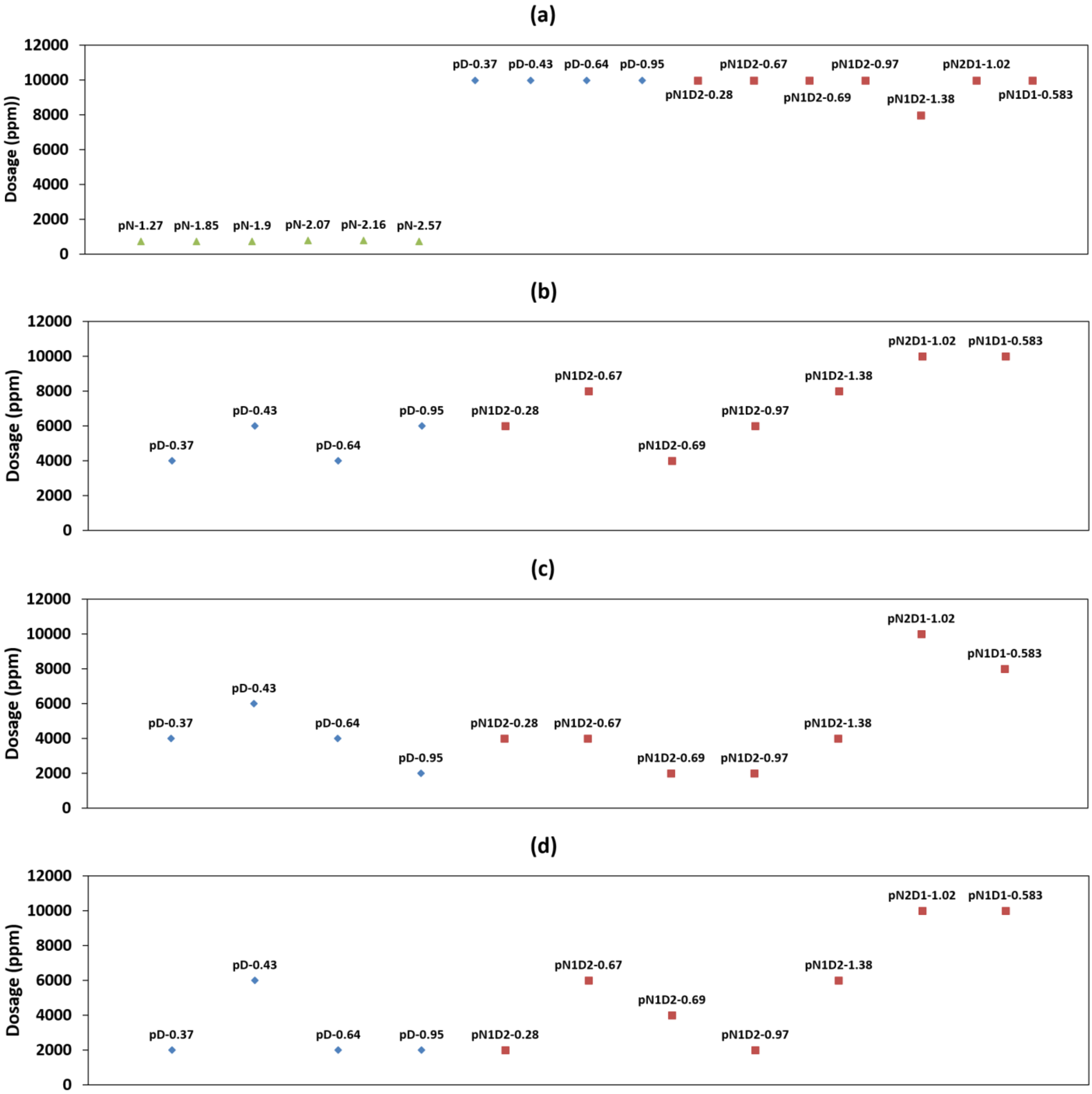

Figure D.0.1. Dosage values for best supernatant turbidity at *t* = 24 h for all polymers different modes CO_2 introduction: **a)** P + MFT **b)** (P+CO_2) + MFT **c)** P + (MFT+CO_2) and **d)** (P+CO_2) + (MFT+CO_2).